

IEEE Guide for Performing Arc-Flash Hazard Calculations

IEEE Industry Applications Society

Sponsored by the
Petroleum and Chemical Industry Committee

IEEE
3 Park Avenue
New York, NY 10016-5997
USA

IEEE Std 1584™-2018
(Revision of IEEE Std 1584-2002,
as amended by IEEE Std 1584a™-2004
and IEEE Std 1584b™-2011)

IEEE Std 1584™-2018

(Revision of IEEE Std 1584-2002,
as amended by IEEE Std 1584a™-2004
and IEEE Std 1584b™-2011)

IEEE Guide for Performing Arc-Flash Hazard Calculations

Sponsor

**Petroleum and Chemical Industry Committee
of the
IEEE Industry Applications Society**

Approved 27 September 2018

IEEE-SA Standards Board

Abstract: This guide provides mathematical models for designers and facility operators to apply in determining the arc-flash hazard distance and the incident energy to which workers could be exposed during their work on or near electrical equipment.

Keywords: arc blast, arc fault currents, arc flash, arc-flash boundary, arc-flash hazard, arc-flash hazard analysis, arc-flash hazard marking, arc in enclosures, arc in open air, electrical hazard, IEEE 1584™, incident energy, personal protective equipment, PPE, protective device coordination study, short-circuit study, working distances

Information related to the topic of this standard is available at https://standards.ieee.org/content/dam/ieee-standards/standards/web/download/1584-2018_downloads.zip and <https://ieee-dataport.org/documents/arc-flash-phenomena>.

The Institute of Electrical and Electronics Engineers, Inc.
3 Park Avenue, New York, NY 10016-5997, USA

Copyright © 2018 by The Institute of Electrical and Electronics Engineers, Inc.
All rights reserved. Published 30 November 2018. Printed in the United States of America.

IEEE, 3000 Standards Collection, and Color Books are registered trademarks in the U.S. Patent & Trademark Office, owned by The Institute of Electrical and Electronics Engineers, Incorporated.

National Electrical Code, NEC, NFPA 70, and NFPA 70E are registered trademarks in the U.S. Patent & Trademark Office, owned by the National Fire Protection Association.

National Electrical Safety Code and NESC are registered trademarks and service marks of the Institute of Electrical and Electronics Engineers, Incorporated.

PDF: ISBN 978-1-5044-5262-5 STD23380
Print: ISBN 978-1-5044-5263-2 STDPD23380

*IEEE prohibits discrimination, harassment, and bullying.
For more information, visit <http://www.ieee.org/web/aboutus/whatis/policies/p9-26.html>.
No part of this publication may be reproduced in any form, in an electronic retrieval system or otherwise, without the prior written permission of the publisher.*

Important Notices and Disclaimers Concerning IEEE Standards Documents

IEEE documents are made available for use subject to important notices and legal disclaimers. These notices and disclaimers, or a reference to this page, appear in all standards and may be found under the heading "Important Notices and Disclaimers Concerning IEEE Standards Documents." They can also be obtained on request from IEEE or viewed at <http://standards.ieee.org/ipr/disclaimers.html>.

Notice and Disclaimer of Liability Concerning the Use of IEEE Standards Documents

IEEE Standards documents (standards, recommended practices, and guides), both full-use and trial-use, are developed within IEEE Societies and the Standards Coordinating Committees of the IEEE Standards Association ("IEEE-SA") Standards Board. IEEE ("the Institute") develops its standards through a consensus development process, approved by the American National Standards Institute ("ANSI"), which brings together volunteers representing varied viewpoints and interests to achieve the final product. IEEE Standards are documents developed through scientific, academic, and industry-based technical working groups. Volunteers in IEEE working groups are not necessarily members of the Institute and participate without compensation from IEEE. While IEEE administers the process and establishes rules to promote fairness in the consensus development process, IEEE does not independently evaluate, test, or verify the accuracy of any of the information or the soundness of any judgments contained in its standards.

IEEE Standards do not guarantee or ensure safety, security, health, or environmental protection, or ensure against interference with or from other devices or networks. Implementers and users of IEEE Standards documents are responsible for determining and complying with all appropriate safety, security, environmental, health, and interference protection practices and all applicable laws and regulations.

IEEE does not warrant or represent the accuracy or content of the material contained in its standards, and expressly disclaims all warranties (express, implied and statutory) not included in this or any other document relating to the standard, including, but not limited to, the warranties of: merchantability; fitness for a particular purpose; non-infringement; and quality, accuracy, effectiveness, currency, or completeness of material. In addition, IEEE disclaims any and all conditions relating to: results; and workmanlike effort. IEEE standards documents are supplied "AS IS" and "WITH ALL FAULTS."

Use of an IEEE standard is wholly voluntary. The existence of an IEEE standard does not imply that there are no other ways to produce, test, measure, purchase, market, or provide other goods and services related to the scope of the IEEE standard. Furthermore, the viewpoint expressed at the time a standard is approved and issued is subject to change brought about through developments in the state of the art and comments received from users of the standard.

In publishing and making its standards available, IEEE is not suggesting or rendering professional or other services for, or on behalf of, any person or entity nor is IEEE undertaking to perform any duty owed by any other person or entity to another. Any person utilizing any IEEE Standards document, should rely upon his or her own independent judgment in the exercise of reasonable care in any given circumstances or, as appropriate, seek the advice of a competent professional in determining the appropriateness of a given IEEE standard.

IN NO EVENT SHALL IEEE BE LIABLE FOR ANY DIRECT, INDIRECT, INCIDENTAL, SPECIAL, EXEMPLARY, OR CONSEQUENTIAL DAMAGES (INCLUDING, BUT NOT LIMITED TO: PROCUREMENT OF SUBSTITUTE GOODS OR SERVICES; LOSS OF USE, DATA, OR PROFITS; OR BUSINESS INTERRUPTION) HOWEVER CAUSED AND ON ANY THEORY OF LIABILITY, WHETHER IN CONTRACT, STRICT LIABILITY, OR TORT (INCLUDING NEGLIGENCE OR OTHERWISE) ARISING IN ANY WAY OUT OF THE PUBLICATION, USE OF, OR RELIANCE UPON ANY STANDARD, EVEN IF ADVISED OF THE POSSIBILITY OF SUCH DAMAGE AND REGARDLESS OF WHETHER SUCH DAMAGE WAS FORESEEABLE.

Translations

The IEEE consensus development process involves the review of documents in English only. In the event that an IEEE standard is translated, only the English version published by IEEE should be considered the approved IEEE standard.

Official statements

A statement, written or oral, that is not processed in accordance with the IEEE-SA Standards Board Operations Manual shall not be considered or inferred to be the official position of IEEE or any of its committees and shall not be considered to be, or be relied upon as, a formal position of IEEE. At lectures, symposia, seminars, or educational courses, an individual presenting information on IEEE standards shall make it clear that his or her views should be considered the personal views of that individual rather than the formal position of IEEE.

Comments on standards

Comments for revision of IEEE Standards documents are welcome from any interested party, regardless of membership affiliation with IEEE. However, IEEE does not provide consulting information or advice pertaining to IEEE Standards documents. Suggestions for changes in documents should be in the form of a proposed change of text, together with appropriate supporting comments. Since IEEE standards represent a consensus of concerned interests, it is important that any responses to comments and questions also receive the concurrence of a balance of interests. For this reason, IEEE and the members of its societies and Standards Coordinating Committees are not able to provide an instant response to comments or questions except in those cases where the matter has previously been addressed. For the same reason, IEEE does not respond to interpretation requests. Any person who would like to participate in revisions to an IEEE standard is welcome to join the relevant IEEE working group.

Comments on standards should be submitted to the following address:

Secretary, IEEE-SA Standards Board
445 Hoes Lane
Piscataway, NJ 08854 USA

Laws and regulations

Users of IEEE Standards documents should consult all applicable laws and regulations. Compliance with the provisions of any IEEE Standards document does not imply compliance to any applicable regulatory requirements. Implementers of the standard are responsible for observing or referring to the applicable regulatory requirements. IEEE does not, by the publication of its standards, intend to urge action that is not in compliance with applicable laws, and these documents may not be construed as doing so.

Copyrights

IEEE draft and approved standards are copyrighted by IEEE under U.S. and international copyright laws. They are made available by IEEE and are adopted for a wide variety of both public and private uses. These include both use, by reference, in laws and regulations, and use in private self-regulation, standardization, and the promotion of engineering practices and methods. By making these documents available for use and adoption by public authorities and private users, IEEE does not waive any rights in copyright to the documents.

Photocopies

Subject to payment of the appropriate fee, IEEE will grant users a limited, non-exclusive license to photocopy portions of any individual standard for company or organizational internal use or individual, non-commercial use only. To arrange for payment of licensing fees, please contact Copyright Clearance Center, Customer Service, 222 Rosewood Drive, Danvers, MA 01923 USA; +1 978 750 8400. Permission to photocopy portions of any individual standard for educational classroom use can also be obtained through the Copyright Clearance Center.

Updating of IEEE Standards documents

Users of IEEE Standards documents should be aware that these documents may be superseded at any time by the issuance of new editions or may be amended from time to time through the issuance of amendments, corrigenda, or errata. A current IEEE document at any point in time consists of the current edition of the document together with any amendments, corrigenda, or errata then in effect.

Every IEEE standard is subjected to review at least every ten years. When a document is more than ten years old and has not undergone a revision process, it is reasonable to conclude that its contents, although still of some value, do not wholly reflect the present state of the art. Users are cautioned to check to determine that they have the latest edition of any IEEE standard.

In order to determine whether a given document is the current edition and whether it has been amended through the issuance of amendments, corrigenda, or errata, visit IEEE Xplore at <http://ieeexplore.ieee.org/> or contact IEEE at the address listed previously. For more information about the IEEE-SA or IEEE's standards development process, visit the IEEE-SA Website at <http://standards.ieee.org>.

Errata

Errata, if any, for IEEE standards can be accessed via <https://standards.ieee.org/standard/index.html>. Search for standard number and year of approval to access the web page of the published standard. Errata links are located under the Additional Resources Details section. Errata are also available in IEEE Xplore: <https://ieeexplore.ieee.org/browse/standards/collection/ieee>.

Patents

Attention is called to the possibility that implementation of this standard may require use of subject matter covered by patent rights. By publication of this standard, no position is taken by the IEEE with respect to the existence or validity of any patent rights in connection therewith. If a patent holder or patent applicant has filed a statement of assurance via an Accepted Letter of Assurance, then the statement is listed on the IEEE-SA Website at <http://standards.ieee.org/about/sasb/patcom/patents.html>. Letters of Assurance may indicate whether the Submitter is willing or unwilling to grant licenses under patent rights without compensation or under reasonable rates, with reasonable terms and conditions that are demonstrably free of any unfair discrimination to applicants desiring to obtain such licenses.

Essential Patent Claims may exist for which a Letter of Assurance has not been received. The IEEE is not responsible for identifying Essential Patent Claims for which a license may be required, for conducting inquiries into the legal validity or scope of Patents Claims, or determining whether any licensing terms or conditions provided in connection with submission of a Letter of Assurance, if any, or in any licensing agreements are reasonable or non-discriminatory. Users of this standard are expressly advised that determination of the validity of any patent rights, and the risk of infringement of such rights, is entirely their own responsibility. Further information may be obtained from the IEEE Standards Association.

Participants

At the time this IEEE guide was completed, the 1584 Arc-Flash Hazard Calculations Working Group had the following membership:

Daleep Mohla, Chair
Jim Phillips, Vice Chair
D. Ray Crow, Secretary

Arunkumar Aravamudhan	Mark Fisher	John Nelson
James Babcock	Frank Foote	Wheeler O'Harrow
Jane Barber	Robert Fuhr	Sergio Panetta
Louis Barrios	Timothy Gauthier	Thomas Papallo
Kevin Bates	Mikhail Golovkov	Antony Parsons
Patrick Baughman	Lloyd Gordon	Jay Prigmore
Terry Becker	J. Travis Griffith	Rahul Rajvanshi
James Bowen	Jimmy Guerrero	Adam Reeves
Waylon Bowers	John Hempstead	Kenneth Rempe
Matthew Braun	Dennis Hill	David Rewitzer
Rachel Bugaris	Ben C. Johnson	Ruperto Sanchez
Bill Burke	Jason Jonas	Vincent Saporita
Eldridge Byron	David Jones	Edwin Scherry
Brian Cadman	Kenneth Jones	Paul Schroder
Eric Campbell	Mark Kendall	David Shank
Kyle Carr	Hardip Kharbanda	Gregory Shirek
Steven Dittmann†	Michael Lang	Arthur Smith
Daniel Doan	Robert Lau	George Smith
Paul Dobrowsky	Wei-Jen Lee	Jeremy Smith
Mike Doherty	Poojit Lingam	Raymund Torres
Thomas Domitrovich	Kevin Lippert	Namgay Tshering
Gary Donner	Shengyi Liu	David Tucker
Ryan Downey	Afshin Majd	Marcelo Valdes
Gary Dreifuerst	Albert Marroquin	Julie Van Dyne
Andrew Drutel	Larry McGuire	David Wallis
Robert Durham	John McQuilkin	Peter Walsh
David Durocher	Jessica Morales	Matt Westerdale
Paul Eaton	Allan Morse	Kenneth White
Steven Emert	Dennis Neitzel	Alex Wu
Jesse Fairchild		Charles Yung

†Deceased

The following members of the individual balloting committee voted on this guide. Balloters may have voted for approval, disapproval, or abstention.

Steven Alexanderson	Jeffrey Brogdon	D. Ray Crow
Curtis Ashton	Chris Brooks	Alireza Daneshpooy
James Babcock	Demetrio Bucaneg Jr.	Glenn Davis
Jane Barber	Rachel Bugaris	Davide De Luca
Louis Barrios	William Bush	Steven Dittmann
Kevin Bates	William Byrd	Daniel Doan
Terry Becker	Eldridge Byron	Paul Dobrowsky
W. J. (Bill) Bergman	Paul Cardinal	Gary Donner
Thomas Blair	Kyle Carr	Neal Dowling
James Bowen	Raymond Catlett	Andrew Drutel
Clarence Bradley	Michael Chirico	Donald Dunn
Frederick Brockhurst	Timothy Croushore	Robert Durham

David Durocher	Robert Lau	Adam Reeves
Paul Eaton	Michael Lauxman	Kenneth Rempe
Marcia Eblen	Wei-Jen Lee	Charles Rogers
Steven Emert	Duane Leschert	Tim Rohrer
Keith Fager	Steven Liggio	Ryandi Ryandi
Samy Faried	Kevin Lippert	Sasan Salem
Mark Fisher	William Lockley	Hugo Ricardo Sanchez
Gary Fox	Rick Lutz	Reategui
Carl Fredericks	Afshin Majd	Vincent Saporita
Robert Fuhr	Jessica Maldonado	Todd Sauve
Timothy Gauthier	Thomas Malone	Trevor Sawatzky
Pamela Gold	Jose Marrero	Bartien Sayogo
Mikhail Golovkov	Albert Marroquin	Robert Seitz
Lou Grahor	John McAlhaney Jr.	Nikunj Shah
J. Travis Griffith	Larry McGuire	David Shank
Randall Groves	John McQuilkin	Gregory Shirek
Paul Guidry	Daleep Mohla	Tom Short
Charles Haahr	Charles Morse	Neal Simmons
Paul Hamer	Daniel Mulkey	Arthur Smith
Robert Hanna	Warren Naylor	Jerry Smith
Thomas Hawkins	Daniel Neeser	Gary Smullin
John Hempstead	Dennis Neitzel	Wayne Stec
Scott Hietpas	John Nelson	Gregory Steinman
Steve Hinton	Arthur Neubauer	Bill Stewart
Werner Hoelzl	Joe Nims	Paul Sullivan
Robert Hoerauf	Wheeler O'Harrow	Peter Sutherland
Richard Hulett	T. W. Olsen	Wayne Timm
Christel Hunter	David Pace	David Tucker
Ben C Johnson	Lorraine Padden	Marcelo Valdes
Joseph Johnson	Mirko Palazzo	John Vergis
Kenneth Jones	Sergio Panetta	David Wallis
Laszlo Kadar	Thomas Papallo	Peter Walsh
John Kay	Antony Parsons	Keith Waters
Peter Kelly	Bansi Patel	John Webb
Mark Kendall	Christopher Pavese	Craig Wellman
Yuri Khersonsky	Howard Penrose	Matt Westerdale
Jim Kulchisky	Branimir Petosic	Kenneth White
Paneendra Kumar	Jim Phillips	Kenneth White
Saumen Kundu	Jay Prigmore	Terry Woodyard
Mikhail Lagoda	Iulian Profir	John Yale
James Lagree	Rahul Rajvanshi	Jian Yu
Michael Lang		Charles Yung

When the IEEE-SA Standards Board approved this guide on 27 September 2018, it had the following membership:

Jean-Philippe Faure, *Chair*
Gary Hoffman, *Vice Chair*
John D. Kulick, *Past Chair*
Konstantinos Karachalios, *Secretary*

Ted Burse

Guido R. Hiertz

Christel Hunter

Joseph L. Koepfinger*

Thomas Koshy

Hung Ling

Dong Liu

Xiaohui Liu

Kevin Lu

Daleep Mohla

Andrew Myles

Paul Nikolich

Ronald C. Petersen

Annette D. Reilly

Robby Robson

Dorothy Stanley

Mehmet Ulema

Phil Wennblom

Philip Winston

Howard Wolfman

Jingyi Zhou

*Member Emeritus

Introduction

This introduction is not part of IEEE Std 1584-2018, IEEE Guide for Performing Arc-Flash Hazard Calculations.

A technical paper, “The other electrical hazard: electric arc blast burns,” by Ralph Lee [B67]¹ provided insight that electric-arc burns make up a substantial portion of the injuries from electrical malfunctions. Mr. Lee identified that electric arcing is the term applied to current passing through vapor from the arc terminal conductive metal or carbon material. The extremely high temperatures of these arcs can cause fatal burns at up to about 1.5 m (5 ft) and major burns at up to about 3 m (10 ft) distance from the arc. Additionally, electric arcs expel droplets of molten terminal material that shower the immediate vicinity, similar to but more extensive than that from electric arc welding. These findings started to fill a void created by early works that identified electric shock as the major electrical hazard. Mr. Lee’s work also helped establish a relationship between time to human tissue cell death and temperature, as well as a curable skin burn time-temperature relationship. Once forensic analysis of electrical incidents focused on the arc-flash hazard, experience over a period of time indicated that Mr. Lee’s formulas for calculating the distance-energy relationship from the source of arc did not serve to reconcile the greater thermal effect on persons positioned in front of opened doors or removed covers, from arcs inside electrical equipment enclosures.

A technical paper, “Predicting incident energy to better manage the electric arc hazard on 600 V power distribution systems,” by Doughty, Neal, and Floyd [B29] presented the findings from many structured tests using both “arcs in open air” and “arcs in a cubic box.” These three-phase tests were performed at the 600 V rating and are applicable for the range of 16 000 A to 50 000 A short-circuit fault current. It was established that the contribution of heat reflected from surfaces near the arc intensifies the heat directed toward the opening of the enclosure.

The focus of industry on electrical safety and recognition of arc-flash burns highlighted the need for protecting workers from arc-flash hazards. There are limitations in applying the currently known formulas for calculating incident energy and arc-flash boundary as discussed throughout this guide, which uses empirically derived models based on statistical analysis and curve fitting of the overall test data available as well as an understanding of electrical arc physics. This is a guide that can help inform worker and worksite considerations, but specific worksite variables and considerations must be evaluated.

The P1584 working group organized testing and developed a model of incident energy that was published in the 2002 version of this guide. The model detailed in IEEE Std 1584-2002 has been used with success throughout industry. There are numerous variables in addition to those included in the 2002 model that can increase or decrease the value of incident energy from an arcing fault. Other researchers, during their testing, have found significantly different values than those calculated using that model. The updated model of incident energy documented in this guide was developed from further testing organized by the IEEE/NFPA Collaborative Arc Flash Research Project.

¹The numbers in brackets correspond to those of the bibliography in Annex A.

Contents

1. Overview	17
1.1 Scope	17
1.2 Purpose	17
2. Normative references	17
3. Definitions, acronyms, and abbreviations	18
3.1 Definitions	18
3.2 Acronyms and abbreviations	20
4. Model for incident energy calculations	20
4.1 General	20
4.2 Range of model	20
4.3 Model application overview	21
4.4 Intermediate average arcing currents	22
4.5 Arcing current variation correction factor	24
4.6 Intermediate incident energy (E)	25
4.7 Intermediate arc-flash boundary (AFB)	27
4.8 Enclosure size correction factor	28
4.9 Determination of I_{arc} , E , and AFB ($600 \text{ V} < V_{oc} \leq 15\,000 \text{ V}$)	31
4.10 Determination of I_{arc} , E , and AFB ($V_{oc} \leq 600 \text{ V}$)	33
4.11 Single-phase systems	34
4.12 DC systems	34
5. Applying the model	34
6. Analysis process	34
6.1 General overview	34
6.2 Step 1: Collect the system and installation data	35
6.3 Step 2: Determine the system modes of operation	36
6.4 Step 3: Determine the bolted fault currents	36
6.5 Step 4: Determine typical gap and enclosure size based upon system voltages and classes of equipment	37
6.6 Step 5: Determine the equipment electrode configuration	38
6.7 Step 6: Determine the working distances	40
6.8 Step 7: Calculation of arcing current	40
6.9 Step 8: Determine the arc duration	40
6.10 Step 9: Calculate the incident energy	42
6.11 Step 10: Determine the arc-flash boundary for all equipment	43
6.12 Cautions and disclaimers	43
7. Background on the arc-flash hazard	44
7.1 Early papers	44
7.2 Additional references	45
Annex A (informative) Bibliography	46
Annex B (informative) Units of measure	53
Annex C (informative) Determination of incident energy for different equipment types	54
Annex D (informative) Sample incident energy calculations	57
Annex E (informative) Arc flash	75

Annex F (informative) Laboratory test programs.....	76
Annex G (informative) Development of model.....	82
Annex H (informative) Development of special model for current-limiting fuses	124
Annex I (informative) Development of special model for circuit breakers.....	136

List of Figures

Figure 1—Multi-source MCC with motor contribution	43
Figure C.1—Switchgear side-view diagram	55
Figure C.2—Side-view diagram of panel board	56
Figure D.1—Determination of arc duration	59
Figure D.2—Determination of arc duration using reduced arcing current.....	65
Figure D.3—Determination of arc duration for LV case.....	70
Figure D.4—Determination of arc duration using reduced arcing current.....	73
Figure F.1—Test setup A—single-phase arc in air with electrodes in-line and with partial Faraday cage	76
Figure F.2—Test setup B—three-phase arc in air with electrodes in parallel (VOA)	76
Figure F.3—Test setup C—arc in box (VCB).....	77
Figure F.4—Vertical conductors, box, with insulating barrier (VCBB)	78
Figure F.5—Horizontal conductors, box (HCB)	79
Figure F.6—Horizontal conductors, open air (HOA)	79
Figure G.1—VCB (vertical electrodes inside a metal “box” enclosure)	82
Figure G.2—VCBB (vertical electrodes terminated in an insulating “barrier,” inside a metal “box” enclosure)	83
Figure G.3—HCB (horizontal electrodes inside a metal “box” enclosure)	83
Figure G.4—VOA (vertical electrodes in open air)	83
Figure G.5—HOA (horizontal electrodes in open air)	84
Figure G.6—Horizontal electrodes (plasma pushed to the left, horizontal direction)	85
Figure G.7—Vertical electrodes (plasma pushed vertically downward)	85
Figure G.8—VCB, vertical electrodes in enclosure (plasma cloud “spills” out of box)	85
Figure G.9—Arcing current recording from 13.8 kV arc-flash test	86
Figure G.10—DC offset and decay trend of asymmetrical ac current	87
Figure G.11—Filtered and unfiltered rms arcing current comparison	88
Figure G.12—Arcing current recording for a 480 V arc-flash test.....	89
Figure G.14—600 V VOA IE with 50.8 mm (2 in) gap	91
Figure G.13—600 V HOA IE with 50.8 mm (2 in) gap	91
Figure G.15—600 V VCB IE with 50.8 mm (2 in) gap.....	92
Figure G.16—2.7 kV HCB IE with 76.3 mm (3 in) gap.....	92

Figure G.17—2.7 kV HCB IE with 114.3 mm (4.5 in) gap.....	93
Figure G.18—14.3 kV VOA IE in 20 kA bolted fault current.....	93
Figure G.19—14.3 kV HOA IE in 20 kA bolted fault current.....	94
Figure G.20—Sample result for partial regression plotting.....	95
Figure G.22—Parameter selection	96
Figure G.21—Data input interface	96
Figure G.23—Partial regression calculation	97
Figure G.24—Sensitivity analysis for I_{bf} against I_{arc}	97
Figure G.25—Sensitivity analysis for gap against I_{arc}	98
Figure G.26—Sensitivity analysis for distance versus IE	99
Figure G.27—Sensitivity analysis for I_{arc} against IE	99
Figure G.28—Sensitivity analysis for gap against IE	100
Figure G.29—Comparison between original regression and adjusted regression model.....	106
Figure G.30—Curve of current correction factor (the vertical axis is the ratio of I_{arc}/I_{bf} and the horizontal axis is the magnitude of I_{bf} in kiloamperes)	107
Figure G.31—Comparison between the linear curve and the curve with correction factor applied.....	107
Figure G.32— I_{arc} versus V_{oc} for 208 V to 1000 V (comparison of IEEE 1584-2002 and IEEE 1584-2018) .	114
Figure G.33— I_{arc} versus V_{oc} for 1 kV to 15 kV (comparison of IEEE 1584-2002 and IEEE 1584-2018)	114
Figure G.34— I_{arc} variation versus V_{oc} for VCB test results	115
Figure G.35—Example of incident energy variation versus opening size (Wilkins)	117
Figure G.36—VCB incident energy comparisons at different enclosure sizes	118
Figure G.37—VCBB incident energy comparisons at different enclosure sizes	118
Figure G.38—HCB incident energy comparisons at different enclosure sizes	119
Figure G.40—VCB (upper circle) and HCB (lower circle) configuration on the fuse holder	121
Figure G.39—HCB/HOA configuration in switchgear (depends on opening dimension)	122
Figure G.41—VCBB configuration on switchgear	122
Figure G.42—VCB configuration on switchgear	123
Figure G.43—HCB configuration on switchgear	123
Figure H.1—Class L 2000 A fuse—incident energy versus bolted fault current.....	125
Figure H.2—Class L 2000 A fuse—low current segment of model	125
Figure H.3—Class L 2000 A fuse—high current segment of model.....	125

Figure H.4—Class L 1600 A fuse—incident energy versus bolted fault current.....	126
Figure H.5—Class L 1600 A fuse—low current segment of model	126
Figure H.6—Class L 1600 A fuse—upper-middle current segment of model	127
Figure H.7—Class L 1600 A fuse—upper-middle current segment of model	127
Figure H.8—Class L 1600 A fuse—upper current segment of model.....	127
Figure H.9—Class L 2000 A fuse—incident energy versus bolted fault current.....	128
Figure H.10—Class L 1200 A fuse—lower current segment of model.....	128
Figure H.11—Class L 1200 A fuse—middle current segment of model.....	129
Figure H.12—Class L 1200 A fuse—upper current segment of model.....	129
Figure H.13—Class RK1 800 A fuse—incident energy versus bolted fault current	130
Figure H.14—Class RK1 800 A fuse—lower current segment of model.....	130
Figure H.15—Class RK1 800 A fuse—middle current segment of model.....	130
Figure H.16—Class RK1 600 A fuse—lower current segment of model.....	131
Figure H.17—Class RK1 600 A fuse—middle current segment of model.....	131
Figure H.18—Class RK1 200 A fuse—upper current segment of model.....	131
Figure H.19—Class RK1 400 A fuse—incident energy versus bolted fault current	132
Figure H.20—Class RK1 400 A fuse—lower current segment of model.....	132
Figure H.21—Class RK1 400 A fuse—middle current segment of model.....	132
Figure H.22—Class RK1 200 A fuse—incident energy versus bolted fault current	133
Figure H.23—Class RK1 200 A fuse—lower current segment of model.....	133
Figure H.24—Class RK1 200 A fuse—upper current segment of model.....	133
Figure H.25—Class RK1 100 A fuse—lower current segment of model.....	134
Figure H.26—Class RK1 100 A fuse—upper current segment of model.....	134
Figure H.27—Class L 100 A fuse—upper current segment of model.....	134
Figure I.1—Incident energy versus fault current for 100 A to 400 A circuit breakers	136
Figure I.2—Incident energy versus available fault current generalized for circuit breakers.....	137
Figure I.3—Typical circuit breaker time-current characteristic.....	139

List of Tables

Table 1—Coefficients for Equation (1)	23
Table 2—Coefficients for Equation (2)	24
Table 3—Coefficients for Equation (3) , Equation (6) , Equation (7) , and Equation (10)	26
Table 4—Coefficients for Equation (4) and Equation (8)	26
Table 5—Coefficients for Equation (5) and Equation (9)	26
Table 6—Guidelines to determine the equivalent height and width	29
Table 7—Coefficients for Equation (14) and Equation (15)	30
Table 8—Classes of equipment and typical bus gaps	37
Table 9—Correlation between actual equipment and electrode configuration	38
Table 10—Classes of equipment and typical working distances	40
Table F.1—Summary of tests	80
Table G.1—Typical dc offset decay rate in power system	87
Table G.2—600 V and below, arcing current, voltage, and resistance	89
Table G.3—Arc energy comparison on different gap length (horizontal electrodes in open air tests)	90
Table G.4—Arc energy comparison on different gap length (vertical electrodes in open air tests)	90
Table G.5— I_E/E_{arc} comparison.....	90
Table G.6—Template for tabulation of the test setup results	102
Table G.7—($\text{cal}/\text{cm}^2_{avg}$)/MJ for different enclosure dimension, 2700 V tests, VCB	103
Table G.8— I_{arc} estimation models	103
Table G.9—[IE/Cycle] estimation models	103
Table G.10—14.3 kV VCB arcing current modeling data	104
Table G.11—Variables entered/removed.....	104
Table G.12—Model summary	105
Table G.13—Coefficients for arcing current model development	105
Table G.14—Ratio of arcing current and bolted fault current.....	106
Table G.15—14.3 kV VCB incident energy modeling data.....	109
Table G.16—Model summary	109
Table G.17—Enclosure sizes for IEEE 1584-2002 arc-flash model	115
Table G.18—Enclosure sizes for IEEE 1584-2018 arc-flash model	116

Table H.1—Incident energy as a function of bolted fault current for one manufacturer’s 2000 A class L current limiting fuses at 600 V, 460 mm (18.11 in)	125
Table H.2—Incident energy as a function of bolted fault current for one manufacturer’s 1600 A class L current limiting fuses at 600 V, 460 mm (18.11 in)	126
Table H.3—Incident energy as a function of bolted fault current for one manufacturer’s 1200 A class L current limiting fuses at 600 V, 460 mm (18.11 in)	128
Table H.4—Incident energy as a function of bolted fault current for one manufacturer’s 800 A class L current limiting fuses at 600 V, 460 mm (18.11 in)	130
Table H.5—Incident energy as a function of bolted fault current of one manufacturer’s 600 A class RK1 current limiting fuses at 600 V, 460 mm (18.11 in)	131
Table H.6—Incident energy as a function of bolted fault current for one manufacturer’s 400 A class RK1 current limiting fuses at 600 V, 460 mm (18.11 in)	132
Table H.7—Incident energy as a function of bolted fault current for one manufacturer’s 200 A class RK1 current limiting fuses at 600 V, 460 mm (18.11 in)	133
Table H.8—Incident energy as a function of bolted fault current of one manufacturer’s 100 A class RK1 current limiting fuses at 600 V, 460 mm (18.11 in)	134
Table H.9—Constants K1, K2, and K3 for special fuse model equation	135
Table I.1—Equations for incident energy and arc-flash boundary by circuit-breaker type and rating	138

IEEE Guide for Performing Arc-Flash Hazard Calculations

1. Overview

1.1 Scope

This guide provides models and an analytical process to enable calculation of the predicted incident thermal energy and the arc-flash boundary. The process covers the collection of field data if applicable, consideration of power system operating scenarios, and calculation parameters. Applications include electrical equipment and conductors for three-phase alternating current (ac) voltages from 208 V to 15 kV. Calculations for single-phase ac systems and direct current (dc) systems are not a part of this guide, but some guidance and references are provided for those applications. Recommendations for personal protective equipment (PPE) to mitigate arc-flash hazards are not included in this guide.

1.2 Purpose

The purpose of the guide is to enable qualified person(s) to analyze power systems for the purpose of calculating the incident energy to which employees could be exposed during operations and maintenance work. Contractors and facility owners can use this information to help provide appropriate protection for employees in accordance with the requirements of applicable electrical workplace safety standards.

2. Normative references

The following referenced documents are indispensable for the application of this document (i.e., they must be understood and used, so each referenced document is cited in text and its relationship to this document is explained). For dated references, only the edition cited applies. For undated references, the latest edition of the referenced document (including any amendments or corrigenda) applies.

IEEE Std 242TM, IEEE Recommended Practice for Protection and Coordination of Industrial and Commercial Power Systems (*IEEE Buff Book*TM).^{2,3,4,5}

²IEEE publications are available from the Institute of Electrical and Electronics Engineers (<http://standards.ieee.org/>).

³The IEEE standards or products referred to in Clause 2 are trademarks owned by the Institute of Electrical and Electronics Engineers, Incorporated.

⁴IEEE 3000 Standards Collection[®] (formerly known as the IEEE Color Books[®]) is the family of industrial and commercial power systems standards organized into “dot” standards that cover specific technical topics, which have been reorganized and, in some cases, updated from the content of the IEEE Color Books (<https://ieeexplore.ieee.org/browse/standards/collection/ieee/power-and-energy/3000StandardsCollection>).

⁵IEEE 3004 Standards: Protection and Coordination covers material from IEEE Std 242 (*IEEE Buff Book*) and IEEE Std 1015 (*IEEE Blue Book*).

IEEE Std 551™, IEEE Recommended Practice for Calculating AC Short-Circuit Currents in Industrial and Commercial Power Systems (*IEEE Violet Book*)⁶.

IEEE Std 1584.1™, IEEE Guide for the Specification of Scope and Deliverable Requirements for an Arc-Flash Hazard Calculation Study in Accordance with IEEE Std 1584™.

IEEE Std C37.010™, IEEE Application Guide for AC High-Voltage Circuit Breakers > 1000 Vac Rated on a Symmetrical Current Basis.

3. Definitions, acronyms, and abbreviations

For the purposes of this document, the following terms and definitions apply. The *IEEE Standards Dictionary Online* should be consulted for terms not defined in this clause.⁷

3.1 Definitions

arc: A plasma cloud formed in a gap between two electrodes with sufficient potential difference.

arc current: *See:* **arcing fault current.**

arc duration: *See:* **clearing time.**

arc flash: An electric arc event with thermal energy dissipated as radiant, convective, and conductive heat.

NOTE—See Annex E for additional information.⁸

arc-flash boundary: A distance from a prospective arc source at which the incident energy is calculated to be 5.0 J/cm² (1.2 cal/cm²).

arc-flash hazard: A dangerous condition associated with an electric arc likely to cause possible injury.

arc-flash hazard calculation: The use of equations to compute the incident energy at a specific working distance and the arc-flash boundary.

arcing fault current: A fault current flowing through an electrical arc plasma. *Syn:* **arc current.**

available short-circuit current: At a given point in a circuit, the maximum current that the power system can deliver through a given circuit to any negligible-impedance short circuit applied at the given point, or at any other point that causes the highest current to flow through the given point. “Available short-circuit current” and “bolted fault current” are equivalent for a zero fault impedance.

bolted fault: A short-circuit condition that assumes zero impedance exists at the point of the fault.

circuit: A conductor or system of conductors through which an electric current flows.

clearing time: The total time between the beginning of a specified overcurrent and the final interruption of the circuit at rated voltage. *Syn:* **arc duration.**

⁶IEEE 3002 Standards: Power Systems Analysis covers material from IEEE Std 551 (*IEEE Violet Book*) and IEEE Std 399 (*IEEE Brown Book*).

⁷*IEEE Standards Dictionary Online* is available at: <http://dictionary.ieee.org>.

⁸Notes in text, tables, and figures of a standard are given for information only and do not contain requirements needed to implement this standard.

NOTE 1—In regard to fuses, it is the sum of the minimum melting time of a fuse plus tolerance and the arcing time. In regard to circuit breakers with integral trip units (usually rated less than 1000 V), it is the sum of the sensor time, plus opening time and the arcing time. For circuit breakers with separate relaying (usually rated greater than 1000 V), it is the sum of the minimum relay time, plus contact parting time and the arcing time. Sometimes referred to as total clearing time or interrupting time.

NOTE 2—Arc duration is the interval of time between the instant of the first initiation of the arc and the instant of final arc extinction. Arc duration is usually the same or directly related to the clearing time. See [6.9.1](#) for special circumstances where arc duration may be different than clearing time.

electrode configuration: The orientation and arrangement of the electrodes used in the testing performed for the model development.

NOTE 1—Electrodes were placed in open-air (“OA”) or enclosed (“Box”) configurations (with open front end). Electrodes were also oriented vertically and horizontally. Open-tipped and barrier-terminated electrode configurations were also used.

NOTE 2—Refer to [Annex G](#). The following electrode configurations (test arrangements) are defined and listed according to their order of use within the incident energy model:

- **VCB:** Vertical conductors/electrodes inside a metal box/enclosure
- **VCBB:** Vertical conductors/electrodes terminated in an insulating barrier inside a metal box/enclosure
- **HCB:** Horizontal conductors/electrodes inside a metal box/enclosure
- **VOA:** Vertical conductors/electrodes in open air
- **HOA:** Horizontal conductors/electrodes in open air

fault current: A current that flows from one conductor to ground or to another conductor owing to an abnormal connection (including an arc) between the two conductors.

incident energy: The amount of thermal energy impressed on a surface, a certain distance from the source, generated during an electric arc event.

NOTE 1—The incident energy is calculated at the working distance. Incident energy increases as the distance from the potential arc source decreases, and the incident energy decreases as the distance increases. *See: working distance.*

NOTE 2—The units used to measure incident energy are joules per square centimeter (J/cm^2) or calories per square centimeter (cal/cm^2). See [B.2](#).

nominal voltage: A numerical value of a circuit or system for designating its voltage class. (National Electrical Safety Code® (NESC®) (Accredited Standards Committee C2-2012) [\[B1\]](#)⁹)

qualified person: A person who performs arc-flash hazard calculations by using skills and knowledge related to the construction and operation of the electrical equipment and installations and has experience in power system studies and arc-flash hazard analysis.

voltage (nominal): *See: nominal voltage.*

working distance: The distance between the potential arc source and the face and chest of the worker performing the task.

NOTE—Parts of the body closer to the potential arc source other than the face and chest receive a greater incident energy. The arc source is usually energized parts within an equipment enclosure or exposed energized parts in open air.

⁹The numbers in brackets correspond to those of the bibliography in [Annex A](#).

3.2 Acronyms and abbreviations

ac	alternating current
CF	correction factor
dc	direct current
E.C.	electrode configuration
HCB	horizontal conductors/electrodes inside a metal box/enclosure
HOA	horizontal conductors/electrodes in open air
LV	low voltage
MCC	motor control center
MV	medium voltage
OA	open air
PDU	power distribution unit
PPE	personal protective equipment
TCC	time current characteristic
UPS	uninterruptible power supplies
VCB	vertical conductors/electrodes inside a metal box/enclosure
VCBB	vertical conductors/electrodes terminated in an insulating barrier inside a metal box/enclosure
VOA	vertical conductors/electrodes in open air

4. Model for incident energy calculations

4.1 General

An empirically derived model is provided for incident energy calculations. Development of this model is discussed in [Annex G](#). This annex provides more definitions and explains the derivations of the coefficients, variables, and terms used in the equations presented in [4.4](#) to [4.10](#). The equations in the model may be embedded in a spreadsheet or commercial software program, because it may be impractical to solve them by hand.

4.2 Range of model

The following empirically derived model, based upon statistical analysis and curve-fitting programs as well as an understanding of electrical arc physics, is applicable for systems with the following parameter range:

- Voltages in the range of 208 V to 15 000 V, three-phase (line-to-line)

Tests were performed in laboratory conditions using selected open-circuit voltages (V_{oc}). While the model utilizes V_{oc} , pre-fault voltage (system nominal voltage, utilization voltage, etc.) can be used for application of this model.

- Frequency of 50 Hz or 60 Hz
- Bolted fault current (rms symmetrical)
 - 208 V to 600 V: 500 A to 106 000 A
 - 601 V to 15 000 V: 200 A to 65 000 A
- Gaps between conductors
 - 208 V to 600 V: 6.35 mm to 76.2 mm (0.25 in to 3 in)
 - 601 V to 15 000 V: 19.05 mm to 254 mm (0.75 in to 10 in)

- Working distances greater than or equal to 305 mm (12 in) (see G.7.6 for details on the lower limit)
- Fault clearing time: No limit (see G.7.8 for more details)
- Enclosures tested (with open front end) as shown in the following table:

Open-circuit voltage (V)	Enclosure dimensions (H × W × D)	
	SI units (metric)	Imperial units
600	508 mm × 508 mm × 508 mm	20 in × 20 in × 20 in
2 700	660.4 mm × 660.4 mm × 660.4 mm	26 in × 26 in × 26 in
14 300	914.4 mm × 914.4 mm × 914.4 mm	36 in × 36 in × 36 in

- Enclosure dimension limits (established using the enclosures from the 2002 version of this guide)
 - Maximum height or width: 1244.6 mm (49 in)
 - Maximum opening area: 1.549 m² (2401 in²)
 - Minimum width: The width of the enclosure should be larger than four times the gap between conductors (electrodes).
- Electrode configurations (see the definition of *electrode configuration* in 3.1 and Figure G.1 through Figure G.5)

There are alternative calculation methods for system parameters that fall outside of the range of the model. However, no particular recommendation can be made because there are other application details such as bolted fault current levels, voltage, gap length, operating frequency, number of phases, types of faults, etc. The user is advised to properly research alternative calculation methods and their application viabilities.

4.3 Model application overview

The model for incident energy calculations has been divided into the following two parts depending on the system open-circuit voltage, V_{oc} :

- Model for $600 \text{ V} < V_{oc} \leq 15\,000 \text{ V}$
- Model for $208 \text{ V} \leq V_{oc} \leq 600 \text{ V}$

Sustainable arcs are possible but less likely in three-phase systems operating at 240 V nominal or less with an available short-circuit current less than 2000 A.

The model uses a two-step process in which intermediate values of average arc current, incident energy, and arc-flash boundary are interpolated to determine final values. Correction factors for enclosure (box) size and arc current variation are applied to adjust the results.

A summary of the steps required to apply the model is provided as follows:

- a) To determine the arcing current
 - 1) Determine the applicable equipment electrode configuration based on 6.6.
 - 2) If the system voltage is $600 \text{ V} < V_{oc} \leq 15\,000 \text{ V}$, use Equation (1) to find intermediate values at 600 V, 2700 V, and 14 300 V. Use Equation (16), Equation (17), Equation (18), and the guidance provided in 4.9 to find the final value of the arcing current.
 - 3) If the system voltage is $208 \text{ V} \leq V_{oc} \leq 600 \text{ V}$, use Equation (1) to find the intermediate value (600 V only) and Equation (25) to find the final value. Guidance for the determination of the final arcing current is provided in 4.10.

- b) Determine the arc duration or fault clearing time using the arcing current determined in step a). Guidance for determining the arc duration is provided in [6.9](#).
- c) To determine the incident energy
 - 1) Determine the enclosure size correction factor using the guidance provided in [4.8.4](#).
 - 2) If the system voltage is $600 \text{ V} < V_{\text{oc}} \leq 15\,000 \text{ V}$, use [Equation \(3\)](#), [Equation \(4\)](#), and [Equation \(5\)](#) to find intermediate values. Use [Equation \(19\)](#), [Equation \(20\)](#), [Equation \(21\)](#), and the guidance provided in [4.9](#) to find the final value of the incident energy.
 - 3) If the system voltage is $208 \text{ V} \leq V_{\text{oc}} \leq 600 \text{ V}$, use [Equation \(6\)](#). Guidance for determining the final incident energy is provided in [4.10](#).
 - 4) Additional considerations are provided in [6.10](#).
- d) To determine the arc-flash boundary
 - 1) Determine the enclosure size correction factor per [4.8](#).
 - 2) If the system voltage is $600 \text{ V} < V_{\text{oc}} \leq 15\,000 \text{ V}$, use [Equation \(7\)](#), [Equation \(8\)](#), and [Equation \(9\)](#) to find intermediate values. Use [Equation \(22\)](#), [Equation \(23\)](#), [Equation \(24\)](#), and the guidance provided in [4.9](#) to find the final value of the arc-flash boundary.
 - 3) If the system voltage is $208 \text{ V} \leq V_{\text{oc}} \leq 600 \text{ V}$, use [Equation \(10\)](#). Guidance for the determination of the final arc-flash boundary is provided in [4.10](#).
- e) Use the guidance provided in [4.5](#) to account for the arcing current variation. Repeat step b), step c), and step d) using the reduced arcing current. It is possible that the incident energy and arc-flash boundary results obtained using the reduced arcing current are different. The final incident energy or arc-flash boundary is the higher of the two calculated values.

A set of sample calculations for different voltage levels is provided in [Annex D](#) to help illustrate the calculation process for two different system-voltage levels (4160 V and 480 V).

The equations presented in this guide can be applied to other unit systems by using the proper conversion factors.

4.4 Intermediate average arcing currents

The intermediate average arcing currents can be determined using [Equation \(1\)](#) as follows and the coefficients provided in [Table 1](#). The arcing currents are calculated at three different open-circuit voltage (V_{oc}).

$$I_{\text{arc_Voc}} = 10^{(k1+k2\lg I_{\text{bf}}+k3\lg G)} (k4I_{\text{bf}}^6 + k5I_{\text{bf}}^5 + k6I_{\text{bf}}^4 + k7I_{\text{bf}}^3 + k8I_{\text{bf}}^2 + k9I_{\text{bf}} + k10) \quad (1)$$

where

I_{bf}	is the bolted fault current for three-phase faults (symmetrical rms) (kA)
$I_{\text{arc_600}}$	is the average rms arcing current at $V_{\text{oc}} = 600 \text{ V}$ (kA)
$I_{\text{arc_2700}}$	is the average rms arcing current at $V_{\text{oc}} = 2700 \text{ V}$ (kA)
$I_{\text{arc_14300}}$ [is the average rms arcing current at $V_{\text{oc}} = 14\,300 \text{ V}$ (kA)
G	is the gap distance between electrodes (mm)
$k1$ to $k10$	are the coefficients provided in Table 1
\lg	is \log_{10}

Table 1—Coefficients for Equation (1)

E.C. / V_{ac}	k_1	k_2	k_3	k_4	k_5	k_6	k_7	k_8	k_9	k_{10}
VCB	600 V	-0.04287	1.035	-0.083	0	0	-4.783E-09	1.962E-06	-0.000229	0.003141
	2 700 V	0.0065	1.001	-0.024	-1.557E-12	4.556E-10	-4.186E-08	8.346E-07	5.482E-05	-0.003191
	14 300 V	0.005795	1.015	-0.011	-1.557E-12	4.556E-10	-4.186E-08	8.346E-07	5.482E-05	-0.003191
VCBB	600 V	-0.017432	0.98	-0.05	0	0	-5.767E-09	2.524E-06	-0.00034	0.01187
	2 700 V	0.002823	0.995	-0.0125	0	-9.204E-11	2.901E-08	-3.262E-06	0.0001569	-0.004003
	14 300 V	0.014827	1.01	-0.01	0	-9.204E-11	2.901E-08	-3.262E-06	0.0001569	-0.004003
HCB	600 V	0.054922	0.988	-0.11	0	0	-5.382E-09	2.316E-06	-0.000302	0.0091
	2 700 V	0.001011	1.003	-0.0249	0	0	4.859E-10	-1.814E-07	-9.128E-06	-0.0007
	14 300 V	0.008693	0.999	-0.02	0	-5.043E-11	2.233E-08	-3.046E-06	0.000116	-0.001145
VOA	600 V	0.043785	1.04	-0.18	0	0	-4.783E-09	1.962E-06	-0.000229	0.003141
	2 700 V	-0.02395	1.006	-0.0188	-1.557E-12	4.556E-10	-4.186E-08	8.346E-07	5.482E-05	-0.003191
	14 300 V	0.005371	1.0102	-0.029	-1.557E-12	4.556E-10	-4.186E-08	8.346E-07	5.482E-05	-0.003191
HOA	600 V	0.111147	1.008	-0.24	0	0	-3.895E-09	1.641E-06	-0.000197	0.002615
	2 700 V	0.000435	1.006	-0.038	0	0	7.859E-10	-1.914E-07	-9.128E-06	-0.0007
	14 300 V	0.000604	0.999	-0.02	0	0	7.859E-10	-1.914E-07	-9.128E-06	-0.0007

4.5 Arcing current variation correction factor

Calculate a second set of arc duration, using the reduced arcing current $I_{\text{arc_min}}$ to determine if the arcing current variation has an effect on the operating time of protective devices and consequently incident energy. The arcing current variation applies for all system open-circuit voltages within the valid range of the model (208 V to 15 000 V), but it is expected to have the most impact between 208 V and 600 V.

To determine a lower bound of the average rms arcing current, use [Equation \(2\)](#) as follows and the coefficients provided in [Table 2](#):

$$I_{\text{arc_min}} = I_{\text{arc}} \times (1 - 0.5 \times VarC_f) \quad (2)$$

$$VarC_f = k1V_{\text{oc}}^6 + k2V_{\text{oc}}^5 + k3V_{\text{oc}}^4 + k4V_{\text{oc}}^3 + k5V_{\text{oc}}^2 + k6V_{\text{oc}} + k7$$

where

- $VarC_f$ is the arcing current variation correction factor
- I_{arc} is the final or intermediate rms arcing current(s) (kA) (see note)
- $I_{\text{arc_min}}$ is a second rms arcing current reduced based on the variation correction factor (kA)
- V_{oc} is the open-circuit voltage between 0.208 kV and 15.0 kV
- $k1$ to $k7$ are the coefficients provided in [Table 2](#)

Table 2—Coefficients for Equation (2)

E.C.	<i>k1</i>	<i>k2</i>	<i>k3</i>	<i>k4</i>	<i>k5</i>	<i>k6</i>	<i>k7</i>
VCB	0	-0.0000014269	0.000083137	-0.0019382	0.022366	-0.12645	0.30226
VCBB	1.138e-06	-6.0287e-05	0.0012758	-0.013778	0.080217	-0.24066	0.33524
HCB	0	-3.097e-06	0.00016405	-0.0033609	0.033308	-0.16182	0.34627
VOA	9.5606E-07	-5.1543E-05	0.0011161	-0.01242	0.075125	-0.23584	0.33696
HOA	0	-3.1555e-06	0.0001682	-0.0034607	0.034124	-0.1599	0.34629

NOTE—The correction factor $(1 - (0.5 \times VarC_f))$ is applied as follows:

- $208 \text{ V} \leq V_{\text{oc}} \leq 600 \text{ V}$: To I_{arc} (final current only)
- $600 \text{ V} < V_{\text{oc}} \leq 15 000 \text{ V}$: To $I_{\text{arc_600}}$, $I_{\text{arc_2700}}$, and $I_{\text{arc_14300}}$ (intermediate average arcing currents). The final I_{arc} value inherits the correction factor.

The “0.5” coefficient indicates that variation is applied to the average arcing current to obtain a lower-bound value arcing current.

4.6 Intermediate incident energy (E)

Use [Equation \(3\)](#) to [Equation \(6\)](#) as follows and [Table 3](#), [Table 4](#), and [Table 5](#) to determine the intermediate incident energy values:

$$E_{600} = \frac{12.552}{50} T \times 10^{\left(k_1 + k_2 \lg G + \frac{k_3 I_{\text{arc_600}}}{k_4 I_{\text{bf}}^7 + k_5 I_{\text{bf}}^6 + k_6 I_{\text{bf}}^5 + k_7 I_{\text{bf}}^4 + k_8 I_{\text{bf}}^3 + k_9 I_{\text{bf}}^2 + k_{10} I_{\text{bf}}} + k_{11} \lg I_{\text{bf}} + k_{12} \lg D + k_{13} \lg I_{\text{arc_600}} + \lg \frac{1}{CF} \right)} \quad (3)$$

$$E_{2700} = \frac{12.552}{50} T \times 10^{\left(k_1 + k_2 \lg G + \frac{k_3 I_{\text{arc_2700}}}{k_4 I_{\text{bf}}^7 + k_5 I_{\text{bf}}^6 + k_6 I_{\text{bf}}^5 + k_7 I_{\text{bf}}^4 + k_8 I_{\text{bf}}^3 + k_9 I_{\text{bf}}^2 + k_{10} I_{\text{bf}}} + k_{11} \lg I_{\text{bf}} + k_{12} \lg D + k_{13} \lg I_{\text{arc_2700}} + \lg \frac{1}{CF} \right)} \quad (4)$$

$$E_{14300} = \frac{12.552}{50} T \times 10^{\left(k_1 + k_2 \lg G + \frac{k_3 I_{\text{arc_14300}}}{k_4 I_{\text{bf}}^7 + k_5 I_{\text{bf}}^6 + k_6 I_{\text{bf}}^5 + k_7 I_{\text{bf}}^4 + k_8 I_{\text{bf}}^3 + k_9 I_{\text{bf}}^2 + k_{10} I_{\text{bf}}} + k_{11} \lg I_{\text{bf}} + k_{12} \lg D + k_{13} \lg I_{\text{arc_14300}} + \lg \frac{1}{CF} \right)} \quad (5)$$

$$E_{\leq 600} = \frac{12.552}{50} T \times 10^{\left(k_1 + k_2 \lg G + \frac{k_3 I_{\text{arc_600}}}{k_4 I_{\text{bf}}^7 + k_5 I_{\text{bf}}^6 + k_6 I_{\text{bf}}^5 + k_7 I_{\text{bf}}^4 + k_8 I_{\text{bf}}^3 + k_9 I_{\text{bf}}^2 + k_{10} I_{\text{bf}}} + k_{11} \lg I_{\text{bf}} + k_{12} \lg D + k_{13} \lg I_{\text{arc}} + \lg \frac{1}{CF} \right)} \quad (6)$$

where

- E_{600} is the incident energy at $V_{\text{oc}} = 600$ V (J/cm²)
- E_{2700} is the incident energy at $V_{\text{oc}} = 2700$ V (J/cm²)
- E_{14300} is the incident energy at $V_{\text{oc}} = 14\ 300$ V (J/cm²)
- $E_{\leq 600}$ is the incident energy for $V_{\text{oc}} \leq 600$ V (J/cm²)
- T is the arc duration (ms)
- G is the gap distance between conductors (electrodes) (mm)
- $I_{\text{arc_600}}$ is the rms arcing current for 600 V (kA)
- $I_{\text{arc_2700}}$ is the rms arcing current for 2700 V (kA)
- $I_{\text{arc_14300}}$ is the rms arcing current for 14 300 V (kA)
- I_{arc} is rms arcing current for $V_{\text{oc}} \leq 600$ V [obtained using [Equation \(25\)](#)] (kA)
- I_{bf} is bolted fault current for three-phase faults (symmetrical rms) (kA)
- D is the distance between electrodes and calorimeters (working distance) (mm)
- CF is correction factor for enclosure size ($CF = 1$ for VOA and HOA configurations)
- \lg is \log_{10}
- k_1 to k_{13} are the coefficients provided in [Table 3](#), [Table 4](#), and [Table 5](#). For [Equation \(3\)](#) use [Table 3](#), for [Equation \(4\)](#) use [Table 4](#), for [Equation \(5\)](#) use [Table 5](#), and for [Equation \(6\)](#) use [Table 3](#)

Table 3—Coefficients for Equation (3), Equation (6), Equation (7), and Equation (10)

600 V	<i>k</i> ₁	<i>k</i> ₂	<i>k</i> ₃	<i>k</i> ₄	<i>k</i> ₅	<i>k</i> ₆	<i>k</i> ₇	<i>k</i> ₈	<i>k</i> ₉	<i>k</i> ₁₀	<i>k</i> ₁₁	<i>k</i> ₁₂	<i>k</i> ₁₃
VCB	0.753364	0.566	1.752636	0	0	-4.783E-09	0.000001962	-0.000229	0.003141	1.092	0	-1.598	0.957
VCBB	3.068459	0.26	-0.098107	0	0	-5.767E-09	0.000002524	-0.00034	0.01187	1.013	-0.06	-1.809	1.19
HCB	4.073745	0.344	-0.370259	0	0	-5.382E-09	0.000002316	-0.000302	0.0091	0.9725	0	-2.03	1.036
VOA	0.679294	0.746	1.222636	0	0	-4.783E-09	0.000001962	-0.000229	0.003141	1.092	0	-1.598	0.997
HOA	3.470417	0.465	-0.261863	0	0	-3.895E-09	0.000001641	-0.000197	0.002615	1.1	0	-1.99	1.04

Table 4—Coefficients for Equation (4) and Equation (8)

2700 V	<i>k</i> ₁	<i>k</i> ₂	<i>k</i> ₃	<i>k</i> ₄	<i>k</i> ₅	<i>k</i> ₆	<i>k</i> ₇	<i>k</i> ₈	<i>k</i> ₉	<i>k</i> ₁₀	<i>k</i> ₁₁	<i>k</i> ₁₂	<i>k</i> ₁₃
VCB	2.40021	0.165	0.354202	-1.557E-1.2	4.556E-10	-4.186E-08	8.346E-07	5.482E-05	-0.003191	0.9729	0	-1.569	0.9778
VCBB	3.870592	0.185	-0.736618	0	-9.204E-11	2.901E-08	-3.262E-06	0.0001569	-0.004003	0.9825	0	-1.742	1.09
HCB	3.486391	0.177	-0.193101	0	0	4.859E-10	-1.814E-07	-9.128E-06	-0.0007	0.9881	0.027	-1.723	1.055
VOA	3.880724	0.105	-1.906033	-1.557E-12	4.556E-10	-4.186E-08	8.346E-07	5.482E-05	-0.003191	0.9729	0	-1.515	1.115
HOA	3.616266	0.149	-0.761561	0	0	7.859E-10	-1.914E-07	-9.128E-06	-0.0007	0.9981	0	-1.639	1.078

Table 5—Coefficients for Equation (5) and Equation (9)

14 300 V	<i>k</i> ₁	<i>k</i> ₂	<i>k</i> ₃	<i>k</i> ₄	<i>k</i> ₅	<i>k</i> ₆	<i>k</i> ₇	<i>k</i> ₈	<i>k</i> ₉	<i>k</i> ₁₀	<i>k</i> ₁₁	<i>k</i> ₁₂	<i>k</i> ₁₃
VCB	3.825917	0.11	-0.999749	-1.557E-12	4.556E-10	-4.186E-08	8.346E-07	5.482E-05	-0.003191	0.9729	0	-1.568	0.99
VCBB	3.644309	0.215	-0.585522	0	-9.204E-11	2.901E-08	-3.262E-06	0.0001569	-0.004003	0.9825	0	-1.677	1.06
HCB	3.044516	0.125	0.245106	0	-5.043E-11	2.233E-08	-3.046E-06	0.000116	-0.001145	0.9839	0	-1.655	1.084
VOA	3.405454	0.12	-0.93245	-1.557E-12	4.556E-10	-4.186E-08	8.346E-07	5.482E-05	-0.003191	0.9729	0	-1.534	0.979
HOA	2.04049	0.177	1.005092	0	0	7.859E-10	-1.914E-07	-9.128E-06	-0.0007	0.9981	-0.05	-1.633	1.151

4.7 Intermediate arc-flash boundary (*AFB*)

Use [Equation \(7\)](#) to [Equation \(10\)](#) as follows and [Table 3](#), [Table 4](#), and [Table 5](#) to determine the intermediate arc-flash boundary values:

$$AFB_{600} = 10^{\left(\frac{k_1 + k_2 \lg G + \frac{k_3 I_{\text{arc_600}}}{k_4 I_{\text{bf}}^7 + k_5 I_{\text{bf}}^6 + k_6 I_{\text{bf}}^5 + k_7 I_{\text{bf}}^4 + k_8 I_{\text{bf}}^3 + k_9 I_{\text{bf}}^2 + k_{10} I_{\text{bf}}} + k_{11} \lg I_{\text{bf}} + k_{13} \lg I_{\text{arc_600}} + \lg \left(\frac{1}{CF} \right) - \lg \left(\frac{20}{T} \right)}{-k_{12}} \right)} \quad (7)$$

$$AFB_{2700} = 10^{\left(\frac{k_1 + k_2 \lg G + \frac{k_3 I_{\text{arc_2700}}}{k_4 I_{\text{bf}}^7 + k_5 I_{\text{bf}}^6 + k_6 I_{\text{bf}}^5 + k_7 I_{\text{bf}}^4 + k_8 I_{\text{bf}}^3 + k_9 I_{\text{bf}}^2 + k_{10} I_{\text{bf}}} + k_{11} \lg I_{\text{bf}} + k_{13} \lg I_{\text{arc_2700}} + \lg \left(\frac{1}{CF} \right) - \lg \left(\frac{20}{T} \right)}{-k_{12}} \right)} \quad (8)$$

$$AFB_{14300} = 10^{\left(\frac{k_1 + k_2 \lg G + \frac{k_3 I_{\text{arc_14300}}}{k_4 I_{\text{bf}}^7 + k_5 I_{\text{bf}}^6 + k_6 I_{\text{bf}}^5 + k_7 I_{\text{bf}}^4 + k_8 I_{\text{bf}}^3 + k_9 I_{\text{bf}}^2 + k_{10} I_{\text{bf}}} + k_{11} \lg I_{\text{bf}} + k_{13} \lg I_{\text{arc_14300}} + \lg \left(\frac{1}{CF} \right) - \lg \left(\frac{20}{T} \right)}{-k_{12}} \right)} \quad (9)$$

$$AFB_{\leq 600} = 10^{\left(\frac{k_1 + k_2 \lg G + \frac{k_3 I_{\text{arc_600}}}{k_4 I_{\text{bf}}^7 + k_5 I_{\text{bf}}^6 + k_6 I_{\text{bf}}^5 + k_7 I_{\text{bf}}^4 + k_8 I_{\text{bf}}^3 + k_9 I_{\text{bf}}^2 + k_{10} I_{\text{bf}}} + k_{11} \lg I_{\text{bf}} + k_{13} \lg I_{\text{arc}} + \lg \left(\frac{1}{CF} \right) - \lg \left(\frac{20}{T} \right)}{-k_{12}} \right)} \quad (10)$$

where

- AFB_{600} is the arc-flash boundary for $V_{\text{oc}} = 600$ V (mm)
- AFB_{2700} is the arc-flash boundary for $V_{\text{oc}} = 2700$ V (mm)
- AFB_{14300} is the arc-flash boundary for $V_{\text{oc}} = 14\ 300$ V (mm)
- $AFB_{\leq 600}$ is the arc-flash boundary for $V_{\text{oc}} \leq 600$ V (mm)
- G is the gap between electrodes (mm)
- $I_{\text{arc_600}}$ is the rms arcing current for 600 V (kA)
- $I_{\text{arc_2700}}$ is the rms arcing current for 2700 V (kA)
- $I_{\text{arc_14300}}$ is the rms arcing current for 14 300 V (kA)
- I_{arc} is the rms arcing current for $V_{\text{oc}} \leq 600$ V [obtained using [Equation \(25\)](#)] (kA)
- I_{bf} is the bolted fault current for three-phase faults (symmetrical rms) (kA)
- CF is the correction factor for enclosure size ($CF = 1$ for VOA and HOA configurations)
- T is the arc duration (ms)
- \lg is \log_{10}
- k_1 to k_{13} are the coefficients provided in [Table 3](#), [Table 4](#), and [Table 5](#). For [Equation \(7\)](#) use [Table 3](#), for [Equation \(8\)](#) use [Table 4](#), for [Equation \(9\)](#) use [Table 5](#), and for [Equation \(10\)](#) use [Table 3](#)

4.8 Enclosure size correction factor

4.8.1 General

The VCB, VCBB, and HCB equations were normalized for a 508 mm × 508 mm × 508 mm (20 in × 20 in × 20 in) enclosure. This subclause provides instructions on how to adjust the incident energy for smaller and larger enclosures using the correction factor (*CF*) determined from [Equation \(14\)](#) and [Equation \(15\)](#). The method for adjusting the incident energy based on the enclosure size is as follows:

- A set of equivalent height and width values are determined based on the system voltage, electrode configuration, the enclosure height, and width. The depth is not considered unless the width and height are both less than 508 mm (20 in) and the system voltage is less than 600 V. The depth is used to classify the enclosure type as “Typical” or “Shallow” (see [4.8.2](#)).
- The enclosure type, equivalent height, and width are used to determine an equivalent enclosure size parameter, which determines the value of the enclosure size correction factor, *CF*.
- Enclosures with opening areas larger than 1244.6 mm × 1244.6 mm (49 in × 49 in) may be encountered in actual equipment. The correction factor for 1244.6 mm × 1244.6 mm (49 in × 49 in) can be used for such. If either the width or height (or both) exceed 1244.6 mm (49 in), treat them as 1244.6 mm (49 in) for this model application.

4.8.2 Determination of enclosure type—Typical or shallow

The enclosure is “Shallow” when the following conditions are met:

- a) The system voltage is less than 600 V ac.
- b) Both the height and width are less than 508 mm (20 in).
- c) The enclosure depth is less than or equal to 203.2 mm (8 in).

If any of these conditions are not met, the enclosure is considered “Typical.”

4.8.3 Determination of equivalent height and width

Once the enclosure type has been classified, the equivalent height and width need to be determined by comparing their values against specific ranges for each of the three electrode configuration. For certain ranges, the equivalent height and width are determined using [Equation \(11\)](#) and [Equation \(12\)](#) as follows:

$$\text{Width}_1 = \left(660.4 + (\text{Width} - 660.4) \times \left(\frac{V_{oc} + A}{B} \right) \right) \times 25.4^{-1} \quad (11)$$

$$\text{Height}_1 = \left(660.4 + (\text{Height} - 660.4) \times \left(\frac{V_{oc} + A}{B} \right) \right) \times 25.4^{-1} \quad (12)$$

where

- | | |
|-------------------|--|
| Height_1 | is the equivalent enclosure height |
| Width_1 | is the equivalent enclosure width |
| Width | is the actual enclosure width (mm) |
| Height | is the actual enclosure height (mm) |
| V_{oc} | is the open-circuit voltage (system voltage) (kV) |
| A | is a constant equal to 4 for VCB and 10 for VCBB and HCB |
| B | is a constant equal to 20 for VCB, 24 for VCBB, and 22 for HCB |

[Table 6](#) provides the guidelines to determine the equivalent enclosure height and width (Height_1 and Width_1) for different ranges of enclosure dimensions and electrode configurations.

Table 6—Guidelines to determine the equivalent height and width

E.C.	Range	<508 (mm)	≥508 and ≤660.4 (mm)	>660.4 and ≤1244.6 (mm)	>1244.6 (mm)
VCB	Width _l = 20 (if Typical) = 0.03937 × Width (if Shallow ^a)	= 0.03937 × Width	obtained from Equation (11) and actual Width	obtained from Equation (11) with Width = 1244.6 mm	
	Height _l = 20 (if Typical) or = 0.03937 × Height (if Shallow ^a)	= 0.03937 × Height	= 0.03937 × Height	= 49	
VCBB	Width _l = 20 (if Typical) or = 0.03937 × Width (if Shallow ^a)	= 0.03937 × Width	obtained from Equation (11) and actual Width	obtained from Equation (11) with Width = 1244.6 mm	
	Height _l = 20 (if Typical) or = 0.03937 × Height (if Shallow ^a)	= 0.03937 × Height	obtained from Equation (12) and actual Height	obtained from Equation (12) with Height = 1244.6 mm	
HCB	Width _l = 20 (if Typical) or = 0.03937 × Width (if Shallow ^a)	= 0.03937 × Width	obtained from Equation (11) and actual Width	obtained from Equation (11) with Width = 1244.6 mm	
	Height _l = 20 (if Typical) or = 0.03937 × Height (if Shallow ^a)	= 0.03937 × Height	obtained from Equation (12) and actual Height	obtained from Equation (12) with Height = 1244.6 mm	

^aShallow only if $V_{oc} < 600$ V ac and the enclosure depth ≤ 203.2 mm (8 in) otherwise the enclosure is “Typical.”

The equivalent enclosure size (*EES*) is determined using the equivalent width and height using [Equation \(13\)](#) as follows:

$$EES = \frac{\text{Height}_1 + \text{Width}_1}{2} \quad (13)$$

where

- Height_1 is the equivalent enclosure height
- Width_1 is the equivalent enclosure width
- EES is the equivalent enclosure size

4.8.4 Determination of enclosure size correction factor (*CF*)

The correction factor (*CF*) for a “Typical Enclosure” is obtained by using [Equation \(14\)](#) as follows:

$$CF = b1 \times EES^2 + b2 \times EES + b3 \quad (14)$$

Use [Equation \(15\)](#) for correction factor for a “Shallow Enclosure” as follows:

$$CF = \frac{1}{b1 \times EES^2 + b2 \times EES + b3} \quad (15)$$

where

- $b1$ to $b3$ are the coefficients for [Equation \(14\)](#) and [Equation \(15\)](#) provided in [Table 7](#)
- CF is the enclosure size correction factor used in [Equation \(3\)](#) through [Equation \(10\)](#)
- EES is the equivalent enclosure size used to find the correction factor determined using [Equation \(13\)](#). For typical box enclosures the minimum value of *EES* is 20

[Table 7](#) provides the coefficients $b1$ to $b3$ for both typical and shallow enclosure types.

Table 7—Coefficients for [Equation \(14\)](#) and [Equation \(15\)](#)

Box type	E.C.	<i>b1</i>	<i>b2</i>	<i>b3</i>
Typical	VCB	-0.000302	0.03441	0.4325
	VCBB	-0.0002976	0.032	0.479
	HCB	-0.0001923	0.01935	0.6899
Shallow	VCB	0.002222	-0.02556	0.6222
	VCBB	-0.002778	0.1194	-0.2778
	HCB	-0.0005556	0.03722	0.4778

4.9 Determination of I_{arc} , E , and AFB (600 V < V_{oc} ≤ 15 000 V)

To determine the final arcing current, incident energy, and arc-flash boundary at a specific voltage, first calculate the intermediate values for the three voltage levels of 600 V, 2700 V, and 14 300 V. Then use the interpolation [Equation \(16\)](#) to [Equation \(24\)](#) to determine the final estimated values as follows:

Arcing current (I_{arc})

$$I_{\text{arc}_1} = \frac{I_{\text{arc}_2700} - I_{\text{arc}_600}}{2.1} (V_{\text{oc}} - 2.7) + I_{\text{arc}_2700} \quad (16)$$

$$I_{\text{arc}_2} = \frac{I_{\text{arc}_14300} - I_{\text{arc}_2700}}{11.6} (V_{\text{oc}} - 14.3) + I_{\text{arc}_14300} \quad (17)$$

$$I_{\text{arc}_3} = \frac{I_{\text{arc}_1} (2.7 - V_{\text{oc}})}{2.1} + \frac{I_{\text{arc}_2} (V_{\text{oc}} - 0.6)}{2.1} \quad (18)$$

where

- I_{arc_1} is the first I_{arc} interpolation term between 600 V and 2700 V (kA)
- I_{arc_2} is the second I_{arc} interpolation term used when V_{oc} is greater than 2700 V (kA)
- I_{arc_3} is the third I_{arc} interpolation term used when V_{oc} is less than 2700 V (kA)
- V_{oc} is the open-circuit voltage (system voltage) (kV)

When $0.600 < V_{\text{oc}} \leq 2.7$, the final value of arcing current is given as follows:

$$I_{\text{arc}} = I_{\text{arc}_3}$$

When $V_{\text{oc}} > 2.7$, the final value of arcing current is given as follows:

$$I_{\text{arc}} = I_{\text{arc}_2}$$

The arc duration can be determined using I_{arc} . This time is used to determine the incident energy and arc-flash boundary.

Incident energy (E)

$$E_1 = \frac{E_{2700} - E_{600}}{2.1} (V_{\text{oc}} - 2.7) + E_{2700} \quad (19)$$

$$E_2 = \frac{E_{14300} - E_{2700}}{11.6} (V_{\text{oc}} - 14.3) + E_{14300} \quad (20)$$

$$E_3 = \frac{E_1 (2.7 - V_{\text{oc}})}{2.1} + \frac{E_2 (V_{\text{oc}} - 0.6)}{2.1} \quad (21)$$

where

- E_1 is the first E interpolation term between 600 V and 2700 V (J/cm²)
- E_2 is the second E interpolation term used when V_{oc} is greater than 2700 V (J/cm²)
- E_3 is the third E interpolation term used when V_{oc} is less than 2700 V (J/cm²)

Arc-flash boundary (*AFB*)

$$AFB_1 = \frac{AFB_{2700} - AFB_{600}}{2.1} (V_{oc} - 2.7) + AFB_{2700} \quad (22)$$

$$AFB_2 = \frac{AFB_{14300} - AFB_{2700}}{11.6} (V_{oc} - 14.3) + AFB_{14300} \quad (23)$$

$$AFB_3 = \frac{AFB_1(2.7 - V_{oc})}{2.1} + \frac{AFB_2(V_{oc} - 0.6)}{2.1} \quad (24)$$

where

AFB_1 is the first *AFB* interpolation term between 600 V and 2700 V (mm)

AFB_2 is the second *AFB* interpolation term used when V_{oc} is greater than 2700 V (mm)

AFB_3 is the third *AFB* interpolation term used when V_{oc} is less than 2700 V (mm)

When $600 < V_{oc} \leq 2.7$, the final values of incident energy and arc-flash boundary are given as follows:

$$E = E_3$$

$$AFB = AFB_3$$

When $V_{oc} > 2.7$, the final values of incident energy and arc-flash boundary are given as follows:

$$E = E_2$$

$$AFB = AFB_2$$

It is recommended to calculate a second set of arc duration, incident energy, and arc-flash boundary values based on the reduced arcing current I_{arc_min} to account for the arcing current variation effect on the operation of protective devices. The final incident energy or arc-flash boundary is the higher of the two calculated values.

The incident energy (cal/cm²) is obtained by dividing E by 4.184 (1 cal = 4.184 J). See [B.2](#).

4.10 Determination of I_{arc} , E , and AFB ($V_{\text{oc}} \leq 600$ V)

This subclause describes how to determine the final arcing current, incident energy, and arc-flash boundary for a specific open-circuit voltage, $208 \text{ V} \leq V_{\text{oc}} \leq 600 \text{ V}$. First, calculate the arcing current using [Equation \(25\)](#). Using the arcing current, estimate the arc duration and proceed to determine the incident energy and arc-flash boundary.

Arcing current (I_{arc})

The final arcing current can be determined using [Equation \(25\)](#).

$$I_{\text{arc}} = \frac{1}{\sqrt{\left[\frac{0.6}{V_{\text{oc}}}\right]^2 \times \left[\frac{1}{I_{\text{arc_600}}} - \left(\frac{0.6^2 - V_{\text{oc}}^2}{0.6^2 \times I_{\text{bf}}}\right)\right]}} \quad (25)$$

where

- V_{oc} is the open-circuit voltage (kV)
- I_{bf} is the bolted fault current for three-phase faults (symmetrical rms) (kA)
- I_{arc} is the final rms arcing current at the specified V_{oc} (kA)
- $I_{\text{arc_600}}$ is the rms arcing current at $V_{\text{oc}} = 600$ V found using [Equation \(1\)](#) (kA)

The arc duration can be determined using I_{arc} . This time is used to determine the incident energy and arc-flash boundary.

Incident energy (E)

The incident energy is given as follows:

$$E = E_{\leq 600}$$

where

- $E_{\leq 600}$ is the incident energy for $V_{\text{oc}} \leq 600$ V determined using [Equation \(6\)](#) solved using the arc current determined from [Equation \(1\)](#) and [Equation \(25\)](#) (J/cm²)
- E is the final incident energy at specified V_{oc} (J/cm²)

Arc-flash boundary (AFB)

The arc-flash boundary is given as follows:

$$AFB = AFB_{\leq 600}$$

where

- $AFB_{\leq 600}$ is arc-flash boundary for $V_{\text{oc}} \leq 600$ V determined using [Equation \(10\)](#) solved using the arc current determined from [Equation \(1\)](#) and [Equation \(25\)](#) (mm)
- AFB is the final arc-flash boundary at specified V_{oc} (mm)

Calculate a second set of arc duration, incident energy, and arc-flash boundary values based on the reduced arcing current $I_{\text{arc_min}}$ to account for the arcing current variation effect on the operation of protective devices. The final incident energy or arc-flash boundary is the higher of the two calculated values.

4.11 Single-phase systems

This model does not cover single-phase systems. Arc-flash incident energy testing for single-phase systems has not been researched with enough detail to determine a method for estimating the incident energy. Single-phase systems can be analyzed by using the single-phase bolted fault current to determine the single-phase arcing current (using the equations provided in 4.4 and 4.10). The voltage of the single-phase system (line-to-line, line-to-ground, center tap voltage, etc.) can be used to determine the arcing current. The arcing current can then be used to find the protective device opening time and incident energy by using the three-phase equations provided in this guide. The incident energy result is expected to be conservative.

4.12 DC systems

Arc-flash incident energy calculation for dc systems is not part of this model. However, publication references (Ammerman et al. [B1], Das [B16], [B17], Doan [B25], Klement [B62]) provide some guidance for incident energy calculation.

5. Applying the model

The purpose of this clause is to provide an overview of the analysis process required to apply the model. The steps described in this clause may be applied manually, but it may be more convenient to use available short-circuit and protective device coordination programs, which have embedded the steps necessary to apply the model.

[Clause 6](#) provides the following summary of considerations and steps necessary to apply the calculation model:

- An overview of system data collection requirements is provided in [6.2](#). Accurate data collection is an important part of the study process.
- Calculation of bolted fault current levels, considering system operating modes, is discussed in [6.3](#) and [6.4](#).
- Information on equipment-related parameters that are used in the model, such as equipment dimensions, electrode configuration, and working distance, are discussed in [6.5](#), [6.6](#), and [6.7](#).
- [Subclauses 6.8](#) and [6.9](#) discuss calculation of the arcing current and determination of the arcing duration to be used in the model.
- [Subclauses 6.10](#) and [6.11](#) address the calculation of the final incident energy and arc-flash boundary. The discussion of specific equipment types in [Annex C](#) may also be useful.

To illustrate the model application process, two detailed calculation examples are provided in [Annex D](#).

NOTE—[Subclause 4.3](#) covers the equation application procedure.

6. Analysis process

6.1 General overview

An arc-flash hazard analysis can be performed in association with or as a continuation of a short-circuit study and protective-device coordination study. A complete coordination study may not be required, but the protective device opening time in response to arcing currents must be applied during the analysis process. The process and methodology of calculating short-circuit currents and performing protective-device

coordination is covered in standards such as IEEE Std 551™ (*IEEE Violet Book*™),¹⁰ IEC 60909-0 [B51],¹¹ and IEEE Std 242™ (*IEEE Buff Book*™). The results of the short-circuit study enable calculation of the arcing fault currents at selected locations. Protective device time response to the arcing currents is used to evaluate the time required for the protective devices to interrupt during fault conditions.

Deliverables of the arc-flash hazard analysis calculation are the arc-flash boundary and the arc-flash incident energy at defined working distances from the arcing source at the selected locations in the electrical system. The results of the study document the incident energy analysis and may be used by workers as part of an overall electrical safety risk assessment.

6.2 Step 1: Collect the system and installation data

A significant effort in performing an arc-flash hazard study is the collection of electrical system data. Even for a facility with nominally up-to-date single-line diagrams, time-current curves, and short-circuit model on a computer, the data collection portion of the study may take about half of the effort. Even for new facilities, field verification of the single-line diagrams and protection settings is necessary to verify the integrity of documentation of the power system. Facility workers who are familiar with the electrical system and its safety-related work practices may be able to assist or perform this part of the study. Refer to IEEE Std 1584.1 for further information on system data required for an arc-flash hazard analysis.

While the data required for this study is similar to data collected for typical short-circuit and protective-device coordination studies, it goes further in that all low-voltage distribution and control equipment within the scope of the study up through its sources of supply must be included.

Collect information to perform incident energy calculations on electrical equipment that is likely to require examination, adjustment, servicing, or maintenance while energized. This could include equipment such as low- and medium-voltage switchgear, medium-voltage plug-in connectors, motor starters, motor control centers (MCCs), switchboards, switchracks, panelboards, separately-mounted switches and circuit breakers, ac and dc drives, power distribution units (PDUs), uninterruptible power supplies (UPS), transfer switches, industrial control panels, meter socket enclosures, etc.

The study process begins with a review of available single-line diagrams and electrical equipment site and layout arrangement with people who are familiar with the site. The diagrams should be updated to show the current system configuration.

Electrical system studies should have an up-to-date single-line diagram(s). The single-line diagrams include all alternate feeds.

Follow applicable industry standards for performing short-circuit studies. See [Clause 2](#) for examples of industry standards.

Obtain the available fault current and X/R ratio that represents the source. For transformers, generators, large motors, and switchgear, collect relevant nameplate data such as voltage/voltage ranges or tap settings, ampacity, kilowatt or kilovoltamperes, first cycle (momentary or close and latch) and/or interrupting current rating, impedance or transient/subtransient reactance data. Because information regarding box (enclosure) size and electrode configuration may be needed for more detailed calculations, it may be necessary to take measurements if possible or collect other data such as nameplate information or device catalog numbers that will allow for relevant equipment enclosure dimensions and configurations to be estimated.

Next, collect conductor and cable data along with its installation (routing and support method, in magnetic raceway-steel conduit or non-magnetic raceway-aluminum conduit, etc.) for all electrical circuits between the

¹⁰Information on references can be found in [Clause 2](#).

¹¹The numbers in brackets correspond to those of the bibliography in [Annex A](#).

power source and the distribution and control equipment that is part of the study. This information is needed for the calculation of impedances. See IEEE Std 551 for information on how to perform short-circuit calculations.

Data from instrument transformers (current transformers and voltage transformers) and protective-device data that is part of the study must be collected. The data should be collected from sources such as the nameplate and/or time-current curves. If nameplate data is not accessible, data may be available in specifications or in recent maintenance test reports. In any case, the user should verify data is still up to date by checking with the owner's representative and, if necessary, by checking in the field. In some cases, a field inspection is required to determine the types and ratings of fuses actually installed, as well as the settings of circuit breaker trip units and/or the settings of protective relays. Protective devices that have not been properly maintained may have increased fault clearing time, thereby increasing the incident energy.

Determine which protective device(s) will be used for calculations. The mode of operation, the equipment construction, and the arrangement and characteristics of protective devices (time-overcurrent or otherwise) in an assembly can impact the consideration of which device(s) is selected for calculating the duration of the arc. Engineering judgment by a qualified person with skills and knowledge of the electrical equipment is required for determination of the protective device selected for these calculations. See IEEE Std 1584.1 for further details on the protective device(s) to be considered in arc-flash hazard calculations.

6.3 Step 2: Determine the system modes of operation

An electrical installation may have several modes of operation. It is important to determine the available short-circuit current for the mode(s) of operation that provides both the maximum and minimum available short-circuit currents. See IEEE Std 1584.1 for further details.

A complex power system may have many modes of operation, such as the following:

- a) One or more utility feeders in service
- b) Utility interface substation secondary bus tie circuit breaker open or closed
- c) Unit substation with one or two primary feeders
- d) Unit substation with two transformers with secondary tie opened or closed
- e) MCC with one or two feeders, one or both energized
- f) Generators running in parallel with the utility supply or in standby
- g) Utility system normal switching configured for maximum possible fault megavolt amperes
- h) Utility system normal switching configured for minimum possible fault megavolt amperes
- i) Separately derived sources (generators) – maximum capacity on line
- j) Separately derived sources (generators) – minimum number on line
- k) Shutdown or startup situation with all motors in an off condition – reduced fault contribution

It is necessary to consider the actual modes of operation based on site operating plans, whether in maintenance, normal operation, or under special conditions. Run the incident energy calculations for all modes of operation in the power system to determine the highest incident energy and arc-flash boundary result for each arcing location.

6.4 Step 3: Determine the bolted fault currents

The arc-flash study should be based upon an up-to-date short-circuit study for the facility. The study should take into account both the system data and modes of operation. If an existing study is not available, it will

be necessary to perform one as part of the arc-flash study effort. See IEEE Std 551 and IEEE Std 1584.1 for further details.

Systems containing multiple sources of short-circuit current, such as generators, large motors, or more than one utility supply, can be more accurately modeled with a dynamic simulation method. Methods may include multiple calculations to account for decaying short-circuit current contributions from rotating equipment, and the effect on protective device opening times and resulting incident energy.

Available bolted fault currents should be determined at prospective fault locations based on established standards (see 6.1 for examples of applicable standards). Both larger and smaller available short-circuit currents can result in higher available arc-flash energies and should be considered. Higher fault currents may result in shorter trip times for overcurrent protective devices resulting in a lower incident energy. Higher fault currents without a decrease in the opening time of the overcurrent protective device result in a higher incident energy. Lower fault currents may result in a longer opening time for the overcurrent protective device, thereby increasing the incident energy. If in doubt about the actual fault current, it may be necessary to establish a possible range of fault current levels and calculate the overcurrent protective device tripping times and arc-flash incident energy levels over a range rather than for a specific set of conditions.

6.5 Step 4: Determine typical gap and enclosure size based upon system voltages and classes of equipment

For each piece of equipment that is part of the study, the system voltage and the class of equipment can be used to establish typical gaps between conductors (or bus gaps) as shown in Table 8. It may be difficult to measure the gaps or obtain them from the manufacturer. The gap values provided in Table 8 were derived based on the gaps used in the arc-flash tests. Actual gap measurements from the installed equipment may be used if available, but it may be difficult to establish a single value since the gaps may vary at different locations in the equipment. The typical gaps provided are based on the laboratory test setups and not on actual equipment testing, but they may approximate conductor gaps in actual equipment.

Table 8—Classes of equipment and typical bus gaps

Equipment class	Typical bus gaps (mm)	Enclosure Size (H × W × D)	
		SI units (metric)	Imperial units
15 kV switchgear	152	1143 mm × 762 mm × 762 mm	45 in × 30 in × 30 in
15 kV MCC	152	914.4 mm × 914.4 mm × 914.4 mm	36 in × 36 in × 36 in
5 kV switchgear	104	914.4 mm × 914.4 mm × 914.4 mm	36 in × 36 in × 36 in
5 kV switchgear	104	1143 mm × 762 mm × 762 mm	45 in × 30 in × 30 in
5 kV MCC	104	660.4 mm × 660.4 mm × 660.4 mm	26 in × 26 in × 26 in
Low-voltage switchgear	32	508 mm × 508 mm × 508 mm	20 in × 20 in × 20 in
Shallow low-voltage MCCs and panelboards	25	355.6 mm × 304.8 mm × ≤203.2 mm	14 in × 12 in × ≤8 in
Deep low-voltage MCCs and panelboards	25	355.6 mm × 304.8 mm × >203.2 mm	14 in × 12 in × >8 in
Cable junction box	13	355.6 mm × 304.8 mm × ≤203.2 mm or 355.6 mm × 304.8 mm × >203.2 mm	14 in × 12 in × ≤8 in or 14 in × 12 in × >8 in

Table 8 also provides information on the enclosure sizes used for each voltage class. This information provides the relation between voltage class, gaps, and enclosure sizes. The enclosure sizes were used to derive the enclosure size incident energy correction factor.

6.6 Step 5: Determine the equipment electrode configuration

As part of the calculation process, the equipment conductor and enclosure arrangement that most closely resembles the actual electrode configuration(s) need to be identified. Each type of equipment such as switchgear, panelboards, and motor control centers may contain conductors arranged in similar manner as the test setup electrode configurations presented in [Table 9](#). Locations within a piece of equipment may contain conductor arrangements similar to more than one electrode configuration. As an example, a panelboard may contain both VCB and VCBB electrode configurations. Other types of equipment such as switchgear, disconnect switches, and switchboards may have other electrode configurations such as HCB depending on the bus and conductor arrangement.

[Table 9](#) provides some examples of how equipment conductor arrangements could be classified based on their similarity to the electrode configurations. Depending on the task being performed, and also on the presence (or lack thereof) of removable components, a location can change its electrode configuration classification (e.g., medium-voltage metal-clad circuit-breaker enclosure without the circuit breaker inside the cubicle).

Additional guidance regarding the selection of VCB, VCCB, HCB, HOA, and VOA is available in [Annex C](#) and [G.2](#).

Table 9—Correlation between actual equipment and electrode configuration

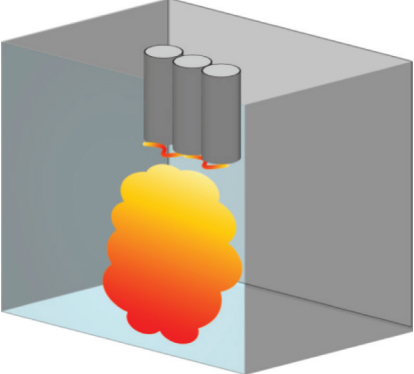
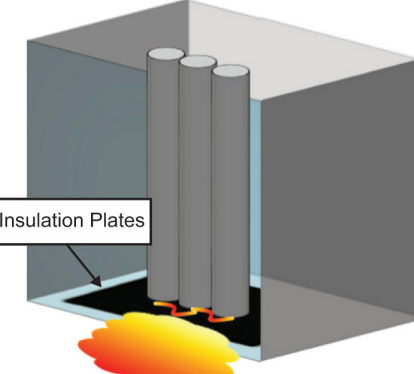
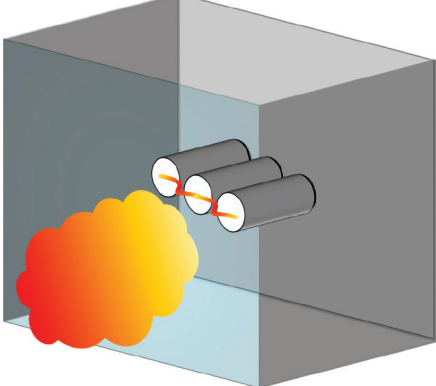
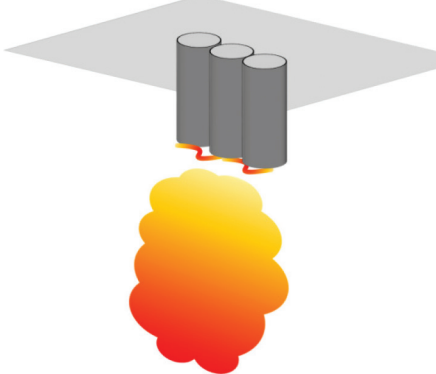
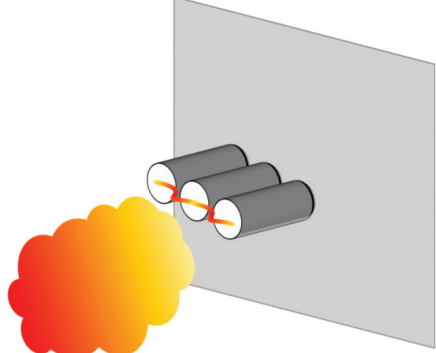
	Electrode configuration in test	Electrode configuration in equipment
VCB		
VCBB		

Table continues

Table 9—Correlation between actual equipment and electrode configuration (continued)

	Electrode configuration in test	Electrode configuration in equipment
HCB		
VOA		
HOA		

6.7 Step 6: Determine the working distances

Arc-flash protection is typically based on the incident energy level on the person's head and torso at the working distance and not the incident energy on the hands or arms. Typical working distances can be found in [Table 10](#) based on the class of equipment. The working distance is used in calculating the incident energy. Alternate working distances may be used depending on the task being performed.

Table 10—Classes of equipment and typical working distances

Equipment class	Working distance	
	mm	in
15 kV switchgear	914.4	36
15 kV MCC	914.4	36
5 kV switchgear	914.4	36
5 kV MCC	914.4	36
Low-voltage switchgear	609.6	24
Shallow low-voltage MCCs and panelboards	457.2	18
Deep low-voltage MCCs and panelboards	457.2	18
Cable junction box	457.2	18

6.8 Step 7: Calculation of arcing current

The arcing current depends primarily on the bolted fault current, as well as other factors such as the gap between conductors, electrode or conductor configuration, and system voltage. The available bolted fault current through each protective device is found from the short-circuit study by looking at contributions and impedance of each circuit. Short-circuit current contributions through each circuit connected to the fault location need to be classified as coming from energizing or non-energizing sources or from temporary sources of current such as induction motors. The total arcing current at a given location is calculated based upon the total bolted fault current available at that location. The arcing current distribution among multiple sources is assumed to be the same as the distribution of bolted fault current among the sources.

The arcing current can be calculated by using the equations shown in [Clause 4](#). The calculated arcing current (I_{arc}) is lower than the bolted fault current due to arc impedance. The total arcing current at the point of concern and the portion of that current passing through the upstream protective device(s) must be determined. The portion of the arcing current flowing through the overcurrent protective device determines the duration that is to be used in the incident energy calculation with the total bus arcing current. In the case of locations being energized by multiple feeders, it is necessary to determine the portion of the total arc current passing through each protective device to determine the clearing time for each device.

6.9 Step 8: Determine the arc duration

6.9.1 General

The arc duration is defined as the time it takes the upstream energizing source(s) of arcing current to stop providing current or energy to the arc fault. Typically, the clearing time of overcurrent protective devices depends on the magnitude and/or direction of the arc current passing through their current sensing equipment (current transformers, relays, etc.). When multiple sources are present, the arc duration depends on the time it takes the last protective device to clear the arc current. Under special circumstances, the arc duration is not totally dependent on protective device opening or trip time, but also on the time it takes the stored energy to

be discharged through the arc. Examples of this condition include, but are not limited to, faults near generator terminals on the line side of the generator circuit breaker.

The arc duration is most commonly dependent on the operating time of a time-overcurrent protective device. The operating time of ground-fault relays is not normally considered for the arc duration, as an arcing fault may or may not involve ground. Other types of protective devices with definite operating times such as differential relays, optical arc-flash light-detecting relays, pressure-sensing devices, etc., should be considered to determine their operating time. If protective device configurations are present that affect the operating time of the protective devices, such as zone-selective interlocking schemes, these also need to be considered. All sources of potential delay should be considered, including protective relay operating time, total clearing time of circuit breakers or operating time of contactors, delays introduced by intermediate devices such as lockout or auxiliary relays, delays related to processing times or communication networks, and other factors as appropriate.

For overcurrent protective devices in series, or at locations where more than one type of protective device could clear the arcing fault (e.g., time-overcurrent relay or differential relay), the operating times must be compared to determine which will operate first. During the field survey, up-to-date time-current curves of overcurrent protective devices may have been obtained or developed as part of a coordination study. If not, they should be created to assist in determining the duration of the arc. Commercially available software typically contains extensive overcurrent protective device libraries to aid in the data collection process. When a manufacturer's time-current curve shows a band, or range, the longest time for the calculated arcing current value should be used. These curves will be used to calculate the arc duration based on the average and minimum values of arcing current (I_{arc} and I_{arc_min}) as discussed in [Clause 4](#).

If the total protective device clearing time is longer than two seconds (2 s); consider how long a person is likely to remain in the location of the arc flash. It is likely that a person exposed to an arc flash will move away quickly if it is physically possible, and 2 s usually is a reasonable assumption for the arc duration to determine the incident energy. However, this also depends on the specific task. A worker in a bucket truck, or inside an equipment enclosure, could need more time to move away. Use engineering judgement when applying any maximum arc duration time for incident energy exposure calculations, because there may be circumstances where a person's egress may be blocked.

6.9.2 Fuses

For fuses, information from the manufacturer's time-current curves should be used. These curves may include both melting and total clearing time. If both are available, the total clearing time that represents the worst-case duration should be used. If the curve only consists of the average melt time, 10% of time plus an additional 0.004 s should be added to determine the total clearing time. If the total clearing time at the arcing fault current is less than 0.01 s, then 0.01 s may be used for the time. For current-limiting fuses, if the arcing current is greater than the current-limiting threshold [obtained from the peak let-through (peak let-thru) curves], then use the manufacturer's recommendation on the total clearing time and effective arc current.

A simplified model for some classes of fuses at 600 V and in a VCB configuration is presented in [Annex H](#). Other electrode configurations besides VCB are not considered in [Annex H](#). See [Annex H](#) for a list of the fuse classes, the ratings tested, and the limitations of the application of these models. The manufacturer should be consulted to confirm the appropriateness of these equations.

6.9.3 Low-voltage circuit breakers

For low-voltage circuit breakers with integral trip units, the manufacturer's time-current curves include both the device tripping time and clearing time in most cases. Note that some low-voltage power circuit breakers may be equipped with retrofit trip units. The time-current curves included with the replacement trip unit may, or may not, include the circuit breaker operating time. If the curves show only the trip unit's operating time, a circuit breaker operating time (typically 0.05 s or three cycles) should be added.

A calculation of arc energy with circuit breakers is more accurate when information from the manufacturer's time-current curves is used. However, when they are not available, a conservative method to determine the incident energy based on circuit breakers has been included in [Annex I](#). This method is based on calculated incident energy levels for the VCB configuration only and may be used only if the arc current is in the instantaneous or magnetic trip range.

For current-limiting circuit breakers, if the arcing current is greater than the current-limiting threshold (obtained from the peak let-through curves), then use the manufacturer's recommendation on the total clearing time and effective arc current.

6.9.4 Overcurrent relays and circuit breakers

The manufacturer(s) of the protective relay(s) and circuit breaker(s) should be consulted for detailed information regarding the operating characteristics and time-current curves. For protection schemes using overcurrent protective relays and circuit breakers, the relay time-current curves illustrate the relay operating time. The circuit breaker interrupting time is added to the relay operating time plus any additional time delays such as for lockout-relays, manufacturer's tolerance, and other additional time delay considerations. Circuit-breaker interrupting times can be verified by consulting the manufacturer's literature or the circuit-breaker nameplate data. Interrupting time is the sum of the circuit-breaker opening time and arcing time. See IEEE Std C37.010-2016 and IEEE Std 551-2006 for additional information.

6.10 Step 9: Calculate the incident energy

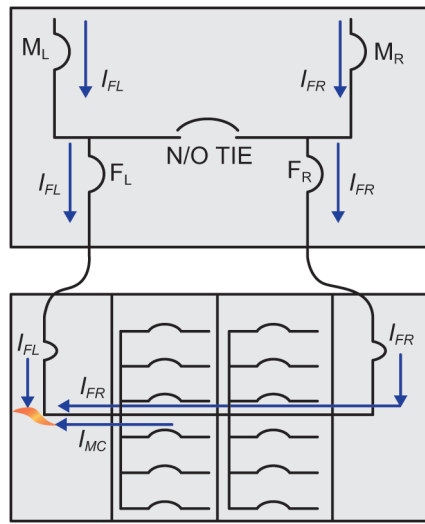
To calculate the incident energy at a specific piece of equipment, the equations in [Clause 4](#) are used. It is important to note that multiple arcing locations can be found within a single piece of equipment as outlined in [6.6](#) and [Annex C](#) and [Annex G](#). Incident energy calculations should be performed at each of the arcing locations that are defined to determine the highest magnitude incident energy or "worst-case" condition.

When a model of the power system is developed, the equipment compartmentalization and fault location need to be considered. The arc fault could occur on the line side, bus side, and load side of protective devices located in different compartments. Refer to IEEE Std 1584.1 for more details on fault location considerations. When evaluating the incident energy at an arcing fault location in the system, the interrupting time of the protective device upstream from the point of the fault must be considered. An integral "main" overcurrent protective device may be considered in the calculation if it is adequately isolated from the bus to prevent escalation to a line-side fault. When the integral main overcurrent protective device is not adequately isolated from the bus, the upstream protective device must be considered as protecting the main and bus.

Systems with motor contribution may require additional considerations for the incident energy calculations. Upstream motor fault current that flows toward the arc-fault location through a feeder may impact the protective device operating time. Downstream motor load contributions also affect the total arcing current and incident energy at the faulted location and need to be accounted for. In other words, the arcing current contribution of motors needs to be considered for its impact on protective device operating time and its effect on the total arcing current and incident energy.

Similar considerations may be needed for systems with multiple sources. Arcing current flows from multiple sources cause protective devices on multiple sources to operate sequentially, causing variation in the arc current flows, arc duration, and incident energy..

[Figure 1](#) shows a dual-source MCC with local mains served from two separate substation feeders with normally open (N/O) tie circuit breaker. A similar concept is applicable for any electrical equipment with multiple sources such as switchgear and switchboards. For the fault on the left side of the MCC main bus, selectivity between the left main (ML) and the left feeder (FL), as well as selectivity between ML and the left MCC main, depends on the current from the left source (IFL). However, the arcing current at the fault consists of current from both main sources (IFL and IFR) and the local motor contribution (IMC).



Source: IEEE Std 1683-2014

Figure 1—Multi-source MCC with motor contribution

The incident energy calculation should consider the change in total arcing current at the fault location caused by the operation of each protective device. The arcing current through each protective device may change based on the removal of other sources of arcing current. The arc energy and incident energy are dependent on the remaining arcing current sources. The total incident energy is then based on the changes to the individual sources of arcing current and their respective durations. The effect of arcing current redistribution after a source of arcing current is removed may also need to be considered. It is possible that the magnitude of the arcing current flowing through a path may change once the impedance of the system changes with each protective device operation. However, the operation and sequence of events presented in this subclause is only an assumption because it is possible that the arc may self-extinguish before the last protective device operation or that it travels to other locations away from its source and develops a different physical behavior.

For each fault current case under consideration, calculate the second incident energy using the minimum arc current and the appropriate arc duration based on the arcing current variation correction factor of 4.5. Choose the higher of the two incident energy values as the calculated incident energy.

6.11 Step 10: Determine the arc-flash boundary for all equipment

To calculate the arc-flash boundary for a given piece of equipment and location, the equations in Clause 4 are used. The arc-flash boundary is the distance from a prospective arc flash where the incident energy is 5.0 J/cm^2 (1.2 cal/cm^2).

6.12 Cautions and disclaimers

As an IEEE guide, this document suggests approaches for conducting an arc-flash hazard analysis but does not contain any mandatory requirements that preclude alternate methods. Following the suggestions in this guide does not guarantee safety, and users should take all reasonable, independent steps necessary to reduce risks from arc-flash events.

Users should be aware that the models in this guide are based upon measured arc-flash incident energy under a specific set of test conditions and on theoretical work. Distances, which are the basis for equations, are based on the measured distance of the test instrument from the arc-flash point source. These models enable users to

calculate the estimated incident energy levels and arc-flash boundary distances. Actual arc-flash exposures may have more or less incident energy than indicated by these models.

This document is intended to provide guidance for the calculation of incident energy and arc-flash boundaries. Once calculated, this information can be used as a basis to develop electrical safety strategies to reduce arc-flash energy exposure.

This information is offered as a tool for conducting an arc-flash hazard analysis. It is intended for use only by qualified persons who are knowledgeable about power system studies, power distribution equipment, and equipment installation practices. It is not intended as a substitute for the engineering judgment and adequate review necessary for such studies.

This guide is based upon testing and analysis of the thermal burn hazard presented by incident energy. Due to the explosive nature of arc-flash incidents, injuries can occur from ensuing molten metal splatters, projectiles, pressure waves, toxic arc by-products, the bright light of the arc, and the loud noise produced. These other effects are not considered in this guide.

This guide is subject to revision as additional knowledge and experience is gained. IEEE, those companies that contributed test data, and those people who worked on the development of this standard make no guarantee of results and assume no obligation or liability whatsoever in connection with this information.

The methodology in this guide assumes that all equipment is installed, operated, and maintained as required by applicable codes, standards, and manufacturers' instructions, and applied in accordance with its ratings. Equipment that is improperly installed or maintained may not operate correctly, possibly increasing the arc-flash incident energy or creating other hazards.

7. Background on the arc-flash hazard

7.1 Early papers

7.1.1 “Arcing fault protection for low-voltage power distribution systems—Nature of the problem” [B59]

This paper identified the potential for personal injury from arcing faults caused by such things as tools contacting bare buses, rodents, dust, insulation failure, or loose connections. The focus was on the nature of arcing faults and the protective equipment and relaying schemes that could be used to extinguish the arc.

7.1.2 “Predicting damage from 277 V single phase to ground arcing faults” [B86]

This paper proposed a method of approximating the degree of burning damage to metal that could be expected from various arcing current values and considerations for coordinating the time and current settings of ground fault protection devices with phase overcurrent protection equipment.

7.1.3 “The other electrical hazard: Electrical arc blast burns” [B67]

The electrical arc-flash hazard was highlighted. The paper described the electrical arc blast as the other electrical hazard. The thermal hazard was described as second-degree burns up to 3.05 m (10 ft) from the arc and third-degree burns up to 1.525 m (5 ft). It also presented theoretical methods of evaluating the open-air arc hazard and gave information on protective measures that should be taken to help avoid or reduce the risk of serious injury.

7.1.4 “The escalating arcing ground-fault phenomenon” [B35]

The possible consequences of arcing ground faults were described in this paper. The phenomena of how low-voltage arcing phase-to-ground faults migrate to three-phase arcs were presented. The observation that the

maximum arcing three-phase fault current is considerably less than the three-phase bolted fault value in 480 V equipment was discussed. The conditions where arcing becomes self-sustaining were described.

7.1.5 “Predicting incident energy to better manage the electric arc hazard on 600 V power distribution systems” [B29]

A method of estimating incident energy on a 600 V, three-phase power distribution system is presented. The effect on incident energy of the arc in a cubic box was considered in developing equations to estimate available bolted fault currents and incident energy at various distances. Benefits of using an estimate of the incident energy in the management of the electrical arc hazard were discussed.

7.1.6 “Report on enclosure internal arcing tests” [B48]

This paper focuses on high-energy arcing faults in enclosures with the compartment door closed. It reports the results of tests in 600 V class MCCs. The need for equipment testing standards in the low-voltage class is identified. Users should identify and provide PPE to personnel working near equipment that cannot contain nor safely vent the arcing hazard.

7.1.7 “Arc and flash burn hazards at various levels of an electrical system” [B55]

This paper presents information from a survey of petrochemical facilities on the PPE used for electrical arc-flash protection. It focuses on the effect of high-energy electrical arcs on humans and presents calculations of distances for curable burn injury at typical industrial/large commercial electrical installations.

7.1.8 “Impact of arc-flash events with outward convective flows on worker protection strategies” [B65]

This paper presents information on additional arc-flash test configurations that increase the convective energy flows outward toward worker. The impact on incident energy predictions is discussed. Further research and modeling method improvements are recommended.

7.2 Additional references

Many other papers have been published on the calculations of arc-flash energy and mitigating the arc-flash hazard, through inherently safer technologies, equipment design improvements, and work practices that reduce the exposure of workers. Reference papers are listed in the bibliography (Annex A). See [B7], [B13], [B14], [B15], [B18], [B20], [B21], [B24], [B28], [B29], [B31] through [B34], [B36] through [B40], [B44], [B46], [B47], [B48], [B50], [B52], [B54], [B55], [B57] through [B66], [B69], [B70], [B73], [B74], [B76] through [B91], [B96], and [B99].

Annex A

(informative)

Bibliography

Bibliographical references are resources that provide additional or helpful material but do not need to be understood or used to implement this standard. Reference to these resources is made for informational use only. The conclusions or recommendations reached in these references have not been validated by testing or endorsed by IEEE 1584.

Additional papers on this subject may be found by searching the IEEE Xplore at <http://ieeexplore.ieee.org/>.

- [B1] Accredited Standards Committee C2-2017, National Electrical Safety Code® (NESC®).¹²
- [B2] Ammerman, R. F., T. Gammon, P. K. Sen, and J. P. Nelson, “DC-Arc Models and Incident-Energy Calculations,” *IEEE Transactions on Industry Applications*, vol. 46, no. 5, pp. 1810–1819, September/October 2010.¹³
- [B3] ASTM F1506-01, Standard Performance Specification for Flame Resistant Textile Materials for Wearing Apparel for Use by Electrical Workers Exposed to Momentary Electric Arc and Related Thermal Hazards.¹⁴
- [B4] ASTM F1959/F1959M-99, Standard Test Method for Determining the Arc Thermal Performance Value of Materials for Clothing.
- [B5] Balasubramanian, I. and A. M. Graham, “Impact of Available Fault Current Variations on Arc-Flash Calculations,” *IEEE Transactions on Industry Applications*, vol. 46, no. 5, pp. 1836–1842, September/October 2010.
- [B6] Baldwin, T. L., M. J. Hittel, L. F. Saunders, and F. Renovich Jr., “Using a Microprocessor-Based Instrument to Predict the Incident Energy from Arc-Flash Hazards,” *IEEE Transactions on Industry Applications*, vol. 40, no. 3, pp. 877–886, May/June 2004.
- [B7] “Blast injury,” *Wikipedia*, last modified October 3, 2008, http://en.wikipedia.org/wiki/Blast_injury.
- [B8] Bowen, J. E., M. W. Wactor, G. H. Miller, and M. Capelli-Schellpfeffer, “Catch the Wave: Modeling of the Pressure Wave Associated with Arc Fault,” *IEEE Industry Applications Magazine*, vol. 10, no. 4, pp. 59–67, July/August 2004.
- [B9] Brown, W. A. and R. Shapiro, “Incident Energy Reduction Techniques: A Comparison Using Low-Voltage Power Circuit Breakers,” *IEEE Industry Applications Magazine*, vol. 15, no. 3, pp. 53–61, May/June 2009.
- [B10] Buff, J. and K. Zimmerman, “Reducing Arc-Flash Hazards,” *IEEE Industry Applications Magazine*, vol. 14, no. 3, pp. 40–47, May/June 2008.
- [B11] Bugaris, R. M. and D. T. Rollay, “Arc-Resistant Equipment,” *IEEE Industry Applications Magazine*, vol. 17, no. 4, pp. 62–70, July/August 2011.

¹²The NESC is available from the Institute of Electrical and Electronics Engineers (<http://standards.ieee.org/>).

¹³IEEE publications are available from the Institute of Electrical and Electronics Engineers (<https://ieeexplore.ieee.org/>).

¹⁴ASTM publications are available from the American Society for Testing and Materials (<http://www.astm.org/>).

- [B12] Cawley, J. C. and B. C. Brenner, “Analyzing On-the-Job Electrical Injuries: A Survey of Selected U.S. Occupational Electrical Injuries from 2003 to 2009,” *IEEE Industry Applications Magazine*, vol. 19, no. 3, pp. 16–20, May/June 2013.
- [B13] Cawley, J. C. and G. T. Homce, “Trends in Electrical Injury in the U.S., 1992–2002,” *IEEE Transactions on Industry Applications*, vol. 44, no. 4, pp. 962–972, July/August 2008.
- [B14] Code of Federal Regulations 29, Subpart R, Part 1910.269, USA Department of Labor Occupational Health and Safety Administration (OSHA) regulations: Electric Power Generation, Transmission, and Distribution, and Subpart S, Part 1910.301 through 1910.399, Occupational Safety and Health Standards—Electrical.
- [B15] Crmko, T. and S. Dyrnes, “Arcing Fault Hazards and Safety Suggestions for Design and Maintenance,” *IEEE Industry Applications Magazine*, vol. 7, no. 3, pp. 23–32, May/June 2001.
- [B16] Das, J. C., “Arc-Flash Hazard Calculations in LV and MV DC Systems—Part I: Short-Circuit Calculations,” *IEEE Transactions on Industry Applications*, vol. 50, no. 3, pp. 1687–1697, May/June 2014.
- [B17] Das, J. C., “Arc-Flash Hazard Calculations in LV and MV DC Systems Part—II: Analysis,” *IEEE Transactions on Industry Applications*, vol. 50, no. 3, pp. 1698–1705, May/June 2014.
- [B18] Das, J. C., “Design Aspects of Industrial Distribution Systems to Limit Arc Flash Hazard,” *IEEE Transactions on Industry Applications*, vol. 41, no. 6, pp. 1467–1475, November/December 2005.
- [B19] Das, J. C., “Protection Planning and System Design to Reduce Arc Flash Incident Energy in a Multi-Voltage-Level Distribution System to 8 cal/cm² (HRC 2) or Less—Part I: Methodology,” *IEEE Transactions on Industry Applications*, vol. 47, no. 1, pp. 398–407, January/February 2011.
- [B20] Das, J. C., “Protection Planning and System Design to Reduce Arc-Flash Incident Energy in a Multi-Voltage-Level Distribution System to 8 cal/cm² (HRC 2) or Less—Part II: Analysis,” *IEEE Transactions on Industry Applications*, vol. 47, no. 1, pp. 408–420, January/February 2011.
- [B21] Doan, D., G. D. Gregory, H. O. Kemp, B. McClung, V. Saporita, and C. M. Wellman, “How to Hamper Hazards: Development of the Guide for Performing Arc-Flash Hazard Calculations,” *IEEE Industry Applications Magazine*, vol. 11, no. 3, pp. 30–39, May/June 2005.
- [B22] Doan, D. R. and R. M. Derer, “Arc Flash Calculations for a 1.3-MW Photovoltaic System,” *IEEE Transactions on Industry Applications*, vol. 51, no. 1, pp. 62–68, January/February 2015.
- [B23] Doan, D. R. and T. E. Neal, “Field Analysis of Arc-Flash Incidents,” *IEEE Industry Applications Magazine*, vol. 16, no. 3, pp. 39–44, May/June 2010.
- [B24] Doan, D. R. and R. A. Sweigart, “A Summary of Arc-Flash Energy Calculations,” *IEEE Transactions on Industry Applications*, vol. 39, no. 4, pp. 1200–1204, July/August 2003.
- [B25] Doan, D. R., “Arc Flash Calculations for Exposures to DC Systems,” *IEEE Transactions on Industry Applications*, vol. 46, no. 6, pp. 2299–2302, November/December 2010.
- [B26] Doan, D. R., “Designing a Site Electrical System With Arc Flash Energy Under 20 cal/cm²,” *IEEE Transactions on Industry Applications*, vol. 45, no. 3, pp. 1180–1183, May/June 2009.
- [B27] Doan, D. R., H. L. Floyd, and T. E. Neal, “Comparison of Methods for Selecting Personal Protective Equipment for Arc Flash Hazards,” *IEEE Transactions on Industry Applications*, vol. 40, no. 4, pp. 963–969, July/August 2004.

- [B28] Doan, D. R., J. K. Slivka, and C. J. Bohrer, “A Summary of Arc Flash Hazard Assessments and Safety Improvements,” *IEEE Transactions on Industry Applications*, vol. 45, no. 4, pp. 1210–1216, July/August 2009.
- [B29] Doughty, R. L., T. E. Neal, and H. L. Floyd, “Predicting Incident Energy to Better Manage the Electric Arc Hazard on 600-V Power Distribution Systems,” *IEEE Transactions on Industry Applications*, vol. 36, no. 1, pp. 257–269, January/February 2000.
- [B30] Doughty, R. L., T. E. Neal, T. A. Dear, and A. H. Bingham, “Testing Update on Protective Clothing and Equipment for Electric Arc Exposure,” *IEEE Industry Applications Magazine*, vol. 5, no. 1, pp. 37–49, January/February 1999.
- [B31] Doughty, R. L., T. E. Neal, G. M. Laverty, and H. Hoagland, “Minimizing Burn Injury: Electric-Arc Hazard Assessment And Personnel Protection,” *IEEE Industry Applications Magazine*, vol. 8, no. 3, pp. 18–25, May/June 2002.
- [B32] Doughty, R. L., T. E. Neal, T. Macalady, V. Saporita, and K. Borgwald, “The Use of Low-Voltage Current-Limiting Fuses to Reduce Arc-Flash Energy,” *IEEE Transactions on Industry Applications*, vol. 36, no. 6, pp. 1741–1749, November/December 2000.
- [B33] Dugan, T. R., “Reducing the flash hazard,” *IEEE Industry Applications Magazine*, vol. 13, no. 3, pp. 51–58, May/June 2007.
- [B34] Dunki-Jacobs, J. R., “The Effects of Arcing Ground Faults on Low-Voltage System Design,” *IEEE Transactions on Industry Applications*, vol. IA-8, no. 3, pp. 223–230, May/June 1972.
- [B35] Dunki-Jacobs, J. R., “The Escalating Arcing Ground-Fault Phenomenon,” *IEEE Transactions on Industry Applications*, vol. IA-22, no. 6, pp. 1156–1161, November/December 1986.
- [B36] Eblen, M. L. and T. A. Short, “Arc-Flash Testing of Typical 480-V Utility Equipment,” *IEEE Transactions on Industry Applications*, vol. 48, no. 2, pp. 581–592, March/April 2012.
- [B37] “Explosions and Blast Injuries: A Primer for Clinicians,” Center for Disease Control, accessed May 9, 2003.¹⁵
- [B38] Floyd, H. L., “Escaping Arc Danger,” *IEEE Industry Applications Magazine*, vol. 14, no. 3, pp. 25–31, May/June 2008.
- [B39] Fox, F. K. and L. B. McClung, “Ground Fault Tests on High-Resistance Grounded 13.8 kV Electrical Distribution System of Modern Large Chemical Plant—I,” *IEEE Transactions on Industry Applications*, vol. IA-10, no. 5, pp. 581–600, September/October 1974.
- [B40] Gammon, T. and J. Matthews, “Conventional and Recommended Arc Power and Energy Calculations and Arc Damage Assessment,” *IEEE Transactions on Industry Applications*, vol. 39, no. 3, pp. 594–599, May/June 2003.
- [B41] Gammon, T. and J. Matthews, “IEEE 1584–2002 Arc Modeling Debate,” *IEEE Industry Applications Magazine*, vol. 14, no. 4, pp. 61–69, July/August 2008.
- [B42] Gammon, T. and J. Matthews, “Instantaneous Arcing-Fault Models Developed for Building System Analysis,” *IEEE Transactions on Industry Applications*, vol. 37, no. 1, pp. 197–203, January/February 2001.

¹⁵Available at <https://www.cdc.gov/masstrama/preparedness/primer.pdf>.

- [B43] Gammon, T. L. and J. H. Matthews, "IEEE 1584–2002: Incident energy factors and simple 480-V incident energy equations," *IEEE Industry Applications Magazine*, vol. 11, no. 1, pp. 23–31, January/February 2005.
- [B44] Golovkov, M., E. Hoagland, H. Schau, and C. Maurice, "Effect of Arc Electrode Geometry and Distance on Cotton Shirt Ignition," *IEEE Transactions on Industry Applications*, vol. 51, no. 1, pp. 36–44, January/February 2015.
- [B45] Graham, A. M., M. Hodder, and G. Gates, "Current Methods for Conducting an Arc-Flash Hazard Analysis," *IEEE Transactions on Industry Applications*, vol. 44, no. 6, pp. 1902–1909, November/December 2008.
- [B46] Gregory, G. and K. J. Lippert, "Applying Low-Voltage Circuit Breakers to Limit Arc-Flash Energy," *IEEE Transactions on Industry Applications*, vol. 48, no. 4, pp. 1225–1229, July/August 2012.
- [B47] Gregory, G. D., I. Lytle, and C. M. Wellman, "Arc Flash Calculations in Systems Protected by Low-Voltage Circuit Breakers," *IEEE Transactions on Industry Applications*, vol. 39, no. 4, pp. 1193–1199, July/August 2003.
- [B48] Heberlein, G. E. Jr., J. A. Higgins, and R. A. Epperly, "Report on Enclosure Internal Arcing Tests," *IEEE Industry Applications Magazine*, vol. 2, no. 3, pp. 35–42, May/June 1996.
- [B49] Hill, D. J., L. W. Bruehler, and P. E. Chmura, "Limiting Arc-Flash Exposure," *IEEE Industry Applications Magazine*, vol. 12, no. 3, pp. 10–21, May/June 2006.
- [B50] Hodder, M., W. Vilchek, F. Croyle, and D. McCue, "Practical Arc-Flash Reduction," *IEEE Industry Applications Magazine*, vol. 12, no. 3, pp. 22–29, May/June 2006.
- [B51] IEC 60909-0, Short-circuit currents in three-phase a.c. systems – Part 0: Calculation of currents.¹⁶
- [B52] IEEE 100, *The Authoritative Dictionary of IEEE Standards Terms*, Seventh Edition, December 1, 2000.
- [B53] IEEE 1584-2002 "Test_results_database.xls" (electronic database containing processed test results)
- [B54] IEEE/ASTM SI 10TM, American National Standard for Metric Practice.¹⁷
- [B55] Jamil, S., R. A. Jones, and L. B. McClung, "Arc and Flash Burn Hazards at Various Levels of an Electrical System," *IEEE Transactions on Industry Applications*, vol. 33, no. 2, pp. 359–366, March/April 1997.
- [B56] Jones, R. A., D. P. Liggett, M. Capelli-Schellpfeffer, T. Macalady, L. F. Saunders, R. E. Downey, L. B. McClung, A. Smith, S. Jamil, and V. J. Saporita, "Staged Tests Increase Awareness of Arc-Flash Hazards in Electrical Equipment," *IEEE Transactions on Industry Applications*, vol. 36, no. 2, pp. 659–667, March/April 2000.
- [B57] Jones, R. A., D. P. Liggett, M. Capelli-Schellpfeffer, T. Macalady, L. F. Saunders, R. E. Downey, L. B. McClung, A. Smith, S. Jamil, and V. J. Saporita, Arc flash hazards in electrical equipment, video plus CD-ROM, prepared during laboratory testing in support of "Staged Tests Increase Awareness of Arc-Flash Hazards in Electrical Equipment," *IEEE Transactions on Industry Applications*, vol. 36, no. 2, pp. 659–667, March/April 2000.

¹⁶IEC publications are available from the International Electrotechnical Commission (<http://www.iec.ch>) and the American National Standards Institute (<http://www.ansi.org/>).

¹⁷The IEEE standards or products referred to in Annex A are trademarks owned by the Institute of Electrical and Electronics Engineers, Incorporated.

- [B58] Kalkstein, E. W., R. L. Doughty, A. E. Paullin, J. M. Jackson, and J. L. Ryner, "Safety Benefits of Arc-Resistant Metalclad Medium-Voltage Switchgear," *IEEE Transactions on Industry Applications*, vol. 31, no. 6, pp. 1402–1411, November/December 1995.
- [B59] Kaufmann, R. H. and J. C. Page, "Arcing Fault Protection for Low-Voltage Power Distribution Systems—Nature of the Problem," *Transactions of the American Institute of Electrical Engineers. Part III: Power Apparatus and Systems*, vol. 79, no. 3, pp. 160–165, April 1960.
- [B60] Kay, J. A., "Meeting the Standards: Testing and certification of medium-voltage control centers to arc-resistance standards," *IEEE Industry Applications Magazine*, vol. 13, no. 5, pp. 49–58, September/October 2007.
- [B61] Kay, J. A., P. B. Sullivan, and M. Wactor, "Arc-Resistant Motor Control Equipment," *IEEE Industry Applications Magazine*, vol. 16, no. 1, pp. 57–64, January/February 2010.
- [B62] Klement, K., "DC Arc Flash Studies for Solar Photovoltaic Systems: Challenges and Recommendations," *IEEE Transactions on Industry Applications*, vol. 51, no. 5, pp. 4239–4244, September/October 2015.
- [B63] Land, H. B., "The Behavior of Arcing Faults in Low-Voltage Switchboards," *IEEE Transactions on Industry Applications*, vol. 44, no. 2, pp. 437–444, March/April 2008.
- [B64] Lang, M. and K. Jones, "Investigation of Factors Affecting the Sustainability of Arcs Below 250 V," *IEEE Transactions on Industry Applications*, vol. 48, no. 2, pp. 784–793, March/April 2012.
- [B65] Lang, M., K. Jones, and T. Neal, "Impact of Arc Flash Events with Outward Convective Flows on Worker Protection Strategies," *IEEE Transactions on Industry Applications*, vol. 47, no. 4, pp. 1597–1604, July/August 2011.
- [B66] Lee, R. H., "Pressures Developed by Arcs," *IEEE Transactions on Industry Applications*, vol. IA-23, no. 4, pp. 760–763, July 1987.
- [B67] Lee, R. H., "The Other Electrical Hazard: Electrical Arc Blast Burns," *IEEE Transactions on Industry Applications*, vol. IA-18, no. 3, pp. 246–251, May 1982.
- [B68] Lee, W.-J., M. Sahni, K. Methaprayoon, C. Kwan, Z. Ren, and J. M. Sheeley, "A Novel Approach for Arcing Fault Detection for Medium-/Low-Voltage Switchgear," *IEEE Transactions on Industry Applications*, vol. 45, no. 4, pp. 1475–1483, July/August 2009.
- [B69] Lippert, K. J., D. M. Colaberardino, and C. W. Kimblin, "Understanding IEEE 1584 Arc Flash Calculations—A clarification of the use of the Arc Flash Calculator," *IEEE Industry Applications Magazine*, vol. 11, no. 3, pp. 69–75, May/June 2005.
- [B70] McClung, L. B. and B. W. Whittington, "Ground Fault Tests on High-Resistance Grounded 13.8 kV Electrical Distribution System of Modern Large Chemical Plant—II," *IEEE Transactions on Industry Applications*, vol. IA-10, no. 5, pp. 601–617, September 1974.
- [B71] Neal, T. E., A. H. Bingham, and R. L. Doughty, "Protective Clothing Guidelines for Electric Arc Exposure," *IEEE Transactions on Industry Applications*, vol. 33, no. 4, pp. 1041–1054, July/August 1997.
- [B72] Neal, T. E. and R. F. Parry, "Shrapnel, Pressure, And Noise—Specialized PPE testing for electric arc hazards beyond heat exposure," *IEEE Industry Applications Magazine*, vol. 11, no. 3, pp. 49–53, May/June 2005.

- [B73] Nelson, J. P., J. D. Billman, and J. E. Bowen, “The Effects of System Grounding, Bus Insulation, and Probability on Arc Flash Hazard Reduction—The Missing Links,” *IEEE Transactions on Industry Applications*, vol. 50, no. 5, pp. 3141–3152, July/August 2014.
- [B74] Nepveux, F., “In A Flash—Use of Instantaneous Trip Functions with Current-Limiting Fuses to Reduce Arc Flash Energy Without Losing Coordination,” *IEEE Industry Applications Magazine*, vol. 13, no. 5, pp. 68–72, September/October 2007.
- [B75] NFPA 70®, National Electrical Code® (NEC®).¹⁸
- [B76] NFPA 70E®, Standard for Electrical Safety in the Workplace®.
- [B77] NFPA/IEEE Research and Testing Planning Committee, Final Report, July 28, 2005.
- [B78] OSHA records with “electric arc” key term, released between March 2005 and September 2008.
- [B79] Papallo, T., “Arc Flash Calculations Using a Physics-Based Circuit Model,” *IEEE Transactions on Industry Applications*, vol. 48, no. 4, pp. 1230–1236, July/August 2012.
- [B80] Roop, D. W. and N. G. Vidonic, “Arcing Fault Protection on VEPCO’S 480Y/277 Volt Secondary Spot Networks,” *IEEE Transactions on Power Apparatus and Systems*, vol. PAS-102, no. 2, pp. 364–372, February 1983.
- [B81] Roscoe, G., T. Papallo, and M. Valdes, “Fast Energy Capture: Arc-flash energy mitigation methods,” *IEEE Industry Applications Magazine*, vol. 17, no. 4, pp. 43–52, July/August 2011.
- [B82] SFPE Engineering Guide to Predicting First and Second Degree Skin Burns, Society of Fire Protection Engineers Task Group on Engineering Practices.
- [B83] Shah, K. R., A. L. Cinsavich, and P. De Silva, “Impact of Arc Flash Hazards on Medium-Voltage Switchgear,” *IEEE Transactions on Industry Applications*, vol. 44, no. 6, pp. 1859–1863, November/December 2008.
- [B84] Shields, F. J., “The Problem of Arcing Faults in Low-Voltage Power Distribution Systems,” *IEEE Transactions on Industrial and General Applications*, vol. IGA-3, no. 1, pp. 15–25, January 1967.
- [B85] Short, T. A., “Arc-Flash Analysis Approaches for Medium-Voltage Distribution,” *IEEE Transactions on Industry Applications*, vol. 47, no. 4, pp. 1902–1909, July/August 2011.
- [B86] Sprem, N., S. Branica, and K. Dawidowsky, “Tympanoplasty After War Blast Lesions of the Eardrum: Retrospective Study,” Croatian Medical Journal, vol. 42, no. 6, pp. 642–645, December 2001.
- [B87] Stanback, H. I. Jr., “Predicting Damage from 277-V Single Phase to Ground Arcing Faults,” *IEEE Transactions on Industry Applications*, vol. IA-13, no. 4, pp. 307–314, July 1977.
- [B88] Stokes, A. D. and D. K. Sweeting, “Electric Arcing Burn Hazards,” *IEEE Transactions on Industry Applications*, vol. 42, no. 1, pp. 134–141, January/February 2006.
- [B89] Sutherland, P. E., “Arc Flash and Coordination Study Conflict in an Older Industrial Plant,” *IEEE Transactions on Industry Applications*, vol. 45, no. 2, pp. 569–574, March/April 2009.

¹⁸NFPA publications are published by the National Fire Protection Association (<http://www.nfpa.org/>).

- [B90] Sweeting, D., "Arcing Faults in Electrical Equipment," *IEEE Transactions on Industry Applications*, vol. 47, no. 1, pp. 387–397, January/February 2011.
- [B91] Teresi, J. D., "A review of research on flash blindness," USNRDL-TR-68-76 Final report. Radiological Defense Laboratory, San Francisco, CA, July 1, 1968.
- [B92] Thiele, O. and V. E. Beachum, "Are Real-World Power Systems Really Safe? Case Studies in Arc Flash Reduction," *IEEE Industry Applications Magazine*, vol. 15, no. 4, pp. 76–81, July/August 2009.
- [B93] Tinsley, H. W. III, M. Hodder, and A. M. Graham, "Arc Flash Hazard Calculations: Myths, Facts, and Solutions," *IEEE Industry Applications Magazine*, vol. 13, no. 1, pp. 58–64, January/February 2007.
- [B94] Tinsley, H. W. III and M. Hodder, "A Practical Approach to Arc Flash Hazard Analysis and Reduction," *IEEE Transactions on Industry Applications*, vol. 41, no. 1, pp. 144–154, January/February 2005.
- [B95] Valdes, M. E., S. Hansen, and P. Sutherland, "Optimized Instantaneous Protection Settings: Improving Selectivity and Arc-Flash Protection," *IEEE Industry Applications Magazine*, vol. 18, no. 3, pp. 66–73, May/June 2012.
- [B96] Wallace, G. L., "Blast Injury Basics: A Primer for the Medical Speech-Language Pathologist," *ASHA Leader*, vol. 11, no. 9, pp. 26–28, July 2006.¹⁹
- [B97] Wilkins, R., M. Allison, and M. Lang, "Calculating Hazards," *IEEE Industry Applications Magazine*, vol. 11, no. 3, pp. 40–48, May/June 2005.
- [B98] Wilkins, R., M. Lang, and M. Allison, "Effect of Insulating Barriers in Arc Flash Testing," *IEEE Transactions on Industry Applications*, vol. 44, no. 5, pp. 1354–1359, September/October 2008.
- [B99] Wilson, R. A., R. Harju, J. Keisala, and S. Ganesan, "Tripping with the Speed of Light: Arc Flash Protection," *Proceedings of the 60th Annual Conference for Protective Relay Engineers*, College Station, TX, USA, Mar. 27–29, 2007, pp. 226–238.
- [B100] Wu, H., X. Li, D. Stade, and H. Schau, "Arc fault model for low-voltage AC systems," *IEEE Transactions on Power Delivery*, vol. 20, no. 2, pp. 1204–1205, April 2005.

¹⁹Available at <https://leader.pubs.asha.org/article.aspx?articleid=2278223>.

Annex B

(informative)

Units of measure

B.1 IEEE Policy 9.16

In 1995, IEEE implemented a new metric policy that called for measured and calculated values of quantities to be expressed in metric units in IEEE publications as of January 2000, following the detailed guidance for SI (Système International d'Unités)-based metric practice. (See IEEE/ASTM SI 10 [B54] for guidance in metric practice.) This means that new and revised standards submitted for approval shall use metric units exclusively in the normative portions of the standard. Inch-pound data may be included, if necessary, in footnotes or annexes that are informative only.

B.2 Incident energy

Incident energy is measured in joules per square centimeter (J/cm^2) in the SI system. A joule is defined as one watt-second. Multiply by 4.184 to convert calories per square centimeter (cal/cm^2) to J/cm^2 . An incident energy of $5.0\ J/cm^2$ ($1.2\ cal/cm^2$) is likely to cause the onset of a second-degree burn. If a butane lighter is held 1 cm away from a person's finger for 1 s and the finger is in the blue flame, $1\ cm^2$ area of the finger is exposed to about $5.0\ J/cm^2$ ($1.2\ cal/cm^2$).

Annex C

(informative)

Determination of incident energy for different equipment types

C.1 Low-voltage drawout switchgear

An arc flash may occur in or behind a circuit-breaker (CB) compartment as follows:

- a) With CB racked in but stab not on studs or not secure
- b) With no CB present – accidental contact during cleaning or inspection
- c) If CB fails because of over-duty or water or other contamination or internal mechanical failure

Faults may also occur in cable-termination compartments, meter compartments, and in instrument or control power transformer compartments (PT or CPT).

Determine which equipment configuration that was tested is most similar to the possible fault causes. Refer to [Table 9](#).

Case 1: If a CB is present, but the CB stabs are not securely connected to a stud (bus run back), for an arc traveling away from the source of supply, then HCB might appear to be the best solution. But because the arc cannot come straight out at the worker, VCB is a better solution. The distance from arc to person is measured from the point where the bus stab connects to the CB, about 30.48 cm (12 in) behind front of low-voltage (LV) switchgear plus about another 45.7 cm (18 in) to the torso of the worker.

Case 2: If a CB is not present, enclosed equipment with horizontal bus, bus not terminated, HCB is the best selection.

Case 3: If a CB is present and has an internal fault, e.g., when the contacts are not able to interrupt the fault, the arc erupts upward into arc chutes as long as they are present. While the equipment is enclosed, the enclosure will have little effect because the arc occurs near the front of the enclosure, with the CB frame blocking the back. The bus is terminated at contacts in such a way that the arc goes up. VCB is the best selection. Distance from arc to person is measured from the CB contacts inside the CB, about 10.16 cm (4 in) inside the LV CB plus 30.48 cm (12 in) outside.

C.2 Low-voltage motor control center

[Figure C.1](#) also applies to MCCs, except that the stab on the back of the unit plugs directly onto the vertical bus in the bus compartment.

An arc flash may occur in the bus compartment or in a motor control center (MCC) unit or in the mains compartment.

Case 1: A fault in the bus compartment can be caused by bent stabs not making a secure connection, which can cause arcing and/or a ground fault. The arc would likely run down the bus to its end, away from the source of supply. VCB would be the best selection.

Case 2: MCC faults may occur anywhere in the bucket due to testing or equipment failure, and they may arc over to the line-side lugs. VCB would be the selection.

Case 3: A fault may occur in a protective device or switch, which would be another VCB case.

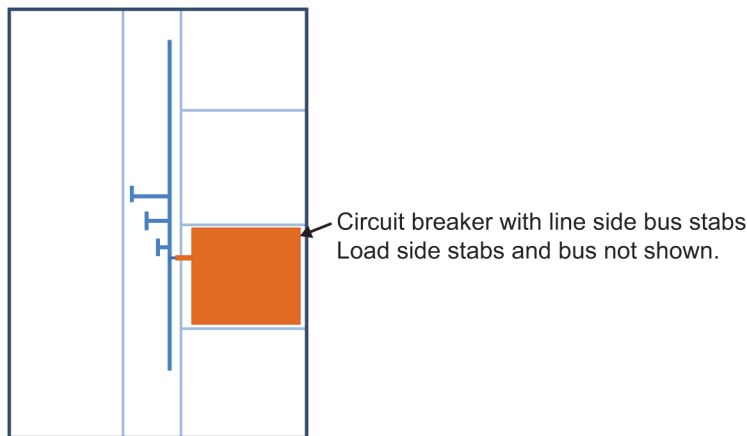


Figure C.1—Switchgear side-view diagram

C.3 NEMA 600 V panelboard

Bus faults may occur in a panelboard as follows:

- a) When workers are installing or removing a CB without de-energizing the bus
- b) When cables are being pulled into or removed from the panelboard
- c) When a CB fails because of over-duty or water or other contaminants in the CB

CB load-side faults may also occur; however, the arc-flash incident energy would be less than or equal to the incident energy for line-side faults.

The worst-case configuration for a panelboard appears to be VCBB, whether the bus is terminated by a branch circuit breaker or not. A bus fault on the main lugs would likely go down the bus to the first CB and that would be the termination point. A bus fault below the CBs would go down to the end of the bus with no termination, so VCB would be the configuration. But this situation would not be as conservative as the situation where the fault occurred above the CBs.

C.4 Enclosed switch

Except for the dimensions, the application is similar to [Figure C.2](#) for panelboards. VCBB is likely the best configuration.

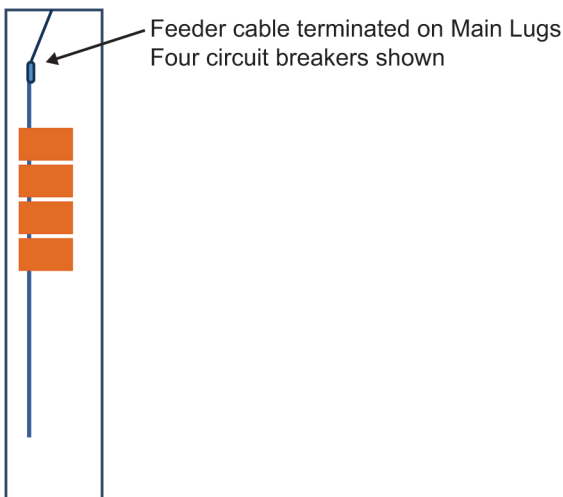


Figure C.2—Side-view diagram of panel board

Annex D

(informative)

Sample incident energy calculations

D.1 Sample arc-flash incident energy calculation for a medium-voltage system

This is an example of an incident energy and arc-flash boundary calculation for a medium-voltage system. The steps used in this sample calculation are provided in 4.3. The input parameters were selected based on the typical data provided in Clause 6.

$$\text{Configuration} := 1 \quad \text{For VCB} \quad (\text{D.1})$$

Three-phase system voltage:

$$V_{\text{oc}} := 4.160 \quad \text{kV rms} \quad (\text{D.2})$$

Three-phase bolted fault current:

$$I_{\text{bf}} := 15 \quad \text{kA symm rms} \quad (\text{D.3})$$

Gap between conductors (electrodes):

$$G := 104 \quad \text{mm} \quad (\text{D.4})$$

Working distance:

$$D := 914.4 \quad \text{mm} \quad (\text{D.5})$$

Enclosure dimensions:

$$\text{Width} := 762 \quad \text{mm} \quad (\text{D.6})$$

$$\text{Height} := 1143 \quad \text{mm} \quad (\text{D.7})$$

Step 1: Determine the intermediate arcing currents using the equations in 4.4.

For 600 V:

$$\begin{aligned} k1 &:= -0.04287 & k2 &:= 1.035 & k3 &:= -0.083 & k4 &:= 0 & k5 &:= 0 \\ k6 &:= -4.783 \cdot 10^{-9} & k7 &:= 1.962 \cdot 10^{-6} & k8 &:= -0.000229 & k9 &:= 0.003141 & k10 &:= 1.092 \end{aligned}$$

$$I_{\text{arc_600}} := 10^{(k1+k2 \cdot \log(I_{\text{bf}}) + k3 \cdot \log(G))} \cdot (k4 \cdot I_{\text{bf}}^6 + k5 \cdot I_{\text{bf}}^5 + k6 \cdot I_{\text{bf}}^4 + k7 \cdot I_{\text{bf}}^3 + k8 \cdot I_{\text{bf}}^2 + k9 \cdot I_{\text{bf}} + k10) \quad (\text{D.8})$$

$$I_{\text{arc_600}} = 11.117 \quad \text{kA} \quad (\text{D.9})$$

For 2700 V:

$$\begin{aligned} k1 &:= 0.0065 & k2 &:= 1.001 & k3 &:= -0.024 & k4 &:= -1.557 \cdot 10^{-12} & k5 &:= 4.556 \cdot 10^{-10} \\ k6 &:= -4.186 \cdot 10^{-8} & k7 &:= 8.346 \cdot 10^{-7} & k8 &:= 5.482 \cdot 10^{-5} & k9 &:= -0.003191 & k10 &:= 0.9729 \end{aligned}$$

$$I_{\text{arc_2700}} := 10^{(k1+k2 \cdot \log(I_{\text{bf}}) + k3 \cdot \log(G))} \cdot (k4 \cdot I_{\text{bf}}^6 + k5 \cdot I_{\text{bf}}^5 + k6 \cdot I_{\text{bf}}^4 + k7 \cdot I_{\text{bf}}^3 + k8 \cdot I_{\text{bf}}^2 + k9 \cdot I_{\text{bf}} + k10) \quad (\text{D.10})$$

$$I_{\text{arc_2700}} = 12.816 \quad \text{kA} \quad (\text{D.11})$$

For 14300 V:

$$\begin{aligned} k1 &:= 0.005795 & k2 &:= 1.015 & k3 &:= -0.011 & k4 &:= -1.557 \cdot 10^{-12} & k5 &:= 4.556 \cdot 10^{-10} \\ k6 &:= -4.186 \cdot 10^{-8} & k7 &:= 8.346 \cdot 10^{-7} & k8 &:= 5.482 \cdot 10^{-5} & k9 &:= -0.003191 & k10 &:= 0.9729 \end{aligned}$$

$$I_{\text{arc_14300}} := 10^{(k1+k2 \cdot \log(I_{\text{bf}}) + k3 \cdot \log(G))} \cdot (k4 \cdot I_{\text{bf}}^6 + k5 \cdot I_{\text{bf}}^5 + k6 \cdot I_{\text{bf}}^4 + k7 \cdot I_{\text{bf}}^3 + k8 \cdot I_{\text{bf}}^2 + k9 \cdot I_{\text{bf}} + k10) \quad (\text{D.12})$$

$$I_{\text{arc_14300}} = 14.116 \quad \text{kA} \quad (\text{D.13})$$

Step 2: Find the final arcing current per the equations and instructions provided in 4.9.

$$I_{\text{arc_1}} := \frac{I_{\text{arc_2700}} - I_{\text{arc_600}}}{2.1} \cdot (V_{\text{oc}} - 2.7) + I_{\text{arc_2700}} = 13.997 \quad \text{kA} \quad (\text{D.14})$$

$$I_{\text{arc_2}} := \frac{I_{\text{arc_14300}} - I_{\text{arc_2700}}}{11.6} \cdot (V_{\text{oc}} - 14.3) + I_{\text{arc_14300}} = 12.979 \quad \text{kA} \quad (\text{D.15})$$

$$I_{\text{arc_3}} := \frac{I_{\text{arc_1}} \cdot (2.7 - V_{\text{oc}})}{2.1} + \frac{I_{\text{arc_2}} \cdot (V_{\text{oc}} - 0.6)}{2.1} = 12.272 \quad \text{kA} \quad (\text{D.16})$$

The final arcing current is:

$$I_{\text{arc}} := I_{\text{arc_2}} = 12.979 \quad \text{kA} \quad (\text{D.17})$$

$$T := 197 \quad \text{ms} \quad (\text{D.18})$$

Figure D.1 shows how the arc duration would be obtained from a sample MV power fuse time current characteristic (TCC) curve.

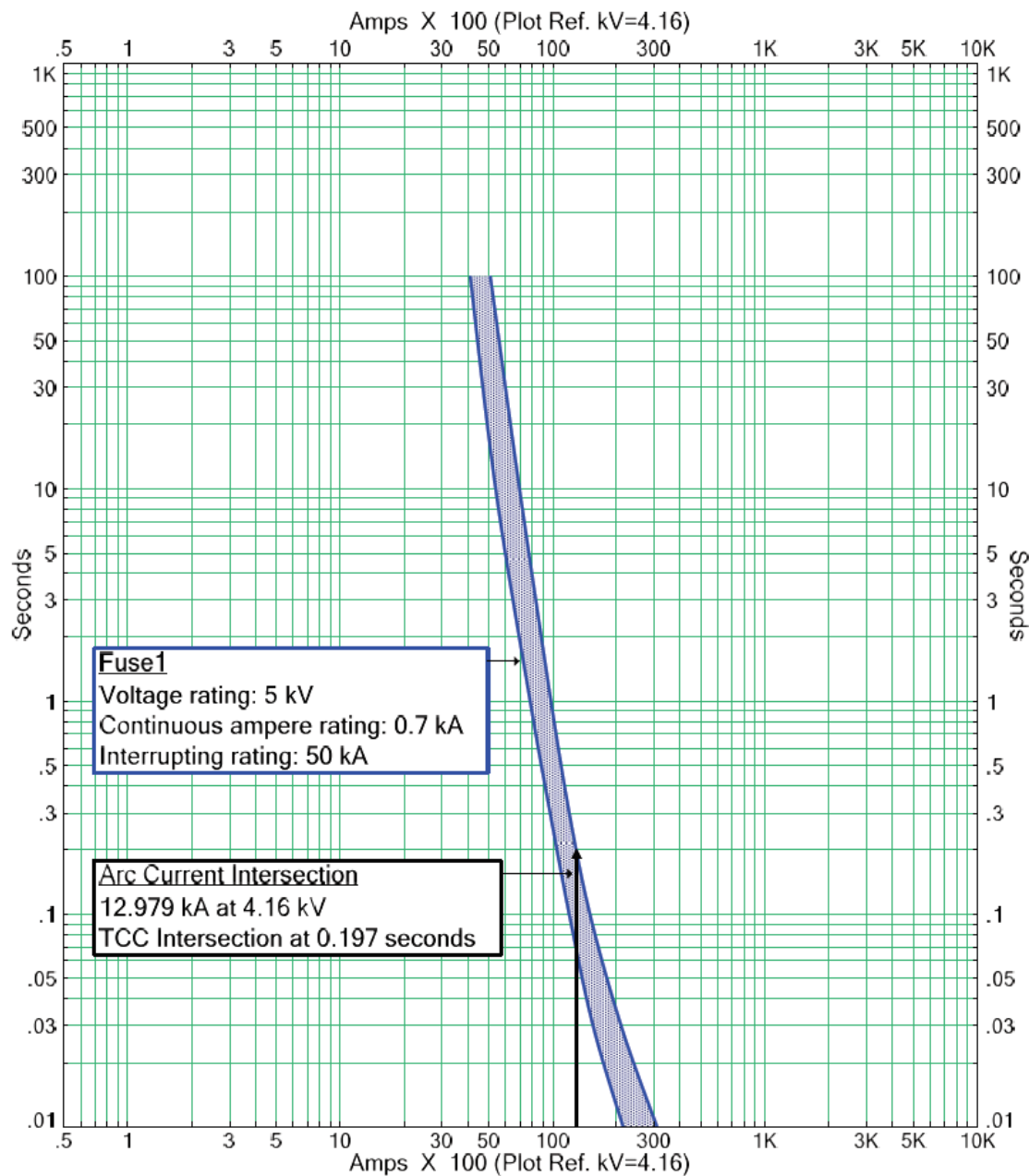


Figure D.1—Determination of arc duration

Step 3: Find the enclosure size correction factor per the equations and instructions provided in 4.8.

$$\text{Width}_1 := \left[660.4 + (\text{Width} - 660.4) \cdot \left(\frac{V_{oc} + 4}{20} \right) \right] \cdot 25.4^{-1} = 27.632 \quad (\text{D.19})$$

Since for $508 \text{ mm} < \text{Width} \leq 1244.6 \text{ mm}$, [Equation \(11\)](#) should be used.

Where Width_1 is the adjusted width used to find the equivalent box size

$$\text{Height}_1 := 0.03937 \cdot \text{Height} = 45 \quad (\text{D.20})$$

Since for $508 \text{ mm} < \text{Height} \leq 1244.6 \text{ mm}$, the height should be used directly.

Where Height_1 is the adjusted height used to find the equivalent box size, the equivalent enclosure size value is:

$$EES := \frac{\text{Height}_1 + \text{Width}_1}{2} = 36.316 \quad (\text{D.21})$$

The correction factor for a VCB electrode configuration is:

$$CF := -0.000302 \cdot EES^2 + 0.03441 \cdot EES + 0.4325 = 1.284 \quad (\text{D.22})$$

Step 4: The intermediate values of incident energy can be found per 4.6.

Using the coefficients from [Table 3](#) and [Equation \(3\)](#), find the intermediate incident energy for 600 V:

$$\begin{aligned} k1 &:= 0.753364 & k2 &:= 0.566 & k3 &:= 1.752636 & k4 &:= 0 \\ k5 &:= 0 & k6 &:= -4.783 \cdot 10^{-9} & k7 &:= 0.000001962 & k8 &:= -0.000229 \\ k9 &:= 0.003141 & k10 &:= 1.092 & k11 &:= 0 & k12 &:= -1.598 & k13 &:= 0.957 \end{aligned}$$

$$E_{600} := \frac{12.552}{50} \cdot T \cdot 10^{\left[k1 + k2 \cdot \log(G) + \frac{(k3 \cdot I_{arc_600})}{(k4 \cdot I_{bf}^7 + k5 \cdot I_{bf}^6 + k6 \cdot I_{bf}^5 + k7 \cdot I_{bf}^4 + k8 \cdot I_{bf}^3 + k9 \cdot I_{bf}^2 + k10 \cdot I_{bf})} + (k11 \cdot \log(I_{bf}) + k12 \cdot \log(D) + k13 \cdot \log(I_{arc_600}) + \log(\frac{1}{CF})) \right]} \quad (\text{D.23})$$

$$E_{600} = 8.652 \quad \text{J/cm}^2 \quad (\text{D.24})$$

Using the coefficients from [Table 4](#) and [Equation \(4\)](#), find the intermediate incident energy for 2700 V:

$$\begin{aligned} k1 &:= 2.40021 & k2 &:= 0.165 & k3 &:= 0.354202 & k4 &:= -1.557 \cdot 10^{-12} \\ k5 &:= 4.55 \cdot 10^{-10} & k6 &:= -4.186 \cdot 10^{-8} & k7 &:= 8.346 \cdot 10^{-7} & k8 &:= 5.482 \cdot 10^{-5} \\ k9 &:= -0.003191 & k10 &:= 0.9729 & k11 &:= 0 & k12 &:= -1.569 & k13 &:= 0.9778 \end{aligned}$$

$$E_{2700} := \frac{12.552}{50} \cdot T \cdot 10^{\left[k1 + k2 \cdot \log(G) + \frac{(k3 \cdot I_{arc_2700})}{(k4 \cdot I_{bf}^7 + k5 \cdot I_{bf}^6 + k6 \cdot I_{bf}^5 + k7 \cdot I_{bf}^4 + k8 \cdot I_{bf}^3 + k9 \cdot I_{bf}^2 + k10 \cdot I_{bf})} + (k11 \cdot \log(I_{bf}) + k12 \cdot \log(D) + k13 \cdot \log(I_{arc_2700}) + \log(\frac{1}{CF})) \right]} \quad (D.25)$$

$$E_{2700} = 11.977 \quad \text{J/cm}^2 \quad (D.26)$$

Using the coefficients from [Table 5](#) and [Equation \(5\)](#), find the intermediate incident energy for 14300 V:

$$\begin{aligned} k1 &:= 3.825917 & k2 &:= 0.11 & k3 &:= -0.999749 & k4 &:= -1.557 \cdot 10^{-12} \\ k5 &:= 4.556 \cdot 10^{-10} & k6 &:= -4.186 \cdot 10^{-8} & k7 &:= 8.346 \cdot 10^{-7} & k8 &:= 5.482 \cdot 10^{-5} \\ k9 &:= -0.003191 & k10 &:= 0.9729 & k11 &:= 0 & k12 &:= -1.568 & k13 &:= 0.99 \end{aligned}$$

$$E_{14300} := \frac{12.552}{50} \cdot T \cdot 10^{\left[k1 + k2 \cdot \log(G) + \frac{(k3 \cdot I_{arc_14300})}{(k4 \cdot I_{bf}^7 + k5 \cdot I_{bf}^6 + k6 \cdot I_{bf}^5 + k7 \cdot I_{bf}^4 + k8 \cdot I_{bf}^3 + k9 \cdot I_{bf}^2 + k10 \cdot I_{bf})} + (k11 \cdot \log(I_{bf}) + k12 \cdot \log(D) + k13 \cdot \log(I_{arc_14300}) + \log(\frac{1}{CF})) \right]} \quad (D.27)$$

$$E_{14300} = 13.367 \quad \text{J/cm}^2 \quad (D.28)$$

Step 5: The final value of incident energy can be determined per [4.9](#).

$$E_1 := \frac{E_{2700} - E_{600}}{2.1} \cdot (V_{oc} - 2.7) + E_{2700} = 14.288 \quad \text{J/cm}^2 \quad (D.29)$$

$$E_2 := \frac{E_{14300} - E_{2700}}{11.6} \cdot (V_{oc} - 14.3) + E_{14300} = 12.152 \quad \text{J/cm}^2 \quad (D.30)$$

$$E_3 := \frac{E_1 \cdot (2.7 - V_{oc})}{2.1} + \frac{E_2 \cdot (V_{oc} - 0.6)}{2.1} = 10.667 \quad \text{J/cm}^2 \quad (D.31)$$

The final incident energy is:

$$E := E_2 = 12.152 \quad \text{J/cm}^2 \quad (D.32)$$

Step 6: The intermediate values of arc-flash boundary can be determined per 4.7.

Using the coefficients from [Table 3](#) and [Equation \(7\)](#), find the intermediate arc-flash boundary for 600 V:

$$\begin{aligned} k1 &:= 0.753364 & k2 &:= 0.566 & k3 &:= 1.752636 & k4 &:= 0 \\ k5 &:= 0 & k6 &:= -4.783 \cdot 10^{-9} & k7 &:= 0.000001962 & k8 &:= -0.000229 \\ k9 &:= 0.003141 & k10 &:= 1.092 & k11 &:= 0 & k12 &:= -1.598 & k13 &:= 0.957 \end{aligned}$$

$$AFB_{600} := 10 \frac{\left(k3 \cdot I_{arc_600} \right)}{\left(k4 \cdot I_{bf}^7 + k5 \cdot I_{bf}^6 + k6 \cdot I_{bf}^5 + k7 \cdot I_{bf}^4 + k8 \cdot I_{bf}^3 + k9 \cdot I_{bf}^2 + k10 \cdot I_{bf} \right)} + \left(k11 \cdot \log(I_{bf}) + k13 \cdot \log(I_{arc_600}) + \log\left(\frac{1}{CF}\right) - \log\left(\frac{20}{T}\right) \right) \quad (D.33)$$

$$AFB_{600} := 1.285 \times 10^3 \quad \text{mm} \quad (D.34)$$

Using the coefficients from [Table 4](#) and [Equation \(8\)](#), find the intermediate arc-flash boundary for 2700 V:

$$\begin{aligned} k1 &:= 2.40021 & k2 &:= 0.165 & k3 &:= 0.354202 & k4 &:= -1.557 \cdot 10^{-12} \\ k5 &:= 4.55 \cdot 10^{-10} & k6 &:= -4.186 \cdot 10^{-8} & k7 &:= 8.346 \cdot 10^{-7} & k8 &:= 5.482 \cdot 10^{-5} \\ k9 &:= -0.003191 & k10 &:= 0.9729 & k11 &:= 0 & k12 &:= -1.569 & k13 &:= 0.9778 \end{aligned}$$

$$AFB_{2700} := 10 \frac{\left(k3 \cdot I_{arc_2700} \right)}{\left(k4 \cdot I_{bf}^7 + k5 \cdot I_{bf}^6 + k6 \cdot I_{bf}^5 + k7 \cdot I_{bf}^4 + k8 \cdot I_{bf}^3 + k9 \cdot I_{bf}^2 + k10 \cdot I_{bf} \right)} + \left(k11 \cdot \log(I_{bf}) + k13 \cdot \log(I_{arc_2700}) + \log\left(\frac{1}{CF}\right) - \log\left(\frac{20}{T}\right) \right) \quad (D.35)$$

$$AFB_{2700} = 1.591 \times 10^3 \quad \text{mm} \quad (D.36)$$

Using the coefficients from [Table 5](#) and [Equation \(9\)](#), find the intermediate arc-flash boundary for 14300 V:

$$\begin{aligned} k1 &:= 3.825917 & k2 &:= 0.11 & k3 &:= -0.999749 & k4 &:= -1.557 \cdot 10^{-12} \\ k5 &:= 4.556 \cdot 10^{-10} & k6 &:= -4.186 \cdot 10^{-8} & k7 &:= 8.346 \cdot 10^{-7} & k8 &:= 5.482 \cdot 10^{-5} \\ k9 &:= -0.003191 & k10 &:= 0.9729 & k11 &:= 0 & k12 &:= -1.568 & k13 &:= 0.99 \end{aligned}$$

$$AFB_{14300} := 10 \frac{\left(k3 \cdot I_{arc_14300} \right)}{\left(k4 \cdot I_{bf}^7 + k5 \cdot I_{bf}^6 + k6 \cdot I_{bf}^5 + k7 \cdot I_{bf}^4 + k8 \cdot I_{bf}^3 + k9 \cdot I_{bf}^2 + k10 \cdot I_{bf} \right)} + \left(k11 \cdot \log(I_{bf}) + k13 \cdot \log(I_{arc_14300}) + \log\left(\frac{1}{CF}\right) - \log\left(\frac{20}{T}\right) \right) \quad (D.37)$$

$$AFB_{14300} := 1.707 \times 10^3 \quad \text{mm} \quad (D.38)$$

Step 7: The final value of the arc-flash boundary can be determined per 4.9.

$$AFB_1 := \frac{AFB_{2700} - AFB_{600}}{2.1} \cdot (V_{oc} - 2.7) + AFB_{2700} = 1.804 \times 10^3 \quad (\text{D.39})$$

$$AFB_2 := \frac{AFB_{14300} - AFB_{2700}}{11.6} \cdot (V_{oc} - 14.3) + AFB_{14300} = 1.606 \times 10^3 \quad (\text{D.40})$$

$$AFB_3 := \frac{AFB_1 \cdot (2.7 - V_{oc})}{2.1} + \frac{AFB_2 \cdot (V_{oc} - 0.6)}{2.1} = 1.468 \times 10^3 \quad (\text{D.41})$$

The final arc-flash boundary is:

$$AFB := AFB_2 = 1.606 \times 10^3 \quad \text{mm} \quad (\text{D.42})$$

Step 8: To account for the arcing current variation, use the equations in 4.5 to find the correction factor.

For VCB, the coefficients from Table 2 are as follows:

$$\begin{aligned} k1 &:= 0 & k2 &:= -0.0000014269 & k3 &:= 0.000083137 \\ k4 &:= -0.0019382 & k5 &:= 0.022366 & k6 &:= -0.12645 & k7 &:= 0.30226 \end{aligned}$$

The VarCf value is:

$$VarC_f := k1 \cdot V_{oc}^6 + k2 \cdot V_{oc}^5 + k3 \cdot V_{oc}^4 + k4 \cdot V_{oc}^3 + k5 \cdot V_{oc}^2 + k6 \cdot V_{oc} + k7 = 0.047 \quad (\text{D.43})$$

$$1 - 0.5 \cdot VarC_f = 0.977 \quad \text{Correction factor} \quad (\text{D.44})$$

Step 9: Adjust the intermediate values of arcing current using the correction factor.

For 600 V:

$$I_{\text{arc_600_min}} := I_{\text{arc_600}} \cdot (1 - 0.5 \cdot VarC_f) = 10.856 \quad \text{kA} \quad (\text{D.45})$$

For 2700 V:

$$I_{\text{arc_2700_min}} := I_{\text{arc_2700}} \cdot (1 - 0.5 \cdot VarC_f) = 12.515 \quad \text{kA} \quad (\text{D.46})$$

For 14300 V:

$$I_{\text{arc_14300_min}} := I_{\text{arc_14300}} \cdot (1 - 0.5 \cdot VarC_f) = 13.786 \quad \text{kA} \quad (\text{D.47})$$

Step 10: Find the reduced final arcing current per the equations and instructions provided in 4.9.

$$I_{\text{arc_1}} := \frac{I_{\text{arc_2700_min}} - I_{\text{arc_600_min}}}{2.1} \cdot (V_{\text{oc}} - 2.7) + I_{\text{arc_2700_min}} = 13.669 \quad \text{kA} \quad (\text{D.48})$$

$$I_{\text{arc_2}} := \frac{I_{\text{arc_14300_min}} - I_{\text{arc_2700_min}}}{11.6} \cdot (V_{\text{oc}} - 14.3) + I_{\text{arc_14300_min}} = 12.675 \quad \text{kA} \quad (\text{D.49})$$

$$I_{\text{arc_3}} := \frac{I_{\text{arc_1}} \cdot (2.7 - V_{\text{oc}})}{2.1} + \frac{I_{\text{arc_2}} \cdot (V_{\text{oc}} - 0.6)}{2.1} = 11.984 \quad \text{kA} \quad (\text{D.50})$$

The reduced final arcing current is:

$$I_{\text{arc_min}} := I_{\text{arc_2}} = 12.675 \quad \text{kA} \quad (\text{D.51})$$

$$T := 223 \quad \text{ms} \quad (\text{D.52})$$

Figure D.2 shows how the arc duration was obtained from the reduced arcing current.

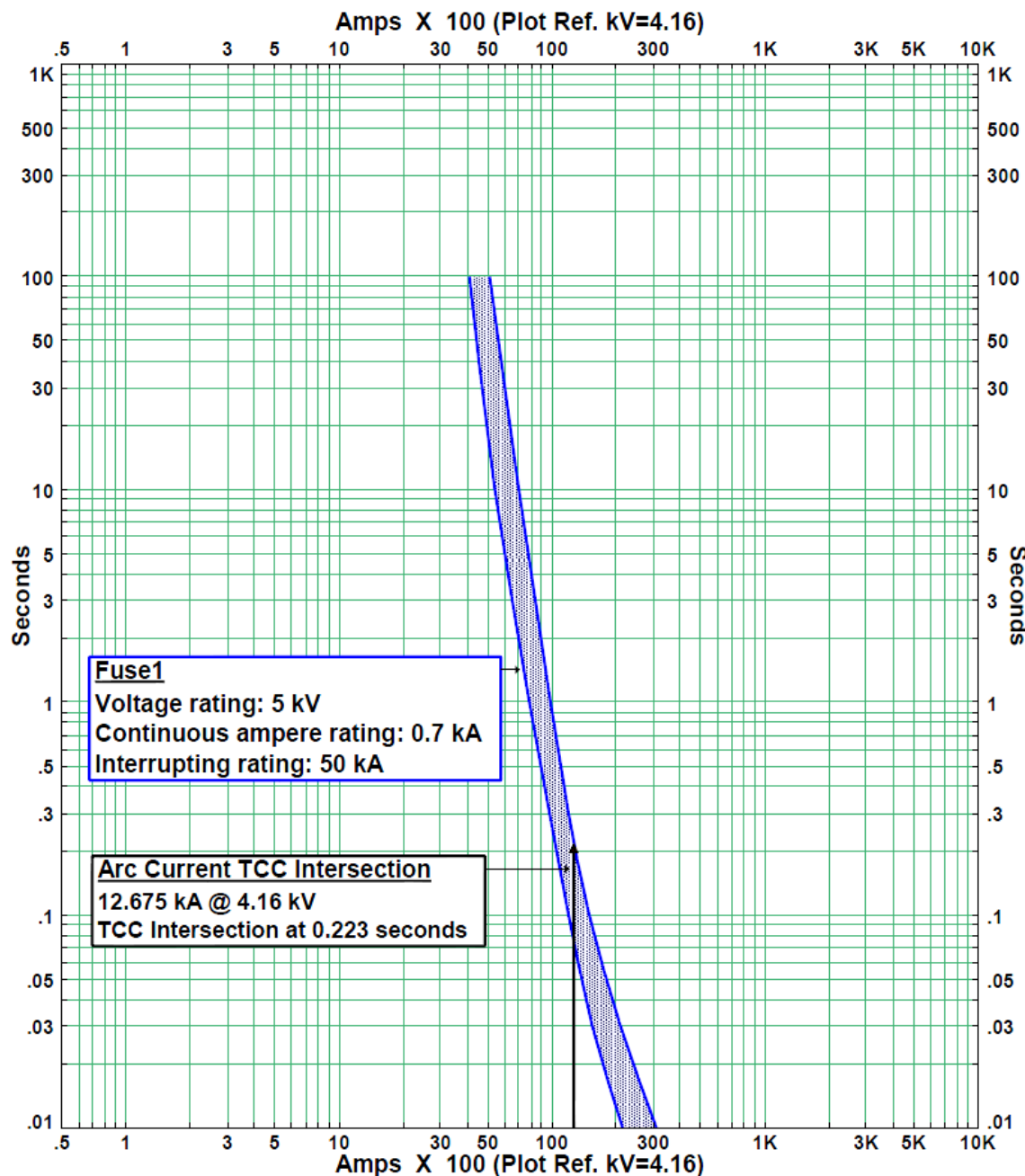


Figure D.2—Determination of arc duration using reduced arcing current

Step 11: Repeat step 4 using the reduced intermediate currents

Using the coefficients from [Table 3](#) and [Equation \(3\)](#), find the intermediate incident energy for 600 V:

$$\begin{aligned} k1 &:= 0.753364 & k2 &:= 0.566 & k3 &:= 1.752636 & k4 &:= 0 \\ k5 &:= 0 & k6 &:= -4.783 \cdot 10^{-9} & k7 &:= 0.000001962 & k8 &:= -0.000229 \\ k9 &:= 0.003141 & k10 &:= 1.092 & k11 &:= 0 & k12 &:= -1.598 & k13 &:= 0.957 \end{aligned}$$

$$E_{600} := \frac{12.552}{50} \cdot T \cdot 10^{\left[k1 + k2 \cdot \log(G) + \frac{(k3 \cdot I_{arc_600_min})}{(k4 \cdot I_{bf}^7 + k5 \cdot I_{bf}^6 + k6 \cdot I_{bf}^5 + k7 \cdot I_{bf}^4 + k8 \cdot I_{bf}^3 + k9 \cdot I_{bf}^2 + k10 \cdot I_{bf})} + (k11 \cdot \log(I_{bf}) + k12 \cdot \log(D) + k13 \cdot \log(I_{arc_600_min}) + \log(\frac{1}{CF})) \right]} \quad (D.53)$$

$$E_{600} := 8.98 \quad \text{J/cm}^2 \quad (D.54)$$

Using the coefficients from [Table 4](#) and [Equation \(4\)](#), find the intermediate incident energy for 2700 V:

$$\begin{aligned} k1 &:= 2.40021 & k2 &:= 0.165 & k3 &:= 0.354202 & k4 &:= -1.557 \cdot 10^{-12} \\ k5 &:= 4.55 \cdot 10^{-10} & k6 &:= -4.186 \cdot 10^{-8} & k7 &:= 8.346 \cdot 10^{-7} & k8 &:= 5.482 \cdot 10^{-5} \\ k9 &:= -0.003191 & k10 &:= 0.9729 & k11 &:= 0 & k12 &:= -1.569 & k13 &:= 0.9778 \end{aligned}$$

$$E_{2700} := \frac{12.552}{50} \cdot T \cdot 10^{\left[k1 + k2 \cdot \log(G) + \frac{(k3 \cdot I_{arc_2700_min})}{(k4 \cdot I_{bf}^7 + k5 \cdot I_{bf}^6 + k6 \cdot I_{bf}^5 + k7 \cdot I_{bf}^4 + k8 \cdot I_{bf}^3 + k9 \cdot I_{bf}^2 + k10 \cdot I_{bf})} + (k11 \cdot \log(I_{bf}) + k12 \cdot \log(D) + k13 \cdot \log(I_{arc_2700_min}) + \log(\frac{1}{CF})) \right]} \quad (D.55)$$

$$E_{2700} := 13.018 \quad \text{J/cm}^2 \quad (D.56)$$

Using the coefficients from [Table 5](#) and [Equation \(5\)](#), find the intermediate incident energy for 14300 V:

$$\begin{aligned} k1 &:= 3.825917 & k2 &:= 0.11 & k3 &:= -0.999749 & k4 &:= -1.557 \cdot 10^{-12} \\ k5 &:= 4.556 \cdot 10^{-10} & k6 &:= -4.186 \cdot 10^{-8} & k7 &:= 8.346 \cdot 10^{-7} & k8 &:= 5.482 \cdot 10^{-5} \\ k9 &:= -0.003191 & k10 &:= 0.9729 & k11 &:= 0 & k12 &:= -1.568 & k13 &:= 0.99 \end{aligned}$$

$$E_{14300} := \frac{12.552}{50} \cdot T \cdot 10^{\left[k1 + k2 \cdot \log(G) + \frac{(k3 \cdot I_{arc_14300_min})}{(k4 \cdot I_{bf}^7 + k5 \cdot I_{bf}^6 + k6 \cdot I_{bf}^5 + k7 \cdot I_{bf}^4 + k8 \cdot I_{bf}^3 + k9 \cdot I_{bf}^2 + k10 \cdot I_{bf})} + (k11 \cdot \log(I_{bf}) + k12 \cdot \log(D) + k13 \cdot \log(I_{arc_14300_min}) + \log(\frac{1}{CF})) \right]} \quad (D.57)$$

$$E_{14300} := 15.602 \quad \text{J/cm}^2 \quad (D.58)$$

Step 12: Repeat Step 5 using the reduced arcing currents.

$$E_1 := \frac{E_{2700} - E_{600}}{2.1} \cdot (V_{oc} - 2.7) + E_{2700} = 15.825 \quad \text{J/cm}^2 \quad (\text{D.59})$$

$$E_2 := \frac{E_{14300} - E_{2700}}{11.6} \cdot (V_{oc} - 14.3) + E_{14300} = 13.343 \quad \text{J/cm}^2 \quad (\text{D.60})$$

$$E_3 := \frac{E_I(2.7 - V_{oc})}{2.1} + \frac{E_2(V_{oc} - 0.6)}{2.1} = 11.618 \quad \text{J/cm}^2 \quad (\text{D.61})$$

The final incident energy found using the reduced final arcing currents is:

$$E := E_2 = 13.343 \quad \text{J/cm}^2 \quad (\text{D.62})$$

Step 13: Repeat Step 6 using the reduced arcing currents.

Using the coefficients from [Table 3](#) and [Equation \(7\)](#), find the intermediate arc-flash boundary for 600 V:

$$\begin{aligned} k1 &:= 0.753364 & k2 &:= 0.566 & k3 &:= 1.752636 & k4 &:= 0 \\ k5 &:= 0 & k6 &:= -4.783 \cdot 10^{-9} & k7 &:= 0.000001962 & k8 &:= -0.000229 \\ k9 &:= 0.003141 & k10 &:= 1.092 & k11 &:= 0 & k12 &:= -1.598 & k13 &:= 0.957 \end{aligned}$$

$$AFB_{600} := 10 \frac{\frac{(k3 \cdot I_{arc_600_min})}{(k4 \cdot I_{bf}^7 + k5 \cdot I_{bf}^6 + k6 \cdot I_{bf}^5 + k7 \cdot I_{bf}^4 + k8 \cdot I_{bf}^3 + k9 \cdot I_{bf}^2 + k10 \cdot I_{bf})} + \left(k11 \cdot \log(I_{bf}) + k13 \cdot \log(I_{arc_600_min}) + \log\left(\frac{1}{CF}\right) - \log\left(\frac{20}{T}\right) \right)}{-k12} \quad (\text{D.63})$$

$$AFB_{600} := 1.316 \times 10^3 \quad \text{mm} \quad (\text{D.64})$$

Using the coefficients from [Table 4](#) and [Equation \(8\)](#), find the intermediate arc-flash boundary for 2700 V:

$$\begin{aligned} k1 &:= 2.40021 & k2 &:= 0.165 & k3 &:= 0.354202 & k4 &:= -1.557 \cdot 10^{-12} \\ k5 &:= 4.55 \cdot 10^{-10} & k6 &:= -4.186 \cdot 10^{-8} & k7 &:= 8.346 \cdot 10^{-7} & k8 &:= 5.482 \cdot 10^{-5} \\ k9 &:= -0.003191 & k10 &:= 0.9729 & k11 &:= 0 & k12 &:= -1.569 & k13 &:= 0.9778 \end{aligned}$$

$$AFB_{2700} := 10 \frac{\frac{(k3 \cdot I_{arc_2700_min})}{(k4 \cdot I_{bf}^7 + k5 \cdot I_{bf}^6 + k6 \cdot I_{bf}^5 + k7 \cdot I_{bf}^4 + k8 \cdot I_{bf}^3 + k9 \cdot I_{bf}^2 + k10 \cdot I_{bf})} + \left(k11 \cdot \log(I_{bf}) + k13 \cdot \log(I_{arc_2700_min}) + \log\left(\frac{1}{CF}\right) - \log\left(\frac{20}{T}\right) \right)}{-k12} \quad (\text{D.65})$$

$$AFB_{2700} := 1.678 \times 10^3 \quad \text{mm} \quad (\text{D.66})$$

Using the coefficients from [Table 5](#) and [Equation \(9\)](#), find the intermediate arc-flash boundary for 14300 V:

$$\begin{aligned} k1 &:= 3.825917 & k2 &:= 0.11 & k3 &:= -0.999749 & k4 &:= -1.557 \cdot 10^{-12} \\ k5 &:= 4.556 \cdot 10^{-10} & k6 &:= -4.186 \cdot 10^{-8} & k7 &:= 8.346 \cdot 10^{-7} & k8 &:= 5.482 \cdot 10^{-5} \\ k9 &:= -0.003191 & k10 &:= 0.9729 & k11 &:= 0 & k12 &:= -1.568 & k13 &:= 0.99 \end{aligned}$$

$$AFB_{14300} := 10 \frac{(k3 \cdot I_{arc_14300_min})}{(k4 \cdot I_{bf}^7 + k5 \cdot I_{bf}^6 + k6 \cdot I_{bf}^5 + k7 \cdot I_{bf}^4 + k8 \cdot I_{bf}^3 + k9 \cdot I_{bf}^2 + k10 \cdot I_{bf})} + \left[k11 \cdot \log(I_{bf}) + k13 \cdot \log(I_{arc_14300_min}) + \log\left(\frac{1}{CF}\right) - \log\left(\frac{20}{T}\right) \right] \quad (D.67)$$

$$AFB_{14300} := 1.884 \times 10^3 \quad \text{mm} \quad (D.68)$$

Step 14: Repeat Step 7 using the reduced arcing currents.

$$AFB_1 := \frac{AFB_{2700} - AFB_{600}}{2.1} \cdot (V_{oc} - 2.7) + AFB_{2700} = 1.93 \times 10^3 \quad \text{mm} \quad (D.69)$$

$$AFB_2 := \frac{AFB_{14300} - AFB_{2700}}{11.6} \cdot (V_{oc} - 14.3) + AFB_{14300} = 1.704 \times 10^3 \quad \text{mm} \quad (D.70)$$

$$AFB_3 := \frac{AFB_1 (2.7 - V_{oc})}{2.1} + \frac{AFB_2 (V_{oc} - 0.6)}{2.1} = 1.547 \times 10^3 \quad \text{mm} \quad (D.71)$$

The arc-flash boundary found using the reduced arcing currents is:

$$AFB := AFB_2 = 1.704 \times 10^3 \quad \text{mm} \quad (D.72)$$

D.2 Sample arc-flash incident energy calculation for a low-voltage system

This is an example of an incident energy and arc-flash boundary calculation for a medium-voltage system. The steps used in this sample calculation are provided in 4.3. The input parameters were selected based on the typical data provided in Clause 6.

$$\text{Configuration} := 1 \quad \text{For VCB} \quad (\text{D.73})$$

Three-phase system voltage:

$$V_{\text{oc}} := 0.480 \quad \text{kV rms} \quad (\text{D.74})$$

Three-phase bolted fault current:

$$I_{\text{bf}} := 45 \quad \text{kA symm rms} \quad (\text{D.75})$$

Gap between conductors (electrodes):

$$G := 32 \quad \text{mm} \quad (\text{D.76})$$

Working distance:

$$D := 609.6 \quad \text{mm} \quad (\text{D.77})$$

Enclosure dimensions:

$$\text{Width} := 610 \quad \text{mm} \quad (\text{D.78})$$

$$\text{Height} := 610 \quad \text{mm} \quad (\text{D.79})$$

$$\text{Depth} := 254 \quad \text{mm} \quad (\text{D.80})$$

Step 1: Determine the intermediate arcing currents using the equations in 4.4 and 4.10.

For 600 V:

$$k1 := -0.04287 \quad k2 := 1.035 \quad k3 := -0.083 \quad k4 := 0 \quad k5 := 0$$

$$k6 := -4.783 \cdot 10^{-9} \quad k7 := 1.962 \cdot 10^{-6} \quad k8 := -0.000229 \quad k9 := 0.003141 \quad k10 := 1.092$$

$$I_{\text{arc_600}} := 10^{(k1+k2 \cdot \log(I_{\text{bf}}) + k3 \cdot \log(G))} \cdot (k4 \cdot I_{\text{bf}}^6 + k5 \cdot I_{\text{bf}}^5 + k6 \cdot I_{\text{bf}}^4 + k7 \cdot I_{\text{bf}}^3 + k8 \cdot I_{\text{bf}}^2 + k9 \cdot I_{\text{bf}} + k10) \quad (\text{D.81})$$

$$I_{\text{arc_600}} = 32.449 \quad \text{kA} \quad (\text{D.82})$$

Step 2: Find the final arcing current per 4.10.

$$I_{\text{arc}} := \frac{1}{\sqrt{\left(\frac{0.6}{V_{\text{oc}}}\right)^2 \cdot \left[\frac{1}{I_{\text{arc_600}}^2} - \left(\frac{0.6^2 - V_{\text{oc}}^2}{0.6^2 \cdot I_{\text{bf}}^2}\right)\right]}} \quad (\text{D.83})$$

$$I_{\text{arc}} = 28.793 \quad \text{kA} \quad (\text{D.84})$$

$$T := 61.3 \quad \text{ms} \quad (\text{D.85})$$

Figure D.3 shows the how the arc duration is determined from a sample LV fuse TCC curve.

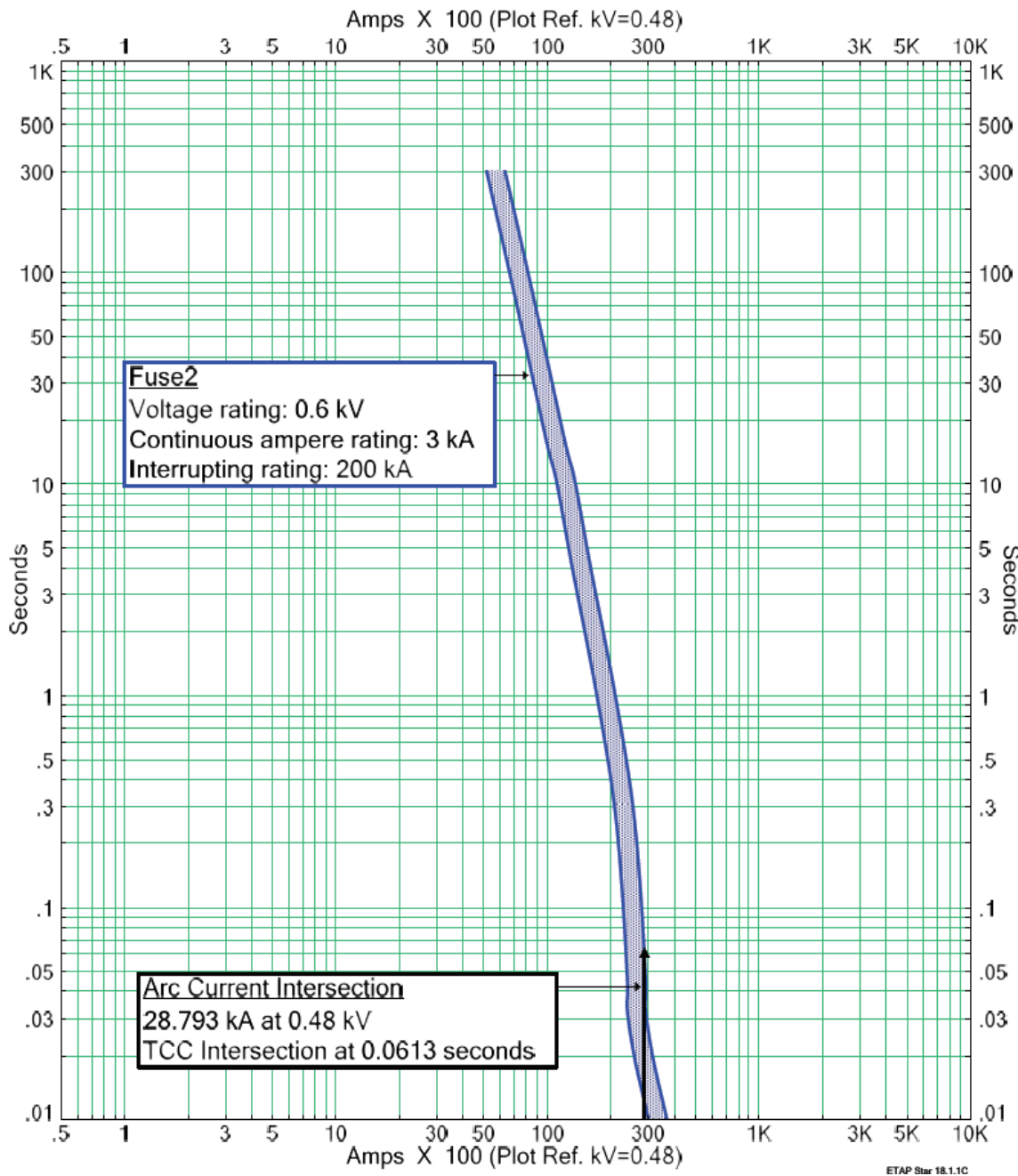


Figure D.3—Determination of arc duration for LV case

Step 3: Find the enclosure size correction factor per the equations and instructions provided in 4.8.

$$\text{Width}_1 := 0.03937 \cdot \text{Width} = 24.016 \quad (\text{D.86})$$

Since for $508 \text{ mm} < \text{Width} \leq 660.4 \text{ mm}$, the width should be used directly.

Where Width_1 is the adjusted width used to find the equivalent box size

$$\text{Height}_1 := 0.03937 \cdot \text{Height} = 24.016 \quad (\text{D.87})$$

Since for $508 \text{ mm} < \text{Width} \leq 1244.64 \text{ mm}$, the height should be used directly.

Where Height_1 is the adjusted height used to find the equivalent box size, the equivalent enclosure size value is:

$$ESS := \frac{\text{Height}_1 + \text{Width}_1}{2} = 24.016 \quad (\text{D.88})$$

The correction factor for a VCB electrode configuration is:

$$CF := -0.000302 \cdot ESS^2 + 0.03441 \cdot ESS + 0.4325 = 1.085 \quad (\text{D.89})$$

Step 4: Determine the intermediate value of incident energy per 4.6.

Using the coefficients from Table 3 and Equation (6), find the intermediate incident energy for $\leq 600 \text{ V}$:

$$\begin{aligned} k1 &:= 0.753364 & k2 &:= 0.566 & k3 &:= 1.752636 & k4 &:= 0 \\ k5 &:= 0 & k6 &:= -4.783 \cdot 10^{-9} & k7 &:= 0.000001962 & k8 &:= -0.000229 \\ k9 &:= 0.003141 & k10 &:= 1.092 & k11 &:= 0 & k12 &:= -1.598 & k13 &:= 0.957 \end{aligned}$$

$$E_{\leq 600} = \frac{12.552}{50} \times T \times 10^{\left(k1 + k2 \cdot \log(G) + \frac{(k3 \cdot I_{arc_600})}{(k4 \cdot I_{bf}^7 + k5 \cdot I_{bf}^6 + k6 \cdot I_{bf}^5 + k7 \cdot I_{bf}^4 + k8 \cdot I_{bf}^3 + k9 \cdot I_{bf}^2 + k10 \cdot I_{bf})} + k11 \cdot \log(I_{bf}) + k12 \cdot \log(D) + k13 \cdot \log(I_{arc}) + \log\left(\frac{1}{CF}\right) \right)} \quad (\text{D.90})$$

$$E_{\leq 600} = 11.585 \quad \text{J/cm}^2 \quad (\text{D.91})$$

Step 5: The final value of incident energy can be determined per 4.10.

The final incident energy is:

$$E = E_{\leq 600} = 11.585 \quad \text{J/cm}^2 \quad (\text{D.92})$$

Step 6: The intermediate value of arc-flash boundary can be determined per 4.7.

Using the coefficients from [Table 3](#) and [Equation \(10\)](#), find the intermediate arc-flash boundary for <600 V:

$$\begin{aligned} k1 &:= 0.753364 & k2 &:= 0.566 & k3 &:= 1.752636 & k4 &:= 0 \\ k5 &:= 0 & k6 &:= -4.783 \cdot 10^{-9} & k7 &:= 0.000001962 & k8 &:= -0.000229 \\ k9 &:= 0.003141 & k10 &:= 1.092 & k11 &:= 0 & k12 &:= -1.598 & k13 &:= 0.957 \end{aligned}$$

$$AFB_{\leq 600} = 10^{\left(\frac{k1+k2 \cdot \log(G) + \frac{k3 \cdot I_{arc_600}}{k4 \cdot I_{bf}^7 + k5 \cdot I_{bf}^6 + k6 \cdot I_{bf}^5 + k7 \cdot I_{bf}^4 + k8 \cdot I_{bf}^3 + k9 \cdot I_{bf}^2 + k10 \cdot I_{bf}} + k11 \cdot \log(I_{bf}) + k13 \cdot \log(I_{arc}) + \log\left(\frac{1}{CF}\right) - \log\left(\frac{20}{T}\right)}{-k12} \right)} \quad (D.93)$$

$$AFB_{\leq 600} = 1029 \quad \text{mm} \quad (D.94)$$

Step 7: The final value of AFB can be determined per 4.10.

The final arc-flash boundary is:

$$AFB = AFB_{\leq 600} = 1029 \quad \text{mm} \quad (D.95)$$

Step 8: To account for the arcing current variation, use the equations in 4.5 to find the correction factor.

For VCB, the coefficients from [Table 2](#) are as follows:

$$\begin{aligned} k1 &:= 0 & k2 &:= -0.0000014269 & k3 &:= 0.000083137 \\ k4 &:= -0.0019382 & k5 &:= 0.022366 & k6 &:= -0.12645 & k7 &:= 0.30226 \end{aligned}$$

The VarCf value is:

$$VarC_f := k1 \cdot V_{oc}^6 + k2 \cdot V_{oc}^5 + k3 \cdot V_{oc}^4 + k4 \cdot V_{oc}^3 + k5 \cdot V_{oc}^2 + k6 \cdot V_{oc} + k7 = 0.247 \quad (D.96)$$

$$1 - 0.5 \cdot VarC_f = 0.877 \quad \text{Correction factor} \quad (D.97)$$

Step 9: Adjust the final values of arcing current using the correction factor.

$$I_{arc_min} := \frac{1}{\sqrt{\left(\frac{0.6}{V_{oc}}\right)^2 \cdot \left[\frac{1}{I_{arc_600}}^2 - \left(\frac{0.6^2 - V_{oc}^2}{0.6^2 \cdot I_{bf}} \right) \right]}} \cdot (1 - 0.5 \cdot VarC_f) \quad (D.98)$$

$$I_{arc_min} = 25.244 \quad \text{kA} \quad (D.99)$$

$$T := 319 \quad \text{ms} \quad (D.100)$$

Figure D.4 shows how the arc duration was obtained using the reduced arcing current.

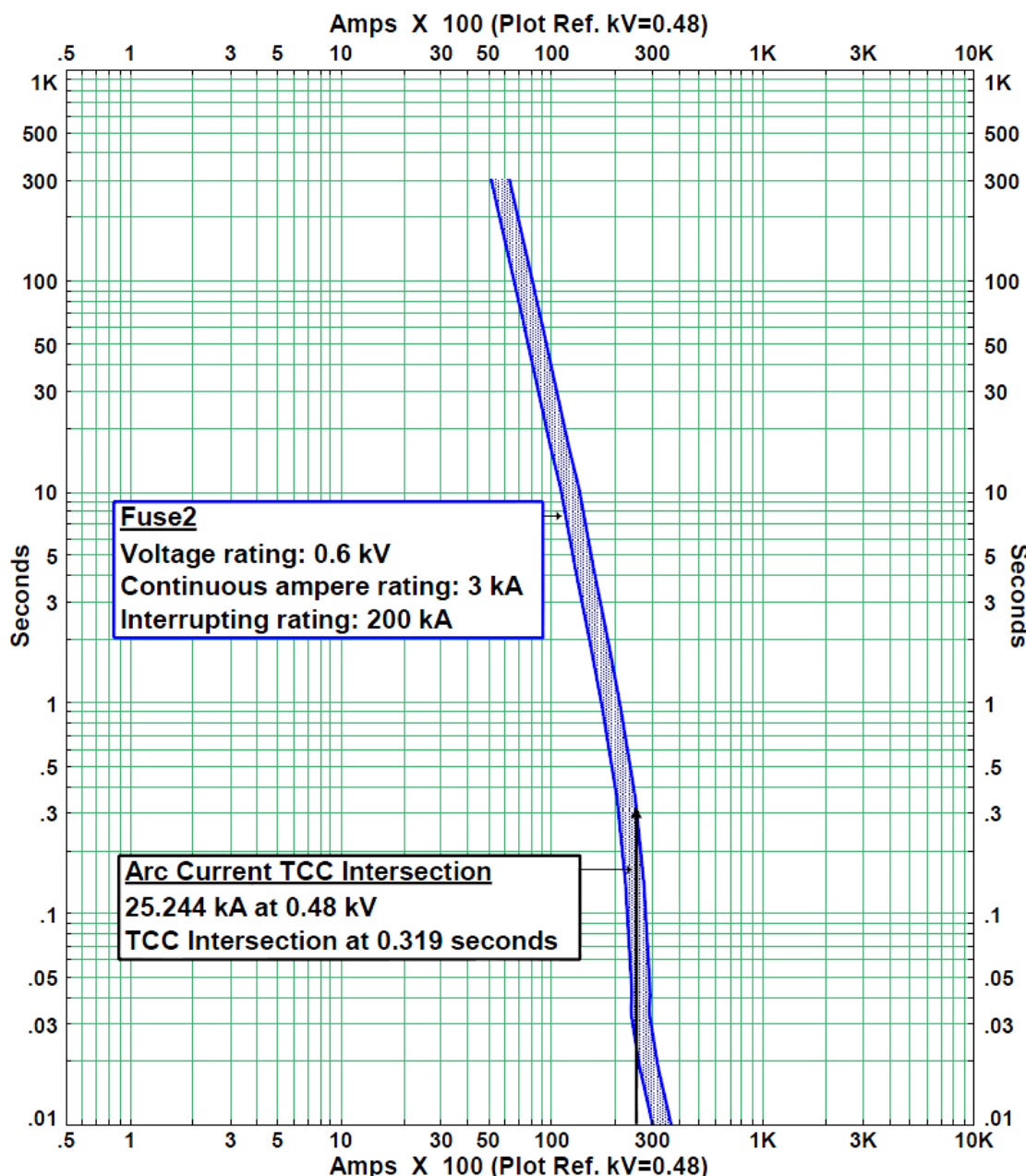


Figure D.4—Determination of arc duration using reduced arcing current

Step 10: Repeat Step 4 using the reduced arcing current.

Using the coefficients from [Table 3](#) and [Equation \(6\)](#), find the intermediate incident energy for ≤ 600 V:

$$\begin{aligned} k1 &:= 0.753364 & k2 &:= 0.566 & k3 &:= 1.752636 & k4 &:= 0 \\ k5 &:= 0 & k6 &:= -4.783 \cdot 10^{-9} & k7 &:= 0.000001962 & k8 &:= -0.000229 \\ k9 &:= 0.003141 & k10 &:= 1.092 & k11 &:= 0 & k12 &:= -1.598 & k13 &:= 0.957 \end{aligned}$$

$$E_{\leq 600} := \frac{12.552}{50} \times T \times 10^{\left(\frac{k1+k2 \cdot \log(G) + \frac{k3 \cdot I_{arc_600}}{k4 \cdot I_{bf}^7 + k5 \cdot I_{bf}^6 + k6 \cdot I_{bf}^5 + k7 \cdot I_{bf}^4 + k8 \cdot I_{bf}^3 + k9 \cdot I_{bf}^2 + k10 \cdot I_{bf}} + k11 \cdot \log(I_{bf}) + k12 \cdot \log(D) + k13 \cdot \log(I_{arc_min}) + \log\left(\frac{1}{CF}\right)}{50} \right)} \quad (D.101)$$

$$E_{\leq 600} := 53.156 \quad \text{J/cm}^2 \quad (D.102)$$

Step 11: The final value of incident energy can be determined per [4.10](#).

The final incident energy is:

$$E = E_{\leq 600} := 53.156 \quad \text{J/cm}^2 \quad (D.103)$$

Step 12: Repeat Step 6 using the reduced arcing current.

Using the coefficients from [Table 3](#) and [Equation \(10\)](#), find the intermediate arc-flash boundary for ≤ 600 V:

$$\begin{aligned} k1 &:= 0.753364 & k2 &:= 0.566 & k3 &:= 1.752636 & k4 &:= 0 \\ k5 &:= 0 & k6 &:= -4.783 \cdot 10^{-9} & k7 &:= 0.000001962 & k8 &:= -0.000229 \\ k9 &:= 0.003141 & k10 &:= 1.092 & k11 &:= 0 & k12 &:= -1.598 & k13 &:= 0.957 \end{aligned}$$

$$AFB_{\leq 600} = 10^{\left(\frac{k1+k2 \cdot \log(G) + \frac{k3 \cdot I_{arc_600}}{k4 \cdot I_{bf}^7 + k5 \cdot I_{bf}^6 + k6 \cdot I_{bf}^5 + k7 \cdot I_{bf}^4 + k8 \cdot I_{bf}^3 + k9 \cdot I_{bf}^2 + k10 \cdot I_{bf}} + k11 \cdot \log(I_{bf}) + k13 \cdot \log(I_{arc_min}) + \log\left(\frac{1}{CF}\right) - \log\left(\frac{20}{T}\right)}{-k12} \right)} \quad (D.104)$$

$$AFB_{\leq 600} = 2669 \quad \text{mm} \quad (D.105)$$

Step 13: The final value of the arc-flash boundary can be determined per [4.10](#).

The final arc-flash boundary is:

$$AFB = AFB_{\leq 600} = 2669 \quad \text{mm} \quad (D.106)$$

Annex E

(informative)

Arc flash

E.1 What is an arc flash? Where and when is it likely to occur?

This annex provides information about arc flashes, their causes and effects, and the places they are likely to occur.

Most arc flashes occur when a person contacts energized terminals or buses with a conducting object. They may be conducting tests or attempting to replace parts. A water leak can also initiate an arc flash. In one case, a roof leak allowed water to enter indoor equipment and run into a 480 V circuit breaker. The circuit breaker exploded and blew open the enclosure door. Tracking can also lead to an arc flash (and may be more likely for system voltage greater than 1000 V).

When an arc flash is initiated, the usually large current generates a strong magnetic field that propels the loose part or tool away. This breaks its contact with the energized parts. As the part moves, the current continues and forms hot arcs that consume conductors, ionizes gases, and generates a plasma cloud. There is a very bright light and the sound of an explosion. The rapidly expanding gases may blow open doors and propel parts, liquid metal droplets, and metal oxide dust. Radiant and convective heat energy may ignite clothing and burn skin on a person a significant distance from the fault. Damage to skin, eyes, ears, and lungs can occur and may be temporary or permanent, and in some cases death may result. Long hospital stays and mental health and family issues can also be common. The injured person may never return to their job.

The arc flash may continue until an upstream overcurrent protective device clears the fault, a time typically from a half cycle to several seconds or it may blow itself out or it may blow out and re-strike.

E.2 Review of incidents in the U.S.

A published paper reviewed the number and types of electrical injuries reported in the U.S. over the 1992 to 2002 timeframe, and is a good starting point for learning about the extent of arc-flash injuries in industry [B13]. The paper was updated with additional data from 2003 to 2009 [B12].

E.3 Analysis of an arc flash in equipment

A recent paper set out to describe the physics of arcing faults in order to describe the energy transfers within fault arcs and, in particular, the three-phase free-burning arcs on parallel electrodes [B90]. This paper and many others in the bibliography (Annex A) are useful for learning about the arcing fault.

Annex F

(informative)

Laboratory test programs

F.1 General

Researchers have conducted test programs at high-power laboratories for the purpose of developing an understanding of the electrical characteristics of arc flashes and the resultant incident energy. Researchers have also endeavored to build a database that could be used to develop empirically based equations or to verify physical model-based equations. This annex includes a description of many tests and a collection of the test data that have been presented in literature.

Three basic types of test setups were employed in the testing as follows:

- Single-phase arc in open air with electrodes in-line as shown in [Figure F.1](#)
- Three-phase arcs in open air with parallel electrodes as shown in [Figure F.2](#)
- Three-phase arcs in a box with parallel electrodes as shown in [Figure F.3](#)

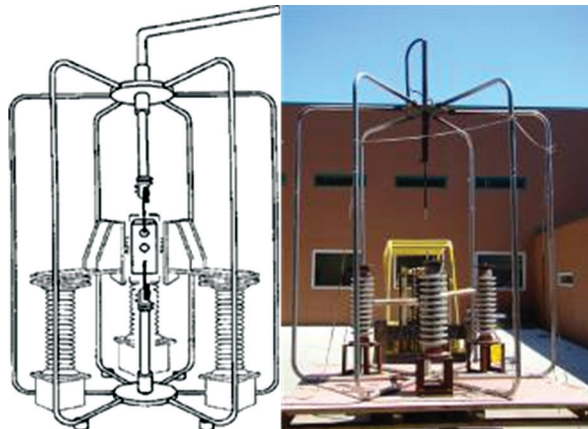


Figure F.1—Test setup A—single-phase arc in air with electrodes in-line and with partial Faraday cage



Figure F.2—Test setup B—three-phase arc in air with electrodes in parallel (VOA)

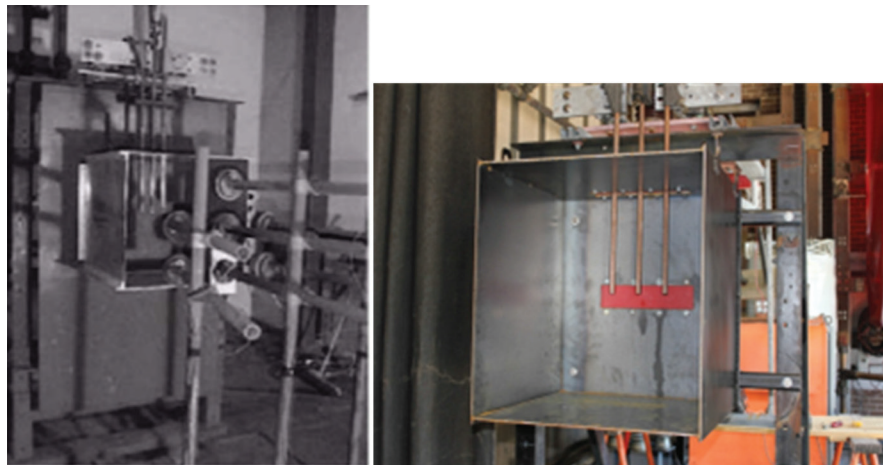


Figure F.3—Test setup C—arc in box (VCB)

F.2 Overview of test programs

The first test program to explore incident energy testing was reported in “Protective clothing guidelines for electric arc exposure” [B71]. Testing was conducted in Laboratory 1 in 2000 using all three of the basic test setups.

The next paper, “Testing update on protective clothing and equipment for electric arc exposure” [B30], used Test setup B and Test setup C. In some cases, only the back of a box was used—a flat panel. In others, a test box of 558.8 mm × 508 mm × 533.4 mm (22 in × 20 in × 21 in) dimensions was used. Testing was conducted in Laboratory 1.

“Predicting incident energy to better manage the electric arc hazard” [B29] was based on Test setup B and Test setup C and employed a 508 mm × 508 mm × 508 mm (20 in × 20 in × 20 in) box. Testing was conducted in Laboratory 1.

“The use of low-voltage current-limiting fuses to reduce arc-flash energy” [B32] used Test setup C, with the addition of current limiting fuses between the laboratory supply and the test box. Tests were also conducted without the fuses to establish a baseline. The box was 508 mm × 508 mm × 508 mm (20 in × 20 in × 20 in) box. Testing was conducted in Laboratory 2.

A basis for incident energy calculations at 2400 V was developed jointly by two laboratories. Test setup B and Test setup C were used in both laboratories. The test box was 1143 mm × 762 mm × 762 mm (45 in × 30 in × 30 in), simulating a medium-voltage equipment enclosure. This data was not previously published.

Testing was performed in Laboratory 1 to develop a verification database for a proprietary analysis program. It used Test setup A, two vertical electrodes in-line or pointed at each other. They were mounted in a partial Faraday cage of the type described in ASTM F1959/F1959M-99. The electrodes were 25.4 mm (1 in) round hard drawn copper.

Testing was performed in Laboratory 3 to investigate the effect of the pressure generated by an arc flash on ship compartments. Incident energy testing was included as part of that program and witnessed by representatives of the IEEE Std 1584-2002 working group. The laboratory used a test chamber that simulated a ship compartment for all tests. It was a 13.6 metric ton (15 tons), 4.9 m × 4.9 m × 3 m (16 ft × 16 ft × 10 ft) enclosure made of steel plate with reinforcing channels and equipped with two naval bulkhead doors. The doors were opened or closed. The test setup was a slight modification of Test setup B, with the electrodes

mounted horizontally and piercing the center of the sidewall of the compartment. Tests were run at 450 V, 4160 V, and 13 800 V ac, and at 1000 V dc.

Further testing was conducted by the IEEE Std 1584-2002 working group in Laboratory 1 to extend the range of 508 mm (20 in) box test data (Test setup C) and thereby extend the range of current limiting fuse data available, and to test used equipment that had been donated. The used equipment included circuit breakers, so that the effects of those circuit breakers on arc-flash energy were documented.

Testing was conducted by the IEEE Std 1584-2002 working group in Laboratory 4. It used Test setup C with a 355.6 mm × 304.8 mm × 190.5 mm (14 in × 12 in × 7.5 in) enclosure. For smaller bus gaps, the electrodes were 6.35 mm × 19.05 mm (0.25 in × 0.75 in) copper bus bars. For larger gaps, they were the standard 19.05 mm (0.75 in) diameter hard drawn copper wire.

Many papers have been published pertaining to the development and use of the 2002 version of this guide [B43], [B21], [B97], [B69], [B93], [B41].

After the publication of IEEE Std 1584-2002, Stokes and Sweeting reported that most of the arc power is stored in the plasma cloud as high temperature enthalpy, and that the convective heating due to the plasma cloud is three times higher than the heating due to radiation alone [B89]. When the calorimeters are placed directly in front of horizontal electrodes in open air as shown in [Figure F.6](#), the arc plasma is driven toward the calorimeters, which results in significantly higher calorimeter measurements than IEEE Std 1584-2002 type setups.

The Institute of Electrical and Electronics Engineers (IEEE) and the National Fire Protection Association (NFPA) formed the Arc Flash Collaborative Research Project in 2004. This initiative supports research and additional testing to increase the understanding of a variety of issues related to arc-flash phenomena. Besides Test setup B and Test setup C, the project team has conducted barrier ([Figure F.4](#)), horizontal in the box ([Figure F.5](#)), and horizontal in the air ([Figure F.6](#)) tests. More than 1800 ac tests have been performed. For each voltage level listed in [Table F.1](#), testing was performed for each combination of bolted-fault current, gap width and one of five configurations. The incident energy was measured at three calorimeter distances from the point of arc initiation. The summary of the conducted tests is shown in [Table F.1](#).



Figure F.4—Vertical conductors, box, with insulating barrier (VCBB)



Figure F.5—Horizontal conductors, box (HCB)

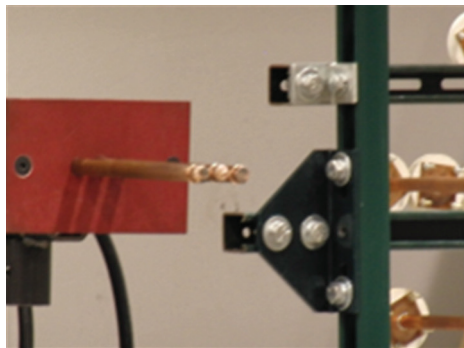


Figure F.6—Horizontal conductors, open air (HOA)

Table F.1—Summary of tests

Voltage (kV)	Current (kA)	Gap		Number of tests ^a	SI units (metric)	Enclosure (H × W × D)	Imperial units
		mm	in				
0.208	2.5–20	6.35–19.05	0.25–0.75	67	355.6 mm × 304.8 mm × 203.2 mm 203.2 mm × 152.4 mm × 152.4 mm	14 in × 12 in × 8 in 8 in × 6 in × 6 in	
0.24	20–41	12.7–25.4	0.50–1.0	25	355.6 mm × 304.8 mm × 203.2 mm	14 in × 12 in × 8 in	
0.3	20–60	25.4–38.1	1.0–38.1	24	355.6 mm × 304.8 mm × 203.2 mm	14 in × 12 in × 8 in	
0.311	17–26	6.35–12.7	0.25–0.5	11	355.6 mm × 304.8 mm × 203.2 mm	14 in × 12 in × 8 in	
0.48	0.5–80.2	10–50.8	0.4–2.0	369	508 mm × 508 mm × 508 mm	20 in × 20 in × 20 in	
0.575	40	25.4–38.1	1.0–1.5	21	508 mm × 508 mm × 508 mm	20 in × 20 in × 20 in	
0.60	0.5–37	12.7–101.6	0.5–4.0	375	508 mm × 508 mm × 508 mm	20 in × 20 in × 20 in	
2.7	0.5–33	38.1–114.3	1.5–4.5	293	660.4 mm × 660.4 mm × 660.4 mm	26 in × 26 in × 26 in	
2.97	37–40	38.1	1.5	32	660.4 mm × 660.4 mm × 660.4 mm 914.4 mm × 914.4 mm × 914.4 mm	26 in × 26 in × 26 in 36 in × 36 in × 36 in	
3.90	60–65	38.1	1.5	18	660.4 mm × 660.4 mm × 660.4 mm 914.4 mm × 914.4 mm × 914.4 mm	26 in × 26 in × 26 in 36 in × 36 in × 36 in	
4.16	20–63	38.1–76.2	1.5–3.0	184	660.4 mm × 660.4 mm × 660.4 mm	26 in × 26 in × 26 in	
14.3	0.5–42	76.2–152.4	3.0–6.0	274	914.4 mm × 914.4 mm × 914.4 mm	36 in × 36 in × 36 in	
0.253 (1-Ph)	5.0–23	6.35–19.05	0.25–0.75	41	Faraday cage		
12	2.3–9.1	254	10	136	Real equipment		
0.6	1.6–33			22	Real equipment		

^aSome unsustainable tests and equipment damage during tests are not included in the list.

F.3 Physical test methodology

The test method for determining the ability of materials to provide protection against electrical arc flashes is defined in ASTM F1959/F1959M-99. The ASTM standard is the basis for the incident energy testing described in this guide. It is intended by ASTM to enable determination of the incident energy that clothing material can withstand up to the point at which there is a 50% probability that skin under the material would receive a second-degree burn. The test methodology works equally well to determine the incident energy to which a worker would be exposed in case of an arc in a specified electrical installation. The results of the two types of tests are complementary.

For each incident energy test, an array of seven copper calorimeters was located in front of the test electrodes, at a distance D from the centerline of the electrodes. A set of three calorimeters was located in a horizontal row at the same height as the tip of the electrodes. A second set of three calorimeters was located in a horizontal row 152.4 mm (6 in) below the elevation of the electrode tips. The middle calorimeters in each set were aligned with the center electrode. A single calorimeter was located 152.4 mm (6 in) above the center electrode tip.

Incident energy was determined by calculation based on the temperature rise of the copper calorimeters mounted in front of the electrodes. Copper calorimeter temperature rise data in degrees Celsius was converted into incident energy in joules per square centimeter (J/cm^2) by multiplying the temperature by 0.565. To calculate incident energy in calories per square centimeter (cal/cm^2), multiply temperature in degrees Celsius by 0.135. Sensor absorption measurements have determined that absorbed energy is equal to or greater than 90% of incident energy for copper calorimeters. Therefore, incident and absorbed energy are considered as equivalent, and the term incident energy is used.

In order to simulate electrical equipment, hard drawn copper wire, 19.05 mm (0.75 in) in diameter, was used for arc electrodes in all cases except where noted. Electrodes were typically vertically oriented or horizontally oriented in a flat configuration with a side-side spacing. Arcs were initiated by applying bolted fault current through a solid 10 AWG or 20 AWG wire that is connected between the ends of the electrodes (20 AWG wire is used in the IEEE/NFPA collaborative project). For all tests, it was necessary to install insulating support blocks between adjacent electrodes to prevent the electrodes from bending outward due to the extremely high magnetic forces created by the arc currents.

The bolted fault current available at the test terminals was measured by shorting the electrodes together at the top. The duration of all arc tests was selected to reduce damage to the test setup but to allow a measurable temperature rise on the calorimeters.

Phase currents and voltages were measured digitally and rms values were computed. Arc power was computed by integrating the products of phase current and voltage and summing the results. Arc energy was computed by integrating arc power over the arc duration. Typically, all of the described data manipulation was performed using the menu/computation functions resident on the digital oscilloscope.

In order to reduce the impact of arc variability, multiple tests were run for each setup. Because arc duration varies slightly from test to test, a time duration correction factor was applied to the temperature rise data from the seven copper calorimeter sensors so that each reported incident energy was based on an arc duration of 200 ms. For the early test programs, the mean incident energy for the seven sensors and the mean maximum incident energy recorded by a single sensor were calculated for each test. In the testing monitored by the committee, each test was reported separately, so mean and maximum incident energy were reported.

Annex G

(informative)

Development of model

G.1 Summary

The new model was developed based on over 1860 tests performed by the project at different voltage levels. The model performance was also evaluated against the existing IEEE Std 1584-2002 test results (approximately 300 tests). The new model performance was evaluated against 932 tests between 0.208 kV to 0.6 kV, 325 tests at 2.7 kV, 202 tests at 4 kV, and over 400 tests between 12 kV and 15 kV.

The new IEEE 1584 arc-flash model is an empirically derived model, and just like the 2002 model, is considered to yield consistent results when applied within the recommended range of its parameters. The model was evaluated as a whole, and its performance was observed using a holistic approach. It is the conclusion that this model produces results that are more accurate than those of its predecessor for configurations common in both models. Further, the new model provides a method to evaluate the incident energy for other configurations not previously considered, such as vertical conductors in a box with a barrier and horizontal conductors in a box and without a box.

G.2 Configurations of the testing

Open-air (OA) and enclosure configurations have been used. The metal enclosures used in the test are with an open front end. Electrodes are open-tipped, and testing has been conducted with vertical and horizontal electrodes; both of which are terminated at the vertical center of the enclosure. In addition, for the “Barrier” configuration, vertical electrodes are terminated at the bottom of the box. The configurations, illustrated in [Figure G.1](#) through [Figure G.5](#), are defined as follows:

- VCB: Vertical Electrodes, Metal “Box” Enclosure ([Figure G.1](#))
- VCBB: Vertical Electrodes terminated in an insulating barrier, Metal “Box” Enclosure ([Figure G.2](#))
- HCB: Horizontal Electrodes, Metal “Box” Enclosure ([Figure G.3](#))
- VOA: Vertical Electrodes, Open Air ([Figure G.4](#))
- HOA: Horizontal Electrodes, Open Air ([Figure G.5](#))



Figure G.1—VCB (vertical electrodes inside a metal “box” enclosure)



Figure G.2—VCBB (vertical electrodes terminated in an insulating “barrier,” inside a metal “box” enclosure)



Figure G.3—HCB (horizontal electrodes inside a metal “box” enclosure)



Figure G.4—VOA (vertical electrodes in open air)

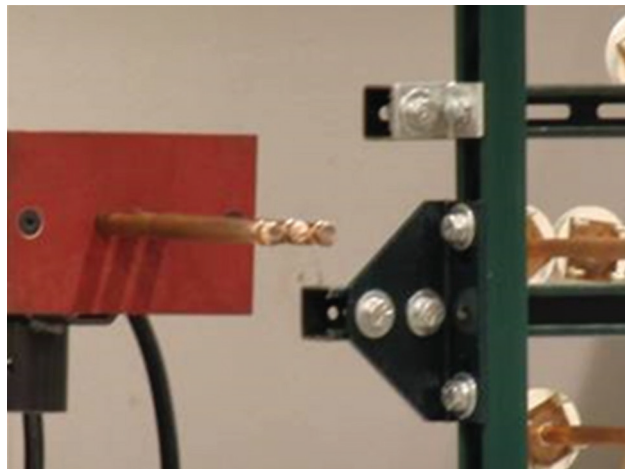


Figure G.5—HOA (horizontal electrodes in open air)

G.3 Summary of conclusions

Analysis of the data allowed the following conclusions:

- a) Based on the relationships among arc energy, incident energy, and arc duration, arc duration has a linear effect on the incident energy.
- b) Distance from the arc to the calorimeters has an inverse exponential affect.
- c) System X/R ratio, frequency, electrode material, and other variables that were considered were found to have little or no effect on arc current and incident energy, and so they are neglected.
- d) Arc current depends primarily on available short-circuit current, bus gap (the distance between conductors at the point of fault), electrode configurations, enclosure size, and system voltage.
- e) Incident energy depends primarily on calculated arc current, arcing duration, and working distance. Bus gap is a smaller factor.

G.4 Observations from test results

The orientation of the electrodes determines the direction of the arc plasma flow, which is most easily observed for the open-air arc tests shown in [Figure G.6](#) and [Figure G.7](#). When calorimeters are placed in front of the horizontal electrodes shown in [Figure G.6](#), the arc plasma is driven directly toward the calorimeters; in contrast in [Figure G.7](#), the vertical electrodes drive the arc plasma in a downward direction that does not intersect the calorimeter surface. Consequently, the horizontal electrode orientation transmits more heat to the calorimeter. The arc-testing program implemented for the development of the initial standard, IEEE 1584-2002, involved vertical electrodes in open air and in enclosures. When an arc has been initiated between vertical electrodes in an enclosure (VCB) as shown for a different test series in [Figure G.8](#), the arc plasma is driven toward the bottom of the box. However, the arc-plasma cloud, somewhat contained by the box, overflows the box's frontal opening in the direction of the calorimeters and more heat flows to the calorimeter surface than for vertical electrodes in open air. Therefore, configuration is an important factor for incident energy estimation. To estimate arc current and incident energy, the user will need to select one of the five configurations that best describes the arrangement of the electrical equipment.



Figure G.6—Horizontal electrodes (plasma pushed to the left, horizontal direction)



Figure G.7—Vertical electrodes (plasma pushed vertically downward)

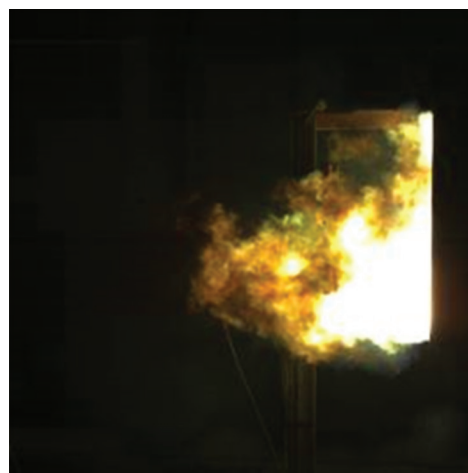


Figure G.8—VCB, vertical electrodes in enclosure (plasma cloud “spills” out of box)

G.5 Model development—Raw test data processing

G.5.1 General

This annex provides a description of the processes used to develop the new IEEE 1584 arc-flash model. It includes examples of raw data processing and describes algorithms and mathematical tools used in its development.

G.5.2 Arcing current data processing

In order to accurately predict the response time for the protective devices to clear a fault current, the arcing current should be precisely estimated. Depending on the fault inception angle and X/R ratio of the Thevenin equivalent impedance at the point of the fault, the arcing current may contain dc component. As shown in [Figure G.9](#), the decaying of dc offset can be seen in a 13.8 kV, 20 kA arc-flash test.

In normal conditions, voltage and current waveforms are relatively symmetrical sine waves. When a fault is suddenly applied to the system, addition of the dc component to the symmetrical short-circuit current gives the asymmetrical fault current. As qualitatively illustrated in [Figure G.9](#), a dc component is introduced at the initiation of the fault due to the system's inductance preventing instantaneous changes in current. [Figure G.10](#) shows the dc offset and decay trend in asymmetrical ac current. [Table G.1](#) provides the typical decay rate of dc offset based on system X/R ratio.

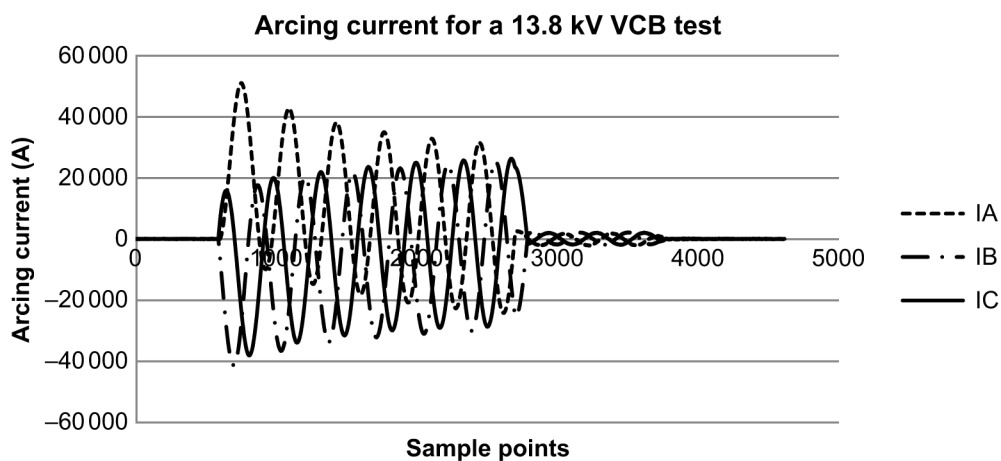


Figure G.9—Arcing current recording from 13.8 kV arc-flash test

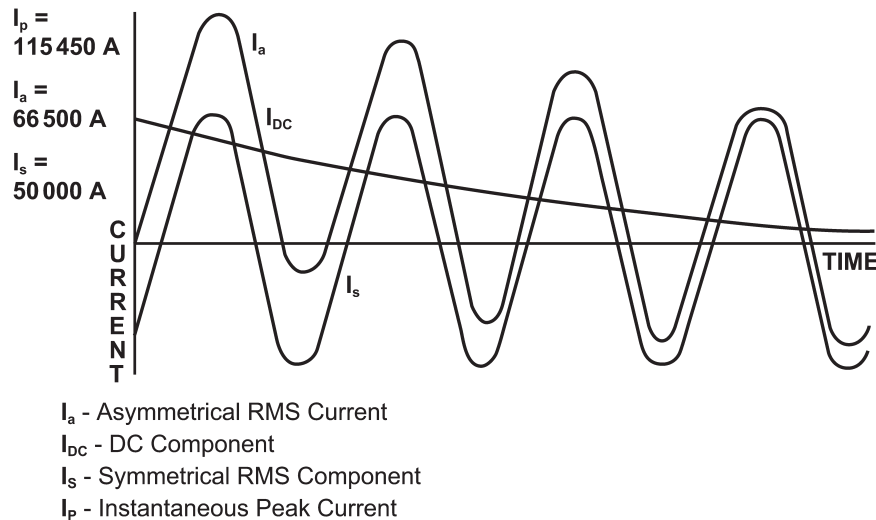


Figure G.10—DC offset and decay trend of asymmetrical ac current

Table G.1—Typical dc offset decay rate in power system

Short-circuit power factor (%)	Short circuit X/R ratio	Maximum 1-Φ instantaneous peak	Maximum 1-Φ rms at half-cycle	Average three-phase rms at half-cycle
10	9.9301	2.455	1.437	1.229
20	4.8990	2.183	1.247	1.127
30	3.1798	1.978	1.130	1.064
40	2.2913	1.819	1.062	1.031
50	1.7321	1.694	1.026	1.013
100	0.000	1.414	1.000	1.000

The decay time of the dc component depends on the X/R ratio of the circuits, and it may affect the fuse-clearing time. However, when microprocessor relay systems are applied, in most cases the dc offset and harmonic components are filtered and the only rms current is used to determine the operating time.

The inception angle of the fault cannot be predicted and the X/R ratio of the system is not typically known with very much accuracy. Neglecting the dc offset and harmonic components when estimating the arcing current should produce the most conservative results.

A filtering algorithm was embedded into the mathematical procedures for arcing current data processing to estimate the arcing current based on the rms value of the fundamental ac component. A commonly used digital filter in the protective relay industry is the cosine filter. The equations for the cosine filter used in the arcing current modeling (using 16 samples per cycle) are shown as follows.

The filter coefficients:

$$CFC_n = \cos\left(\frac{2\pi}{16}n\right) \quad (G.1)$$

The cosine filter:

$$IX_{\text{sample+spc}} = \frac{2}{N+1} \sum_{n=0}^N I_{\text{sample+spc-n}} \cdot CFC_n \quad (G.2)$$

The phasor magnitude:

$$|I_o|_{\text{sample+spc}} = \sqrt{\left(IX_{\text{sample+spc}}\right)^2 + \left(IX_{\text{sample+spc}-\frac{\text{spc}}{4}}\right)^2} \quad (\text{G.3})$$

The phasor output:

$$I_{o_{\text{sample+spc}}} = IX_{\text{sample+spc}} + j \cdot IX_{\text{sample+spc}-\frac{\text{spc}}{4}} \quad (\text{G.4})$$

where

N	= 16
n	= 0, 1, 2 ... N
sample	= sequence of samples 0, 1, 2, 3, ..
spc	= number of samples per cycle (it is 16 for this example)
$I_{\text{sample+spc-n}}$	= current samples
$IX_{\text{sample+spc}}$	= filter output

The filtering process determines the components' change in magnitude when the sampling interval remains fixed and the input frequency is varied. While extracting the fundamental component, the filter rejects the exponentially decaying dc component, as well as harmonics.

The dc offset of the arcing current is thus filtered before performing I_{arc} estimation in the model; however, in incident energy estimation, from a conservative protection point of view, the original unfiltered current data is utilized in incident arc energy calculation process.

The measured arcing current data are processed by a cycle-by-cycle cosine filter applied to the raw data based on the recording sampling rate (typical is 20 k samples per second). A sliding window is employed for each cycle of data to determine the fundamental 60 Hz rms current to remove dc offset and other higher order harmonics. [Figure G.11](#) shows the filtered rms value of arcing current compared to the unfiltered rms value of arcing current.

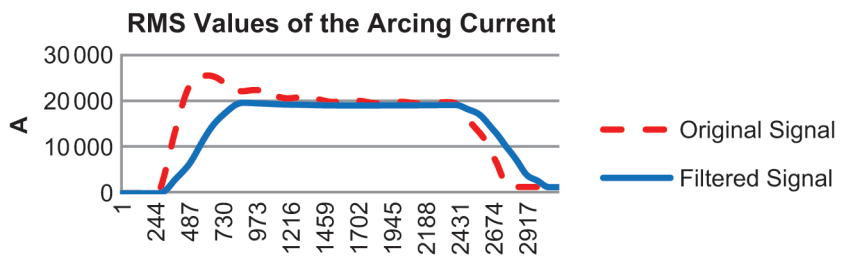


Figure G.11—Filtered and unfiltered rms arcing current comparison

To create stable arcing, it takes some time to melt the trigger wire and establish an arcing path at the beginning of arc initiation. Thus, to allow for the accuracy of the arcing current estimation, two cycles of data are excluded to avoid estimation errors from mixing arcing and non-arcing data in the process. Because lower values are obtained when mixing these two conditions, last two cycles of data after descending order are excluded. An average current will be taken from $N_s \times (N-2)$ current data points where N_s is the number of samples per cycle and N is the arc-flash duration in number of cycles. All three phases are averaged together. As the model is based on the average of all three phases, single-phase clearing effects cannot be applied.

As observed from the test, the arcing current is relatively stable when the open circuit voltage is higher than 2700 V. However, the arcing current becomes dynamic and unstable at lower voltage (below 600 V), which makes it difficult to model I_{arc} based on laboratory test data.

Figure G.12 is a six-cycle arcing current plot on a three-phase 480 V test with 17.2 kA bolted fault current. Compared to the 13.8 kV arcing current recording shown in **Figure G.9**, a 480 V arcing current may have a complex time structure during the arc event. There is no consistent trend during the entire single test.

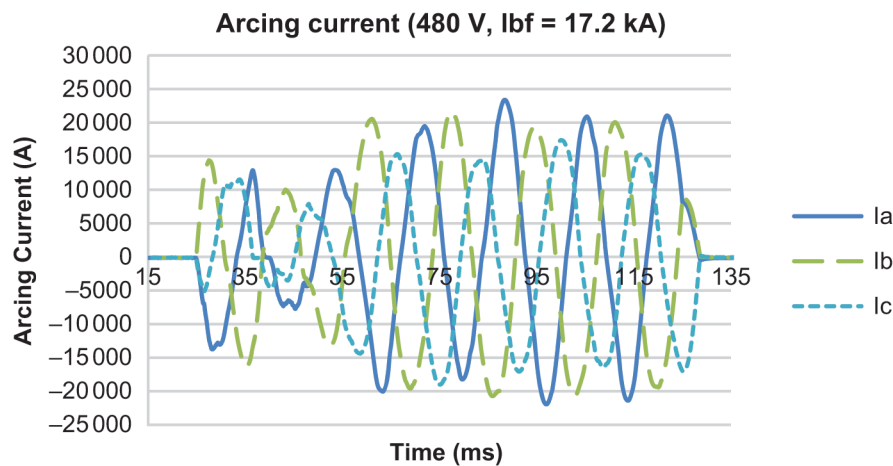


Figure G.12—Arcing current recording for a 480 V arc-flash test

In lower voltage (<600 V) tests, arcing current generally decreases with system voltage when other conditions remain the same. According to published literature [B2], per centimeter voltage drop of the arc column remains almost the same when the arcing current is high enough. Therefore, per centimeter arc column resistance is increased when the open circuit voltage is dropped. On the other hand, lower arcing current produces lower electrical force to reduce the length of the arc column. From the research and the observation of the test results, these two effects offset each other and cause very small variation of the arc resistance when the open circuit voltage of the system is lower. With other conditions remaining the same, it was assumed that the arc resistance remains the same when the system voltage varies between 208 V and 600 V. Based on this, it is possible to derive arcing current below 600 V from well-behaved 600 V estimation results. **Table G.2** provides some sample arcing resistance values recorded for 600 V and below tests.

Table G.2—600 V and below, arcing current, voltage, and resistance

Configuration	V_{oc} (kV)	I_{bf} (kA)	Gap (mm)	I_{arc} (kA)	V_{arc} (V)	R_{arc} (mΩ)
VCBB	0.300	20.000	25.4	13.734	108.66	7.91
VCBB	0.480	20.000	25.4	16.539	114.07	6.90
VCBB	0.300	20.000	25.4	15.736	103.66	6.59
VCBB	0.480	20.000	25.4	16.872	101.96	6.04

The information in **Table G.2** demonstrates that the arcing resistance is similar for the same configuration and bolted fault current.

G.5.3 Incident energy data processing

Arc energy depends on many electrical factor characteristics. Under the same bolted fault current, higher arc voltage typically implies higher arc energy. A greater gap width could also result in increased arc energy as

well. From the observation on arc-flash tests, the arc-column length increases with increases in gaps between conductors, which could cause an increased arc energy by longer gap distance. Sample energy results for horizontal electrode in open air and vertical electrode in open air are provided in [Table G.3](#) and [Table G.4](#).

**Table G.3—Arc energy comparison on different gap length
(horizontal electrodes in open air tests)**

600 V, 20 kA (HOA)			2.7 kV, 20 kA (HOA)		
G mm (in)	Arc energy (MJ)		G mm (in)	Arc energy (MJ)	
	6 cycles	12 cycles		6 cycles	12 cycles
31.75 (1.25)	0.9196	1.8652	76.2 (3.0)	2.0908	4.1432
31.75 (1.25)	0.8796	1.8959	76.2 (3.0)	2.0469	4.0150
31.75 (1.25)	0.8946	1.7772	76.2 (3.0)	2.0409	3.9868
50.8 (2.0)	0.9890	1.9584	114.3 (4.5)	2.1033	4.1882
50.8 (2.0)	0.9859	1.9154	114.3 (4.5)	2.1568	4.1318
50.8 (2.0)	1.0236	1.9285	114.3 (4.5)	2.1527	4.1430

**Table G.4—Arc energy comparison on different gap length
(vertical electrodes in open air tests)**

600 V, 20 kA (VOA)			2.7 kV, 20 kA (VOA)		
G mm (inch)	Arc energy (MJ)		G mm (inch)	Arc energy (MJ)	
	6 cycles	12 cycles		6 cycles	12 cycles
12.7 (0.5)	0.9507	1.8779	76.2 (3.0)	1.9977	4.0263
12.7 (0.5)	0.9954	1.8752	76.2 (3.0)	2.0207	3.8896
12.7 (0.5)	0.9972	1.8529	76.2 (3.0)	1.9754	3.9059
31.75 (1.25)	1.0072	1.9741	114.3 (4.5)	2.4400	4.7643
31.75 (1.25)	1.0027	1.9352	114.3 (4.5)	2.4020	4.6293
31.75 (1.25)	0.9984	1.8876	114.3 (4.5)	2.4225	4.5813

As shown in [Table G.3](#) and [Table G.4](#) in the same configuration, arc energy tends to increase with correspondingly larger gap spacing. Although the arc energy may be different at different voltage levels, the ratio of incident energy to arc energy (IE/E_{arc}) tends to be similar when the bolted fault currents are identical. [Table G.5](#) shows the sample result for horizontal electrode in open-air test.

Table G.5— IE/E_{arc} comparison

Horizontal electrodes in open air arc-flash tests					
600 V, 20 kA (HOA)			2.7 kV, 20 kA (HOA)		
D mm (in)	IE/E_{arc} (cal/cm ² /MJ)		D mm (in)	IE/E_{arc} (cal/cm ² /MJ)	
	Average	Peak		Average	Peak
914.4 (36)	1.2482	1.3116	914.4 (36)	1.2355	1.3097
685.8 (27)	1.9224	2.1035	685.8 (27)	1.8883	2.0972
457.2 (18)	3.6633	4.5528	457.2 (18)	3.7651	4.8112

For HOA configurations on [Table G.5](#), the incident energy to arc energy (IE/E_{arc}) is similar between 600 V and 2.7 kV. The slight difference may be caused by the loss along a longer arc column at higher voltages, or plasma flow partially blocked by calorimeter in a nearer distance. This is just a speculation that attempts to explain this observation. From the standpoint of model development, the differences or errors are within tolerance.

G.5.4 Modeling parameter sensitivity analysis

For the model development process, parameter correlation analysis is the first step to understand the relationships between dependent and independent variables. Observations on the test data provide some basic hints to discover the relationship(s). Representative 600 V energy analysis is provided in [Figure G.13](#) through [Figure G.15](#), which are a horizontal electrode in the open-air test configuration, vertical electrode in the open air test configuration, and vertical electrode in the metal enclosure test configuration, respectively. These data were obtained with a 50.8 mm (2 in) electrode gap width over a 12 cycles arc duration, and the working distance is 457.2 mm (18 in). As shown on these figures, incident energy tends to rise with increasing bolted fault current, in which the arcing energy is increasing. In open-air tests, there is substantially less incident energy because the enclosure may direct the plasma toward to calorimeter array. Similarly, lower incident energy is detected in vertical electrode configurations compared to horizontal setups.

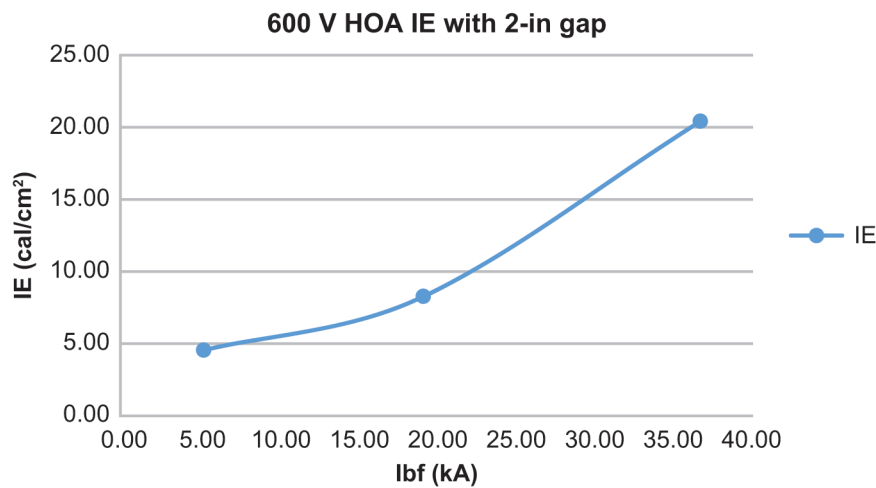


Figure G.13—600 V HOA IE with 50.8 mm (2 in) gap

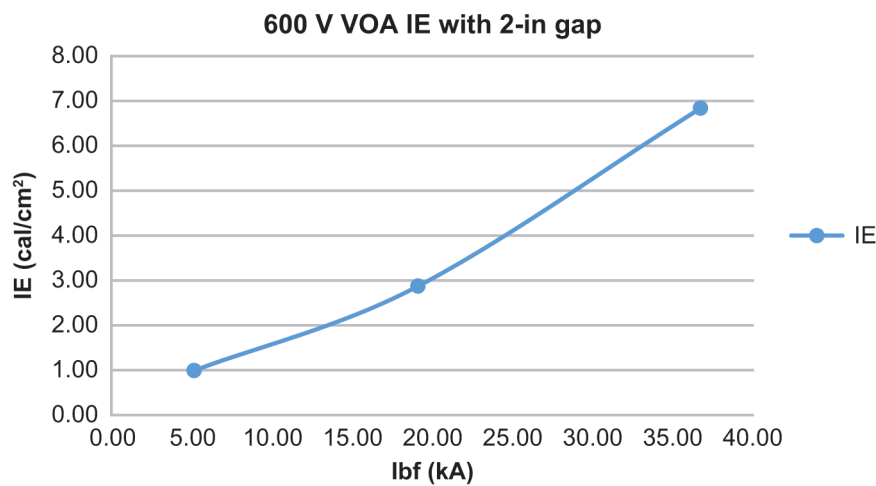


Figure G.14—600 V VOA IE with 50.8 mm (2 in) gap

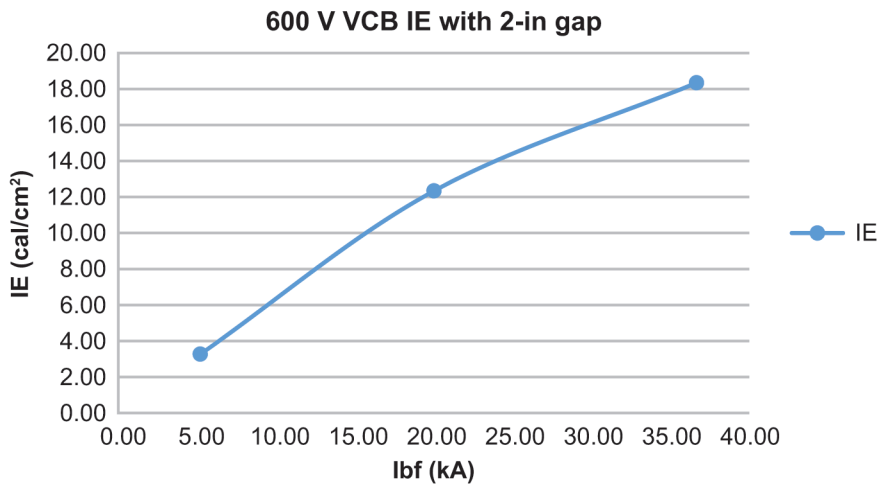


Figure G.15—600 V VCB IE with 50.8 mm (2 in) gap

Figure G.16 and Figure G.17 are representative incident energy plots for a 2.7 kV test for a horizontal electrode in a metal enclosure configuration. Figure G.16 and Figure G.17 show the incident energy of 76.2 mm (3 in) and 114.3 mm (4.5 in) electrode gap setup, respectively. In both cases, the calorimeter was placed 609.6 mm (24 in) from the arcing point. As shown in these figures, the correlation between incident energy level and gap width is relatively strong. In other words, arc energy is proportional to the electrode gap width.

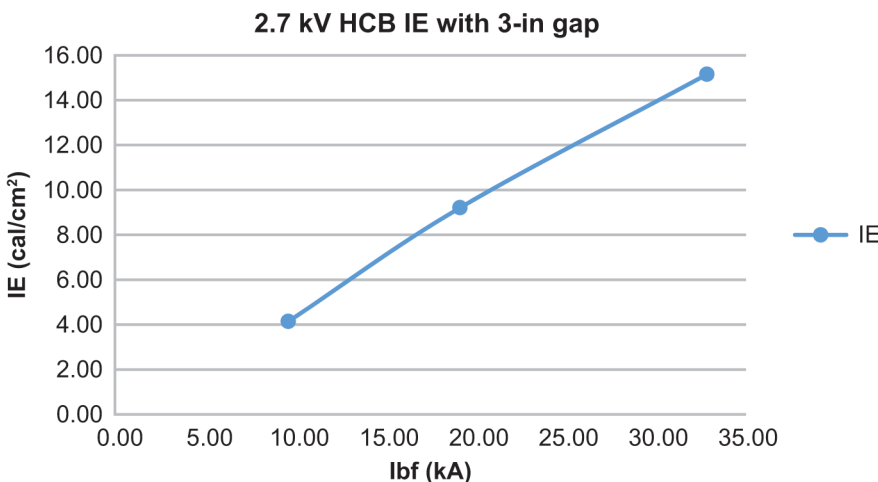


Figure G.16—2.7 kV HCB IE with 76.3 mm (3 in) gap

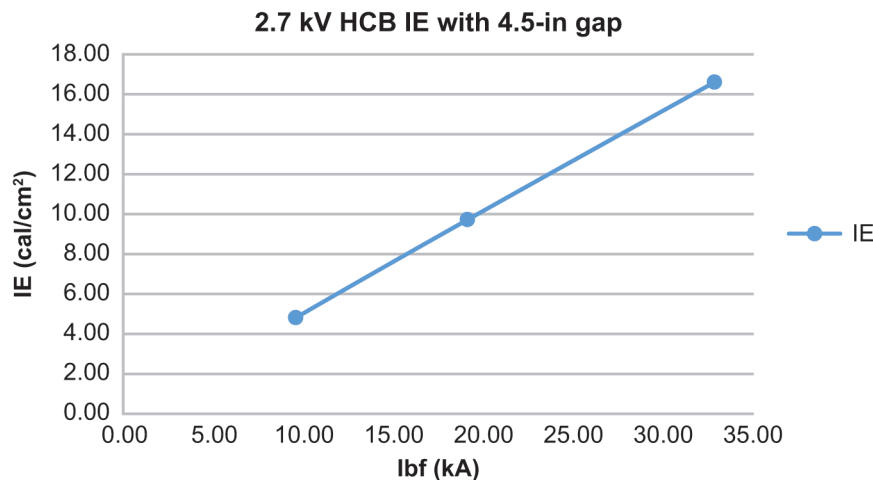


Figure G.17—2.7 kV HCB IE with 114.3 mm (4.5 in) gap

Figure G.18 and Figure G.19 are representative incident energy plots for a 14.3 kV test for vertical electrode in open-air test configuration and horizontal electrode in open air configuration, with 20 kA bolted fault current and 95.25 mm (3.75 in) gap width between electrodes. From these two figures, one can see that the incident energy level falls off with distance. Besides, there is higher incident energy exposure in horizontal electrode configuration as compared to the vertical one. Thus, it can be seen that the test configuration has a substantial impact on incident energy level.

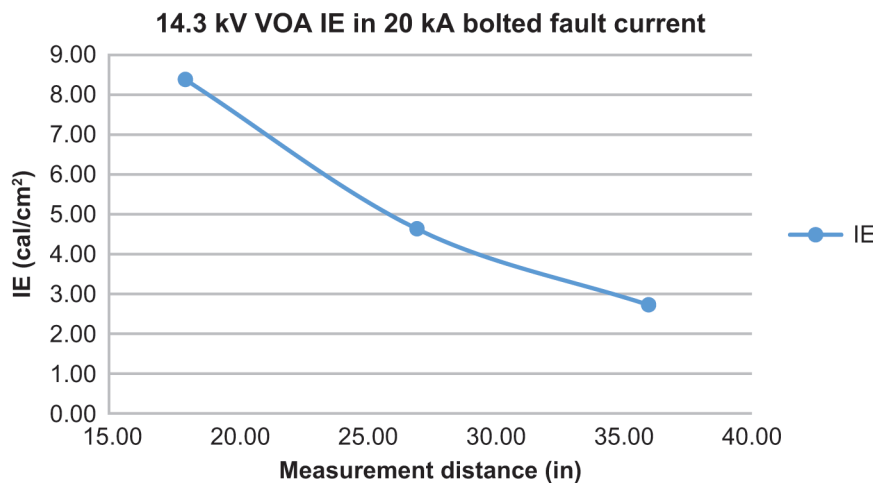


Figure G.18—14.3 kV VOA IE in 20 kA bolted fault current

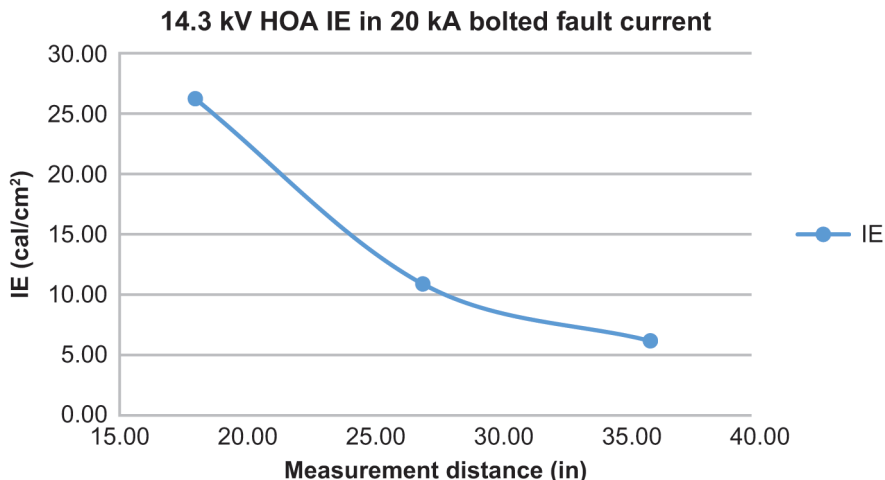


Figure G.19—14.3 kV HOA IE in 20 kA bolted fault current

To provide the theoretical basis, some applied statistic approaches are utilized to analyze parameter sensitivity to incident energy and arcing current.

Although single variable linear regression provides an indication of the nature of the relationship between the independent variable and the dependent variable, multiple independent variables can interact with each other to affect the dependent variable and complicate the analysis. Partial regression analysis is applied to show the effect of adding a variable to a model already having one or more independent variables; also, it may take into account the effect among the other independent variables in the model.

Partial regression is formed by:

- Computing the residuals of regressing the response variable against the independent variables but omitting X_i
- Computing the residuals from regressing X_i against the remaining independent variables
- Plotting the residuals from item a) against the residuals from item b)

For example, [Figure G.20](#) shows one partial regression plots on the arcing current modeling process. This example, plot indicates the dependence between bolted fault current and arcing current.

From the figure, it shows a very good linearization performance between arcing current and bolted fault current. Additionally, the increasing trend from the figure indicates the positive correlation between independent variable and dependent variables.

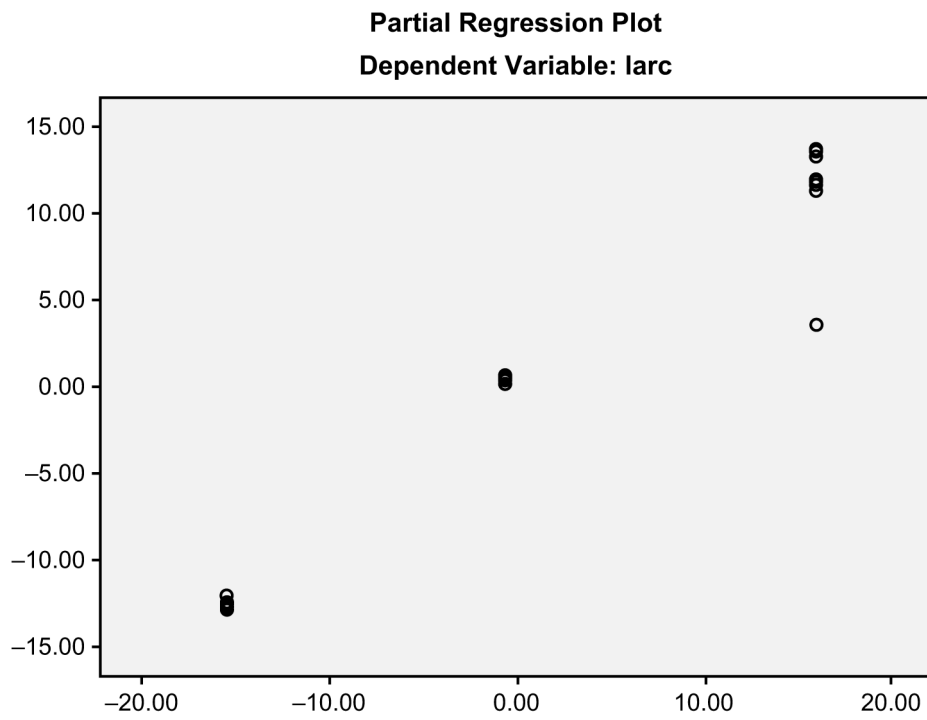


Figure G.20—Sample result for partial regression plotting

G.5.5 Arcing current parameter sensitivity analysis

When performing a partial regression with a single independent variable, a scatter plot of the response variable against the independent variable provides a good indication of the nature of the relationship. This subclause included a detailed example to show the sensitivity analysis for 14.3 kV arcing current analysis steps.

- a) Take logarithm on all variables before regression process.
- b) Convert I_{arc} to $\log I_{\text{arc}}$, I_{bf} to $\log I_{\text{bf}}$, Gap to $\log \text{Gap}$ for model development purposes.
- c) Enter all 14.3 kV converted data into commercially available statistic software. (See [Figure G.21](#).)
- d) Choose $\log I_{\text{arc}}$ as dependent variable Y , $\log I_{\text{bf}}$ and $\log \text{Gap}$ as independent X_1 and X_2 , respectively. (See [Figure G.22](#).)
- e) Compute the residuals of regressing the response variable against the dependent variables Y but omitting X_1 , then X_2 .
- f) Compute the residuals from regressing X_1 , then X_2 against the remaining dependent variables Y .
- g) Plot the residuals from step e) against the residuals from step f). (See [Figure G.23](#).)
- h) The software will generate the regression results and plot the partial regression figures, which is provided in [Figure G.24](#) and [Figure G.25](#).

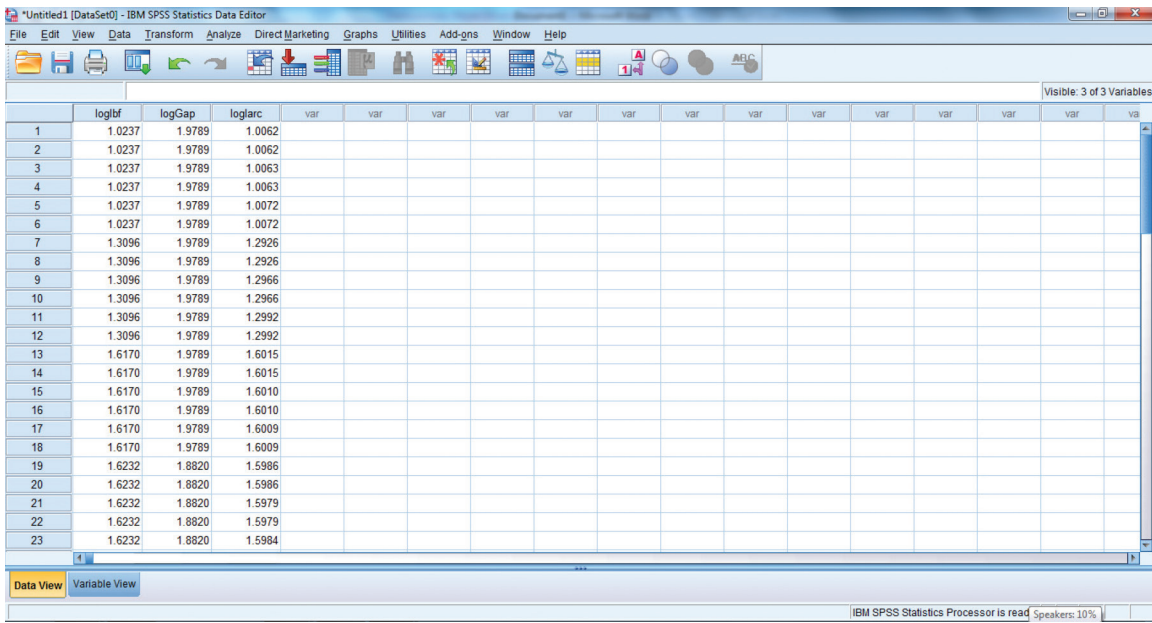


Figure G.21—Data input interface

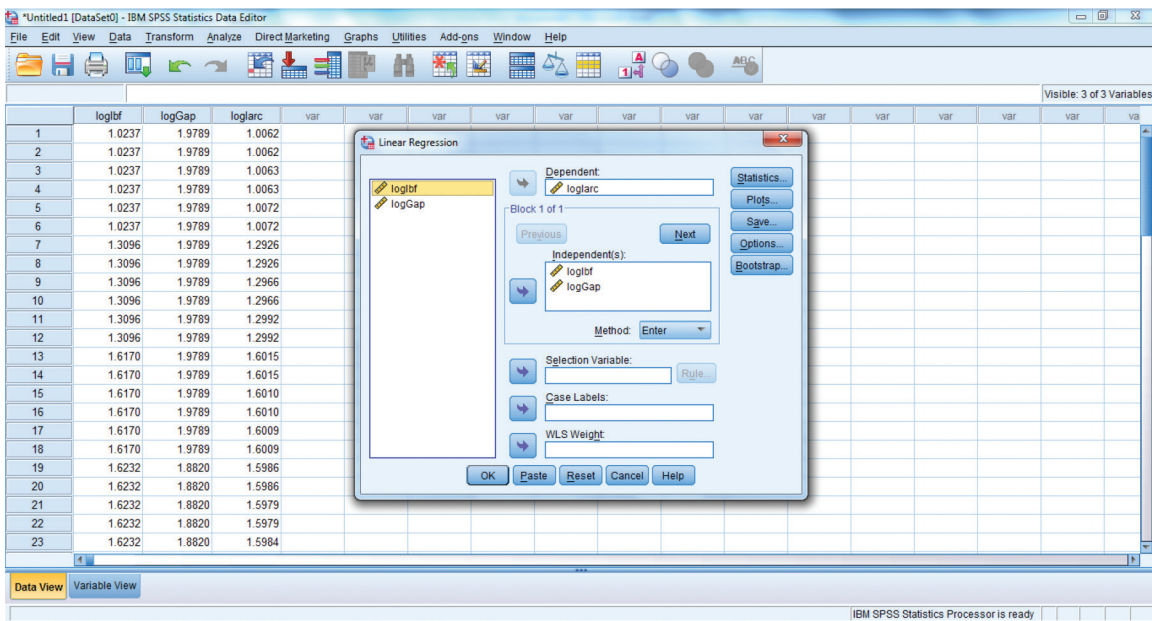


Figure G.22—Parameter selection

From the partial regression plots in [Figure G.24](#) shown above ($\log I_{\text{arc}}$ versus $\log I_{\text{bf}}$), it has strong positive linear correlation between $\log I_{\text{arc}}$ and $\log I_{\text{bf}}$.

From [Figure G.25](#), it is clear to see that there is good linear relationship between $\log I_{\text{arc}}$ and $\log \text{Gap}$. With the same I_{bf} , I_{arc} decreases with the increasing of gap width. Additionally, at the same gap level, I_{ratio} ($I_{\text{arc}}/I_{\text{bf}}$) will decrease when I_{bf} increases.

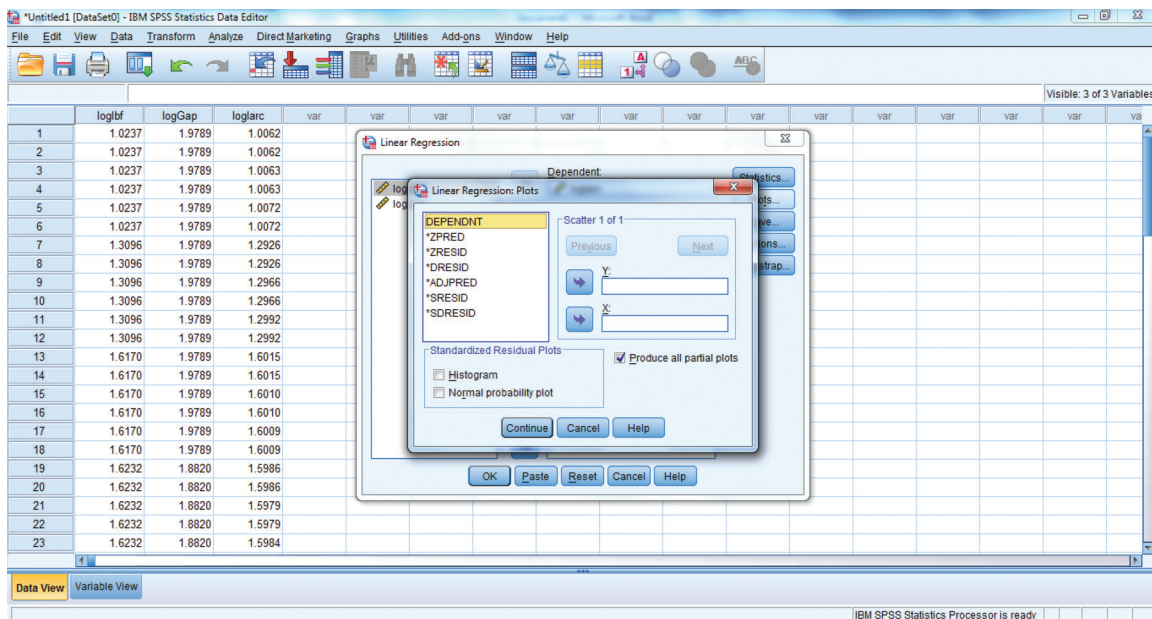


Figure G.23—Partial regression calculation

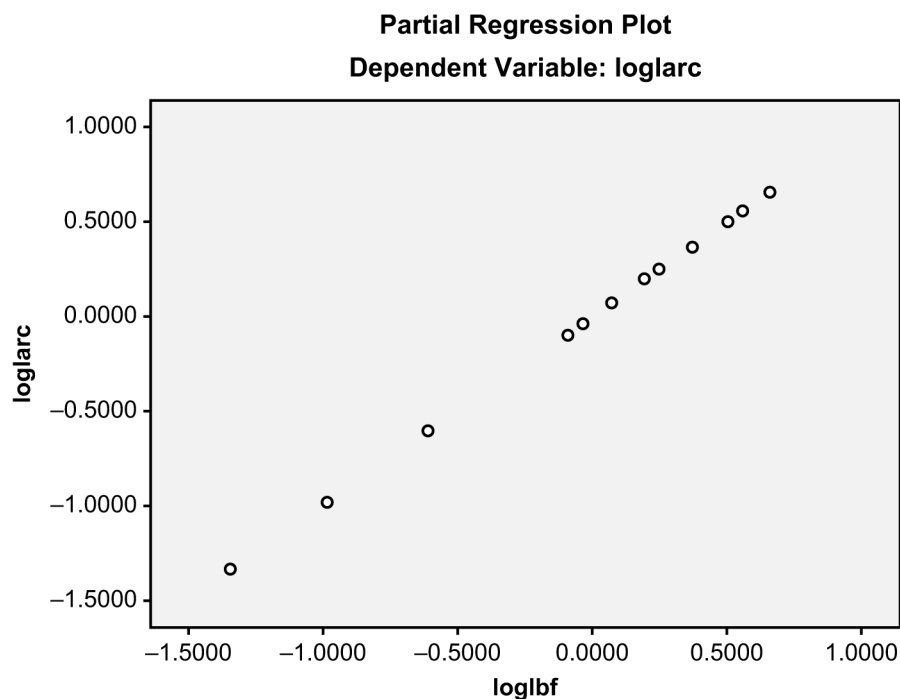


Figure G.24—Sensitivity analysis for I_{bf} against I_{arc}

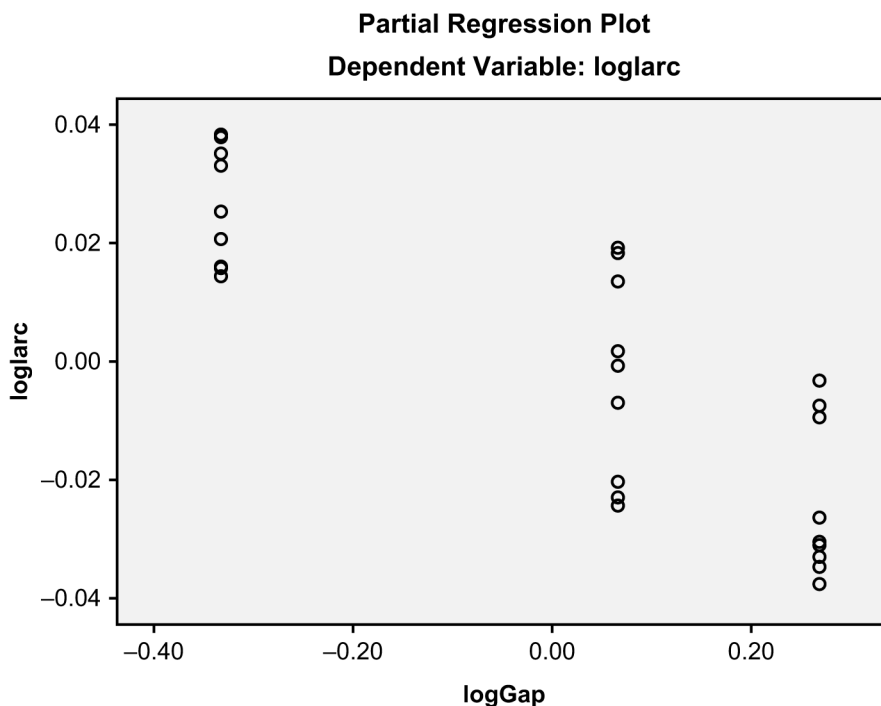


Figure G.25—Sensitivity analysis for gap against I_{arc}

G.5.6 Incident energy parameter sensitivity analysis

The process of incident energy model development involves approximately 150 possible correlations among five variables. A partial regression was performed to find the correlation between incident energy to other parameters. Sample partial regression results are shown in [Figure G.26](#), [Figure G.27](#), and [Figure G.28](#).

From [Figure G.26](#), the partial regression results clearly show the relationship between working distance and incident energy. Shorter distance results in a greater reception of energy during the arc flash.

I_{arc} and IE are positively correlated, as shown in [Figure G.27](#).

The gap width is also a vital factor for incident energy level. From [Figure G.28](#), a larger gap between electrodes causes higher incident energy.

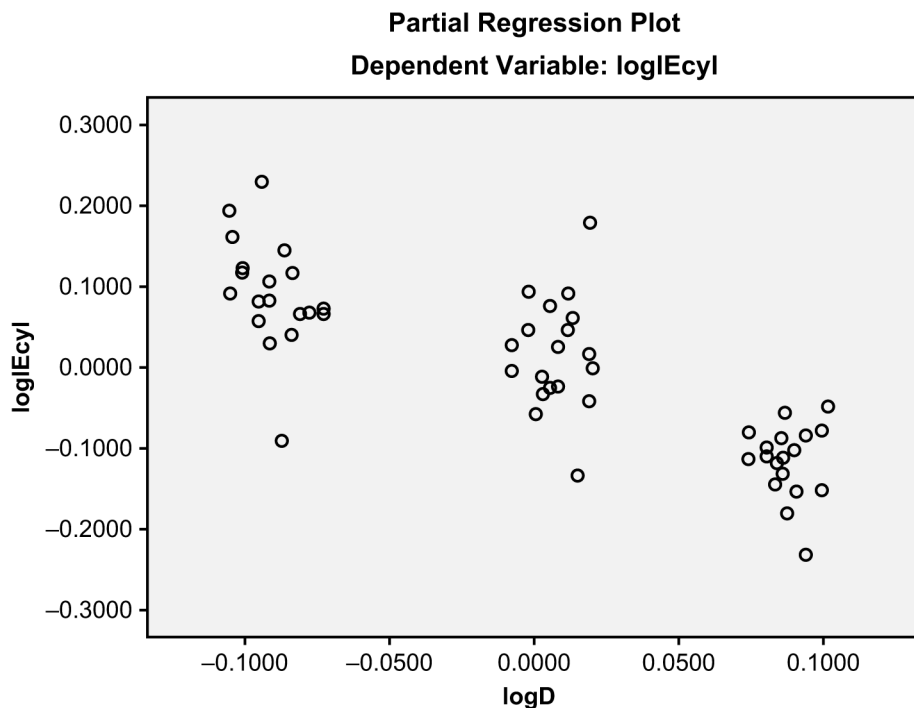


Figure G.26—Sensitivity analysis for distance versus IE

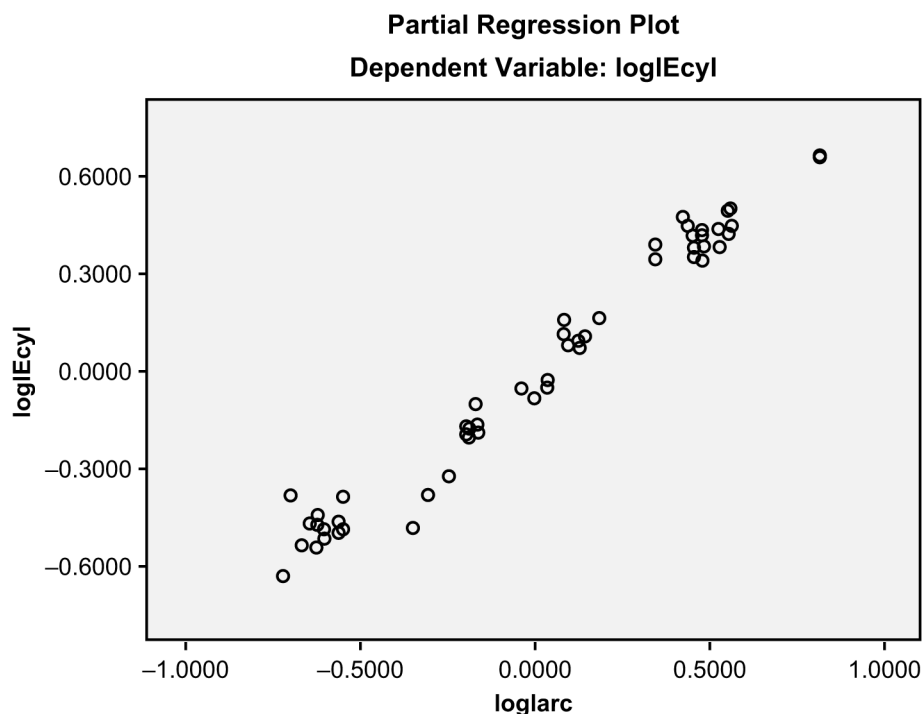


Figure G.27—Sensitivity analysis for I_{arc} against IE

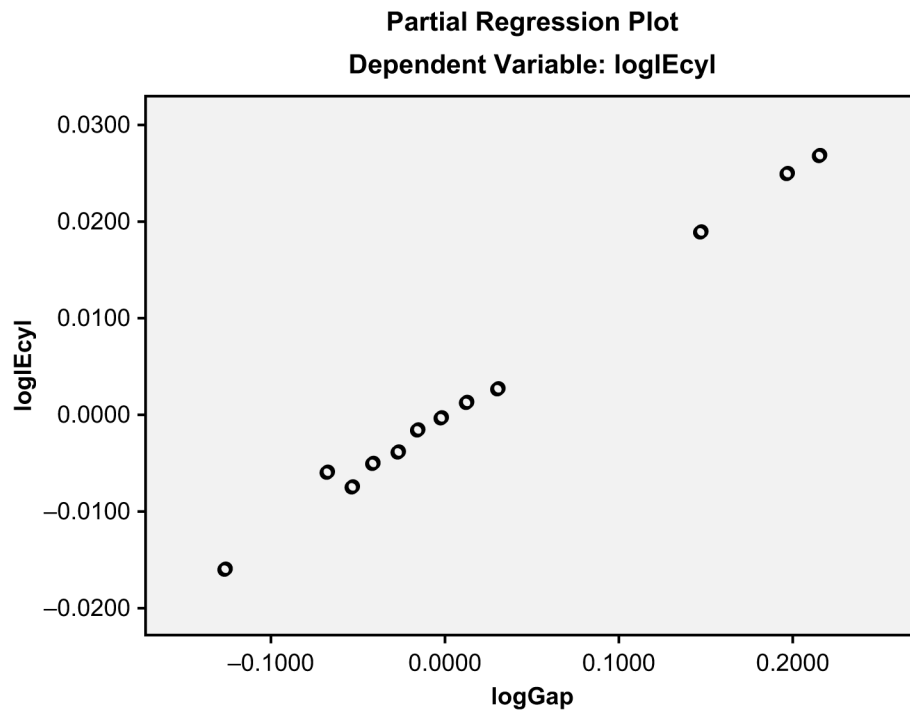


Figure G.28—Sensitivity analysis for gap against I/E

G.5.7 Arcing current and incident energy modeling procedure

Based on test results and parameter sensitivity results, the following factors are known to affect the level of arcing current and incident energy:

- Bolted fault current level
- Open circuit voltage level
- Gap width between electrodes
- Working distance
- Arc duration
- Electrode orientation
- Enclosure configuration

For incident energy model development, the following representative assumptions are used:

- Temperature rise in the calorimeter is proportional to the arc energy during the same event. This assumption allows for generating multiple data points from a single event.
- If test configurations and major ratings, such as bolted fault current, are identical, regardless of voltage level, 1 MJ arc energy will create a similar temperature rise in a calorimeter during the arc flash.

With the above assumptions and observations, data analysis and model development will be carried out through the following procedure. Also, these assumptions provide for the calculation of the box size correction factor when different enclosures are utilized. Brief descriptions of the steps are provided as follows:

Step 1: Select a configuration (representative configuration including VCB, VCBB, VOA, HCB, and HOA) for a specific anchor voltage class (600 V, 2.7 kV and 14.3 kV).

NOTE—The following three voltages were selected to capture potential non-linearity: 600 V was used to provide more consistent LV results, 2.7 kV was selected to be closer to the transition from LV to MV, and the higher voltage tests were normalized to 14.3 kV to minimize the effect of voltage variations between test laboratories.

Step 2: Select a test case from performed tests with typical parameter selections such as bolted fault current, electrode gap, and measurement distance.

Step 3: Arcing current modeling data processing. The rms arcing current will be calculated from the filtered signal for the corresponding period. Average value of $N-2$ cycles descending order data will be utilized as arcing current modeling data.

Step 4: Calculate the total arc energy during the arc event.

Step 5: Obtain maximum incident energy recording. The maximum incident energy IE_{\max} is obtained from recorded data, using the highest temperature rise from any single calorimeter.

Step 6: Calculate IE per MJ based upon the assumption in Step 5. The ratio is defined in units of cal/cm²/MJ. As previously mentioned, depending on model, it may be assumed that the IE/MJ is identical for each configuration.

Step 7: Convert MJ/Cycles to IE/Cycles. To develop a unified data processing procedure, the recording data is analyzed sample by sample. The arc energy for a complete cycle will be calculated by adding energy from one-cycle N_s consecutive sampling points (MJ/Cycles).

Step 8: Using a sliding window to move forward one data point and repeat the procedure over N_s data points representing a cycle. For example, if the sampling rate is 20 k samples/s, and the ac frequency is 60 Hz, this procedure will enable to generate 333 (N_s) data points per cycle.

Step 9: Sort IE/Cycles in descending sequence, and keep top $N_s*(N-2)$ data points. N is the number of cycles of the arc-flash duration and N_s is the number of samples per cycle. Based on cycle-by-cycle analysis, a higher incident energy per cycle is extracted while the initial time for burning the starter wire is excluded. $N_s*(N-2)$ will exclude the time to burning the starter wire or arc trigger delays, which is done in order to not underestimate arc-flash energy.

Step 10: Combine data points for tests with the same configuration and sort them in descending order. The average of the top 50% data points plus two standard deviations will be used for IE estimation.

Step 11: Repeat the procedure until all cases within the configuration for a specific voltage class are completed. The incident energy models are obtained as the function of bolted fault current, open circuit voltage, gap spacing of the electrodes, and distance to arcing point. [Table G.6](#) is a template of the tabulation of each test setup used to derive a function to represent the incident energy.

Table G.6—Template for tabulation of the test setup results

Gap	Bolted fault	Distance	[IE/cycle]	Arcing current
G ₁	I_{bf1}	D ₁	—	—
G ₁	I_{bf1}	D ₂	—	—
G ₁	I_{bf1}	D ₃	—	—
G ₁	I_{bf2}	D ₁	—	—
G ₁	I_{bf2}	D ₂	—	—
G ₁	I_{bf2}	D ₃	—	—
G ₁	I_{bf3}	D ₁	—	—
G ₁	I_{bf3}	D ₂	—	—
G ₁	I_{bf3}	D ₃	—	—
G ₂	I_{bf1}	D ₁	—	—
G ₂	I_{bf1}	D ₂	—	—
G ₂	I_{bf1}	D ₃	—	—
G ₂	I_{bf2}	D ₁	—	—
G ₂	I_{bf2}	D ₂	—	—
G ₂	I_{bf2}	D ₃	—	—
G ₂	I_{bf3}	D ₁	—	—
G ₂	I_{bf3}	D ₂	—	—
G ₂	I_{bf3}	D ₃	—	—
G ₃	I_{bf1}	D ₁	—	—
G ₃	I_{bf1}	D ₂	—	—
G ₃	I_{bf1}	D ₃	—	—
G ₃	I_{bf2}	D ₁	—	—
G ₃	I_{bf2}	D ₂	—	—
G ₃	I_{bf2}	D ₃	—	—
G ₃	I_{bf3}	D ₁	—	—
G ₃	I_{bf3}	D ₂	—	—
G ₃	I_{bf3}	D ₃	—	—

Step 12: Configuration correction. Use the relationships of $(\text{cal}/\text{cm}^2)_{\text{avg}}/\text{MJ}$ at different voltage levels to establish the correction factor for different enclosures. Specifically, the ratio of average incident energy to arc energy is different for different enclosure dimensions. **Table G.7** shows the sample of $(\text{cal}/\text{cm}^2)_{\text{avg}}/\text{MJ}$ for 2700 V with 660.4 mm × 660.4 mm × 660.4 mm (26 in × 26 in × 26 in) enclosure and 2700 V with 914.4 mm × 914.4 mm × 914.4 mm (36 in × 36 in × 36 in) enclosure at VCB. A curve-fitting process is performed to estimate the correction factor at the specified distance (D). It is reasonable to assume that the IE difference between them is caused by the size of the enclosure. This is the basis for box correction factor development. Similar procedures for other configurations (VCBB and HCB) and voltages will be carried out to establish the correction factor. The normalized incident energy on particular enclosure size at first, then it will be corrected to the actual size using the correction factor based on the correction equation for each test configuration.

NOTE—For open air configuration, there is no need to perform this step.

Table G.7—(cal/cm²_{avg})/MJ for different enclosure dimension, 2700 V tests, VCB

2700 V 660.4 mm × 660.4 mm × 660.4 mm (26 in × 26 in × 26 in)		2700 V 914.4 mm × 914.4 mm × 914.4 mm (36 in × 36 in × 36 in)	
Configuration	(cal/cm ² _{avg})/MJ	Configuration	(cal/cm ² _{avg})/MJ
VCB-20-24	2.4335	VCB-20-31	1.9009
VCB-20-33	1.6088	VCB-20-34	1.2567
VCB-20-42	0.9645	VCB-20-43	0.7534

Step 13: Obtain I_{arc} and IE/Cycle models as function of bolted fault current, open circuit voltage, gaps of electrodes, and distance to the arcing point for this configuration at specified voltage through the regression process.

Step 14: Repeat the procedure for all configurations and tested voltages. Depending on application in practice, with the enclosure correction factor, the results for enclosed configurations, such as HCB, VCB, and VCBB, are able to be normalized to 508 mm × 508 mm × 508 mm (20 in × 20 in × 20 in) enclosure.

Step 15: I_{arc} and IE estimation models for each configuration at the two other tested voltages can be created through Step 1 through Step 14 ([Table G.8](#) and [Table G.9](#)). Also, these models may be utilized to determine the arc-flash boundary.

Table G.8—I_{arc} estimation models

Voltage	VCB	VCBB	HCB	HOA	VOA
0.60 kV	$I_{arcVCB-0.6}$	$I_{arcVCBB-0.6}$	$I_{arcHCB-0.6}$	$I_{arcHOA-0.6}$	$I_{arcVOA-0.6}$
2.7 kV	$I_{arcVCB-2.7}$	$I_{arcVCBB-2.7}$	$I_{arcHCB-2.7}$	$I_{arcHOA-2.7}$	$I_{arcVOA-2.7}$
14.3 kV	$I_{arcVCB-14.3}$	$I_{arcVCBB-14.3}$	$I_{arcHCB-14.3}$	$I_{arcHOA-14.3}$	$I_{arcVOA-14.3}$

Table G.9—[IE/Cycle] estimation models

Voltage	VCB	VCBB	HCB	HOA	VOA
0.60 kV	[IE/Cycle] _{VCB-0.6}	[IE/Cycle] _{VCBB-0.6}	[IE/Cycle] _{HCB-0.6}	[IE/Cycle] _{HOA-0.6}	[IE/Cycle] _{VOA-0.6}
2.7 kV	[IE/Cycle] _{VCB-2.7}	[IE/Cycle] _{VCBB-2.7}	[IE/Cycle] _{HCB-2.7}	[IE/Cycle] _{HOA-2.7}	[IE/Cycle] _{VOA-2.7}
14.3 kV	[IE/Cycle] _{VCB-14.3}	[IE/Cycle] _{VCBB-14.3}	[IE/Cycle] _{HCB-14.3}	[IE/Cycle] _{HOA-14.3}	[IE/Cycle] _{VOA-14.3}

Step 16: Use interpolation to estimate the system voltage between 2700 V and 14.3 kV. Use interpolation and extrapolation to estimate system voltage between 600 V and 2700 V.

Step 17: Because the arc-flash behavior becomes more dynamic at low voltage, below 600 V models will be derived directly from 600 V models.

G.6 Model development procedure

G.6.1 Arcing current model

Step 1: Take the logarithm of all variables prior to regression.

Step 2: Convert I_{arc} to $\log I_{\text{arc}}$, I_{bf} to $\log I_{\text{bf}}$, Gap to $\log \text{Gap}$ for model development purpose.

Step 3: Put all 14.3 kV converted data into multiple linear regression process. (See [Table G.10](#).)

Table G.10—14.3 kV VCB arcing current modeling data

Configuration	V_{oc} (kV)	I_{bf} (kA)	Gap (mm)	I_{arc} (kA)
VCB	14.32	10.56	95.25	9.96828
VCB	14.32	10.56	95.25	9.94576
VCB	14.32	10.56	95.25	9.93284
...
...
...
VCB	14.16	2.703	101.6	2.64053
VCB	14.16	2.703	101.6	2.63228
VCB	14.16	1.136	101.6	1.10990

Step 4: Based on the selected parameter and arcing current recording, linear regression can be performed. The linear regression results will be:

$$\log I_{\text{arc}} = -0.121 + 0.99 \times \log I_{\text{bf}} + 0.056 \times \log \text{Gap} \quad (\text{G.5})$$

[Table G.11](#) clearly shows the dependent and independent variables in 14.3 kV I_{arc} model.

Table G.11—Variables entered/removed

Model	Variables entered	Variables removed	Method
1	$\log \text{Gap}$, $\log I_{\text{bf}}$	No	Enter
NOTE 1—Dependent variable: $\log I_{\text{arc}}$			
NOTE 2—All requested variable entered.			

In statistics, R^2 (R squared) is called the coefficient of determination, which provides a measure of how well future outcomes are likely to be predicted by the model and ranges from 0 to 1. The most general definition of R^2 is:

$$R^2 = 1 - \frac{SS_{\text{err}}}{SS_{\text{tot}}} \quad (\text{G.6})$$

$$SS_{\text{tot}} = \sum_i (x_i - \bar{x})^2 \quad (\text{G.7})$$

$$SS_{\text{err}} = \sum_i (x_i - f_i)^2 \quad (\text{G.8})$$

$$SS_{\text{err}} = \sum_i (x_i - f_i)^2 \quad (\text{G.9})$$

where

- x_i is sample value
- f_i is modeled value

From the model summary shown in [Table G.12](#), R^2 equal 1. Based on the definition of R^2 , it indicates independent variables ($\log I_{bf}$ and $\log Gap$) selection can very precisely model the way the dependent variable ($\log I_{arc}$) is changing.

Table G.12—Model summary

Model	R	R^2	Adjusted R^2	Standard error of the estimation
1	1.000a	1.000	1.000	0.00569
NOTE 1—Predictors(Constant): $\log Gap$, $\log I_{bf}$				
NOTE 2—Dependent Variable: $\log I_{arc}$				

Step 5: From [Figure G.10](#), partial regression results show the gap width has a negative relationship with the arcing current value. However, the linear regression model gives a positive relationship indication between gap and arcing current in the model from Step 4.

This contrary phenomenon could be caused by the statistical process. From [Table G.13](#), the coefficients table for arcing current shows the problem very clearly. In last column of the table, t-distribution show the significant difference from $\log I_{bf}$ and $\log Gap$.

Table G.13—Coefficients for arcing current model development

Model		Unstandardized coefficients		Standardized coefficients	t
		B	Standard error		
1	(Constant)	-0.121	0.016		-7.795
	$\log I_{bf}$	0.990	0.001	1.001	755.036
	$\log Gap$	0.056	0.008	0.010	7.276
NOTE—Dependent Variable: $\log I_{arc}$					

From the statistics and pure data point of view, bolted fault current has a more direct relationship to arcing current than does gap to arcing current. Therefore, in regression processes, the correct relation between bolted fault current and arcing current has been put as the first priority. This has caused the opposite trend between I_{arc} and Gap. This may not cause significant estimation error if the gap width is strictly limited to within the test data (data that has been used for regression analysis). However, it may produce undesired estimation results if the gap width is extended to 254 mm (10 in), which is significantly outside the tested range.

Based on the partial regression from [Figure G.29](#), the original regression has been adjusted as in [Equation \(G.10\)](#), which gives the correct relationship indication among arcing current, bolted fault current and gap width. The laboratory testing was performed between 76.2 mm (3 in) and 152.6 mm (6 in) gap width. The following adjusted equation match the original regression results at 114.3 mm (4.5 in). Matching at other gap widths are also derived. The constant and the coefficient of the $\log I_{bf}$ and $\log Gap$ of these equations are used as initial conditions for further tuning process.

$$\log I_{arc} = 0.138 + 0.99 \times \log I_{bf} - 0.0744 \times \log Gap \quad (G.10)$$

Figure G.29 provides the results comparison between the original regression and the adjusted regression model estimation.

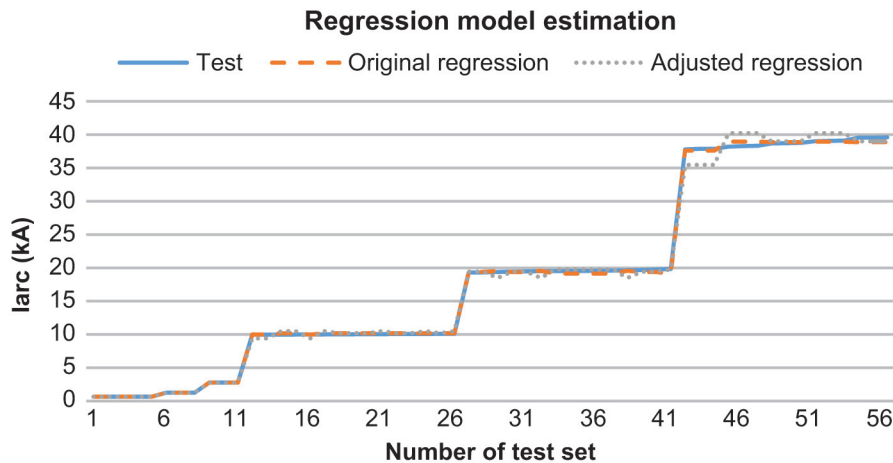


Figure G.29—Comparison between original regression and adjusted regression model

Step 6: Based on the changes of system impedance according to different bolted fault current, the arcing current curve cannot always be expressed in a linear form. In order to take into consideration, the actual characteristics of arcing current with the increasing system voltage and current, an adjustment curve has been applied to the original regression curve to extend the range of the estimator to 65 kA. Table G.14 gives the ratio trend corresponding to current level.

Table G.14—Ratio of arcing current and bolted fault current

Bolted fault current (kA)	Ratio of arcing current and bolted fault current ($I_{\text{arc}}/I_{\text{bf}}$)
42	0.943200952
20.08	0.963315239
10.076	0.978900854
2.703	0.979965594
1.136	0.983667254
0.5	0.997106

Step 7: Based on the trend of I_{ratio} for different levels of I_{bf} (from laboratory test recording), follow the trend to extend the ratio value to 65 kA. Then the fifth degree polynomial is generated by curve fitting. Figure G.30 illustrates the curve of current correction factors.

$$I_{\text{ef}} = -1.557 \times 10^{-12} I_{\text{bf}}^6 + 4.556 \times 10^{-10} I_{\text{bf}}^5 - 4.186 \times 10^{-8} I_{\text{bf}}^4 + 8.346 \times 10^{-7} I_{\text{bf}}^3 + 5.482 \times 10^{-5} I_{\text{bf}}^2 - 0.003191 I_{\text{bf}} + 0.9729 \quad (\text{G.11})$$

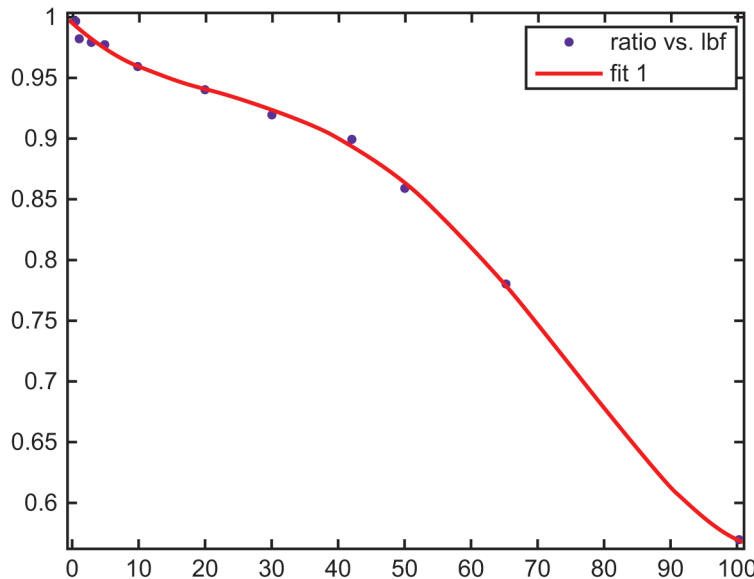


Figure G.30—Curve of current correction factor (the vertical axis is the ratio of I_{arc}/I_{bf} and the horizontal axis is the magnitude of I_{bf} in kiloamperes)

Step 8: Impose the curve into the adjusted linear regression result. Figure G.31 provides the comparison between the adjusted curve and original curve.

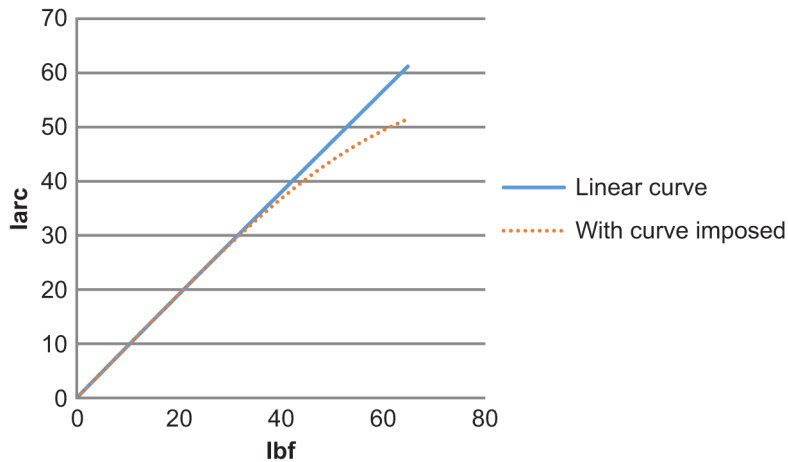


Figure G.31—Comparison between the linear curve and the curve with correction factor applied

Step 9: Based on the adjusted regression model and the adjustment curve, the least square error method and gradient search method are applied to tune the coefficients of the equation to improve the fitting performance. The final 14.3 kV VCB arcing current equations is shown in Equation (G.12):

$$I_{arc} = 10^{(0.005795 + 1.015 \lg I_{bf} - 0.011 \lg Gap)} \\ (-1.557 \times 10^{-12} I_{bf}^6 + 4.556 \times 10^{-10} I_{bf}^5 - 4.186 \times 10^{-8} I_{bf}^4 + 8.346 \times 10^{-7} I_{bf}^3 + 5.482 \times 10^{-5} I_{bf}^2 - 0.003191 I_{bf} + 0.9729) \quad (G.12)$$

G.6.2 Incident energy data processing

Step 1: Obtain maximum IE from the recording data.

Step 2: Calculate the power and multiply by 0.00005 (20 K sample per second) to convert the values into joules.

Step 3: Calculate the total arc energy during the event.

Step 4: Calculate ΔIE per MJ, and MJ/Cycle.

Step 5: Move forward one data point and repeat the procedure. This procedure will generate 333 data points per cycle.

Step 6: Convert MJ/Cycle to IE/Cycle.

Step 7: Sort IE/Cycle in descending order and keep top 50% data points. In other words, based on 20 k sample rate, $333 \times N - 2)/2$ data points. N is the arc-flash duration in cycles. In this example case, $N = 24$, so 3663 data points can be extracted from a 24-cycle arc-flash test.

Step 8: Statistical analysis will be performed to obtain average IE/Cycle and its standard deviation. Statistical analysis is used to calculate the upper bound of a 95% confidence interval for the IE/Cycle value.

G.6.3 Incident energy model

The essential parameters (arcing current, gap width, working distance, ratio of bolted fault current and arcing current) for incident energy modeling can be obtained from sensitivity analysis, then the model development steps can be processed.

NOTE—In the following equations, log refers to log base 10.

Step 1: Take the logarithm on all variables prior to regression.

Step 2: Use I_{ratio} , $\log I_{arc}$, I_{bf} , $\log Gap$, $\log D$ as independent variables for model development.

Step 3: Use $\log(IE/cycle)$ from data processing part as the dependent variable.

Step 4: For 14.3 kV VCB cases, enter data into multiple linear regression process ([Table G.15](#)) to obtain the initial results. Since the model can only match results within the range of the data input, a “modified” linear regression approach is applied to extend the range of the model to 65 kA and 254 mm (10 in) gap. Using the results from the “modified” linear regression approach as initial condition, least square error method and gradient search method are applied to tune the coefficients of the equation to improve the fitting performance.

Table G.15—14.3 kV VCB incident energy modeling data

Config.	V_{oc} (kV)	I_{bf} (kA)	Gap (mm)	D (mm)	Duration (ms)	I_{arc} (kA)	IE_{max} (cal/cm ²)
VCB	14.32	10.56	95.25	1193.8	104.11	9.96828	0.675
VCB	14.32	10.56	95.25	1193.8	206.14	9.94576	1.2555
VCB	14.32	10.56	95.25	990.6	104.03	9.93284	0.864
...
...
...
VCB	14.07	0.5	101.6	1193.8	418.42	0.49700	0.2835
VCB	14.07	0.5	101.6	990.6	429.73	0.49640	0.324
VCB	14.07	0.5	101.6	787.4	414.87	0.49616	0.3645

Step 5: Use I_{arc} equation (from I_{arc} model development) to replace the measured I_{arc}

Step 6: The final IE equation based on the box 914.4 mm × 914.4 mm × 914.4 mm (36 in × 36 in × 36 in) is:

$$IE = \frac{3}{50} t \times 10^{\left(k_1 + k_2 \lg Gap + \frac{k_3 I_{arc_14300}}{k_4 I_{bf}^6 + k_5 I_{bf}^6 + k_6 I_{bf}^5 + k_7 I_{bf}^5 + k_8 I_{bf}^3 + k_9 I_{bf}^2 + k_{10} I_{bf}} + k_{11} \lg I_{bf} + k_{12} \lg D + k_{13} \lg I_{arc_14300} + \lg \frac{1}{CF} \right)} \quad (G.13)$$

where (for VCB configuration):

k_1	k_2	k_3	k_4	k_5	k_6	k_7	k_8	k_9	k_{10}	k_{11}	k_{12}	k_{13}
3.825917	0.11	-0.999749	-1.557E-12	4.556E-10	-4.186E-08	8.346E-07	5.482E-05	-0.003191	0.9729	0	-1.568	0.99

From Table G.16, R^2 equals 0.984, which indicates independent variable selection can reflect the way of dependent variable, IE , changing very precisely.

Table G.16—Model summary

Model	R	R^2	Adjusted R^2	Standard error of the estimate
1	0.992a	0.984	0.982	0.0649722

G.7 IEEE 1584 arc-flash model parameter range determination

G.7.1 General

The range of the parameters was determined based on different criteria. The main consideration was the range of the test data available. The second important consideration was the application of the model to existing and new equipment. Based on collective experience, the range of some of the model parameters was extended to better suit its application to practical equipment sizes with various voltage and short-circuit current levels.

This annex provides some samples of the validation analysis to determine the range of the parameters. Examples include plots that show how the bolted fault current behaves against variation in gaps, voltage, and bolted fault current. The plots also show how the incident energy and arc-flash boundary change as a function of the arc fault duration, working distance, or enclosure size. This analysis is different from the parameter sensitivity analysis described in G.6.

G.7.2 Voltage

The range of the model voltage is 0.208 kV to 15 kV. The voltage range of the new model correlates with the range of its predecessor. Note that the 2002 model tests did not include any tests at voltage values higher than 2.4 kV in enclosed configurations. The new IEEE 1584 arc-flash model is developed based on test results for all configurations (open and enclosed) up to 14.8 kV.

G.7.3 Frequency

The model is considered to be applicable to either 50 Hz or 60 Hz. However, the majority of the tests were performed at 60 Hz. The previous IEEE 1584-2002 frequency range was 50 Hz to 60 Hz. There are no tests available to support incident energy calculations for frequency values outside this range.

G.7.4 Bolted fault current

The range of the bolted short-circuit rms current is different than the one selected in the 2002 standard. The new range is 500 A to 106 kA between the voltages of three-phase 208 V to 600 V and 200 A to 65 kA between the voltages of three-phase 601 V to 15 000 V.

The test results in the low-voltage area only went as high as 80 kA. It was not possible to test at higher currents for low-voltage applications based on the lack of available test laboratories. The model results were extrapolated up to 106 kA based on the expected trend of the results determined from the available tests, and based on comparisons to previous data available from the 2002 arc-flash tests. Note that the extension of the current range to 106 kA was based on considerable analysis of the behavior of the arc current that was not included in the 2002 model.

The test data available could not support model results above 65 kA for medium voltage applications (601 V to 15 000 V). The bolted short-circuit current range should be limited to 0.5 kA to 65 kA based on the available test results.

Overall, it can be concluded that the range of allowable bolted fault current in the new model is less than that used in the 2002 model; however, its selection was based on far more detailed analysis of the data and arc current physical behavior.

G.7.5 Gap between conductors

The gap range was selected as 6.35 mm (0.25 in) to 76.2 mm (3.0 in) between 208 V and 600 V. This was determined based on the available test results. The gaps between conductors were extended to 254 mm (10 in) for voltages from 601 V to 15 kV based on the fact that a lot of medium voltage equipment has longer gaps than 152.4 mm (6 in). The trend in the behavior of the gap between conductors was observed and the extrapolation done between 152.4 mm (6 in) to 254 mm (10 in) gaps produces arc-current results that follow the expected physical behavior and at the same time are expected to yield conservative results.

G.7.6 Working distance

An upper limit on the working distance is not considered necessary. The incident energy was measured at several working distances to be able to determine an accurate relationship of distance versus incident energy for each configuration at different voltage levels. The minimum working distance should be no less than 304.8 mm (12 in). Any smaller working distance could place the worker within the range of the arc plasma cloud and metal droplets. No tests were performed at such short working distances. A minimum working distance of 304.8 mm (12 in) was used because it is considered that the plasma cloud is not considered to have exceeded a radius of 304.8 mm (12 in). The plasma cloud size and effect of direct contact with it should be considered in future arc-flash model revisions.

The range of the test parameters for working distance included 457.2 mm (18 in) to 1193.8 mm (47 in) for 601 V to 15 000 V and 381 mm (15 in) to 914.4 mm (36 in) for 208 V to 600 V. The working distance was extended down to 304.8 mm (12 in) based on the trend of the test results.

G.7.7 Arc-flash boundary

An upper limit beyond the working distance is not considered necessary. In the new arc-flash model, the incident energy at a working distance and arc-flash boundary (AFB) for a certain incident energy use the same equations. The arc-flash boundary equation was derived based on the test results at different working distances.

The arc-flash boundary equation followed the trend of the test results in conservative fashion. The AFB produced by the new model may be more accurate and less over conservative when compared to the IEEE 1584-2002 model results.

G.7.8 Fault clearing time

The fault clearing time is not considered to have any upper limit. The tests performed were normalized to 6- and 12-cycles test; however, the tests included arc durations up to 30 cycles. A linear relationship between time and incident energy is considered acceptable. Linearity beyond 30 cycles is likely unless specific test results for specific equipment determine otherwise.

The testing conducted in multiple laboratories was based on sustaining the arc for a definite period of time. The application of the model is based on the arc sustaining until the clearing time of the upstream protective device. Self-extinguishing arc faults were not used in the model development. The probability of the arc self-extinguishing before the clearing time is feasible but cannot be accurately predicted or modeled.

G.7.9 Equipment enclosure sizes

The IEEE/NFPA Collaboration and IEEE Std 1584-2002 test results [B53] for enclosed configurations were analyzed to determine the enclosure size range. The model enclosure size should have a maximum width or height of 1270 mm (50 in). The maximum box opening size of 1270 mm × 1270 mm (50 in × 50 in) was determined based on the observation of the trend in incident energy reduction for tests with different box sizes but with similar arc energy. Examples of the extrapolation process to extend the model opening area range are shown 4.8. The test box sizes used by the collaboration were 508 mm × 508 mm × 508 mm (20 in × 20 in × 20 in), 660.4 mm × 660.4 mm × 660.4 mm (26 in × 26 in × 26 in) and 914.4 mm × 914.4 mm × 914.4 mm (36 in × 36 in × 36 in). The 355.6 mm × 304.8 mm × 203.2 mm (14 in × 12 in × 8 in) and 1143 mm × 762 mm × 762 mm (45 in × 30 in × 30 in) tests were used to develop the list of allowable enclosure sizes in the new IEEE 1584 arc-flash model (refer to G.9.6 for enclosure size application examples).

Also, the width of the enclosure should be at least four times the gap between conductors to keep the model arc current and incident energy results within the limits of the test setups.

For more information on the equipment enclosure sizes for each voltage level, see G.9.3.

G.7.10 Incident energy

The incident energy has no range and is considered to have a linear relationship with time. That is the incident energy will increase linearly with the arc-fault duration. It was observed that the incident energy/cycle will be different during the first and last cycle (arc ignition and arc extinction).

The raw data measurements from each of seven calorimeters were processed to obtain the highest energy/cycle rate that was obtained from the highest incident energy measurement of all seven calorimeters. The mean energy and max energy measurement are available in the test result summary documents.

Therefore, because the model was developed with these assumptions it is considered to yield adequate results.

G.7.11 System grounding

Contrary to how the IEEE 1584-2002 model interpreted the effect of system grounding, the new IEEE 1584 arc-flash model will not utilize the system grounding configuration as an input parameter. The IEEE/NFPA Collaboration test results did not show any significant impact of the system grounding or bonding on the incident energy released by the arc.

G.8 For I_{arc} and IE estimation at user defined environment

G.8.1 Stage 1: Arcing current estimation

- a) User input data
 - 1) Voltage
 - 2) Configuration
 - 3) Bolted fault current
 - 4) Dimension of the enclosure (for VCB, VCBB, and HCB)
 - 5) Gap of the electrodes
- b) Estimation procedure and output data
 - 1) Based upon user specified configuration (except voltage), calculate average I_{arc} for 600 V, 2700 V, and 14300 V.
 - 2) Use curve-fitting approach to estimate the average I_{arc} at user-specified configuration and voltage.
 - 3) Based upon user specified configuration (except voltage), calculate minimum I_{arc} for 600 V, 2700 V, and 14300 V.
 - 4) Use curve-fitting approach to estimate the minimum I_{arc} at user specified configuration and voltage.

G.8.2 Stage 2: IE estimation

- a) User input data
 - 1) Average and minimum I_{arc}
 - 2) Arc duration at average I_{arc} [based upon the arcing current to determine the fuse or (circuit breaker + relay) operation time by user or third party software]
 - 3) Arc duration at minimum I_{arc} [based upon the arcing current to determine the fuse or (circuit breaker + relay) operation time by user or third party software]
 - 4) Distance to the arcing point
- b) Estimation procedure and output data
 - 1) Based upon user specified configuration (except voltage), calculate IE for 600 V, 2700 V, and 14300 V.

- 2) Use curve-fitting approach to estimate the IE at user specified configuration and voltage with normalized enclosure.
- 3) Apply correction factor for different enclosure dimensions.
- 4) Repeat for minimum I_{arc} .
- 5) Provide IE estimates for specified condition; select larger value.
- 6) Estimate arc-flash boundary at 1.2 cal/cm².

G.9 IEEE 1584 arc-flash model application guidelines

G.9.1 General

This subclause provides application guidelines for the new IEEE 1584 arc-flash model. The application guidelines cover the recommended application of the model to account for variations in current, voltage and enclosure size.

G.9.2 Arc-current variation

The variation of the arc current can be obtained by using [Equation \(2\)](#) from [4.5](#). Similar to what was recommended in IEEE 1584-2002, two calculations should be performed to determine the arc duration or fault clearing time (FCT) of overcurrent protective devices. The first FCT calculation uses the uncorrected average arc current. The second FCT determination can be performed using the average arc current obtained from using [Equation \(2\)](#).

The incident energy and arc-flash boundary can be determined using the fault clearing times obtained from 100% I_{arc} and reduced I_{arc} ($I_{\text{arc_min}}$).

Commercial software programs already implement multiple calculations that account for arc-current variation.

[Figure G.32](#) shows that the variation of the arc current is now continuous and varies as a function of voltage.

[Figure G.33](#) shows that the variation in the arc current decreases as the voltage increases. The plot also shows how the IEEE 1582-2002 model handles arc current and arc-current variation. The plot above shows that the expected current variation is less than 1.5% at 15 kV, approximately 4% at 3 kV and 14.4% at 0.480 kV (~15%, which still agrees with the uniform value used in the 2002 model for any voltage below 1000 V).

[Figure G.34](#) shows the maximum measured variation in the arc current results at each voltage level for the vertical conductors in box configuration. Each point included in [Figure G.34](#) is the percent difference between the highest and lowest arc current recorded for similar tests (e.g., same bolted fault current, voltage, gap, and configuration). The x axis represents the voltage range of the model and the clusters of points represent the groups of tests performed at each voltage level. Each point may represent the variation of several similar tests (4 to 6). The entire set of available IEEE/NFPA Collaboration test data was considered in the analysis. Equations used to represent the arc current variation were derived based on the average of the arc current variation at each voltage level.

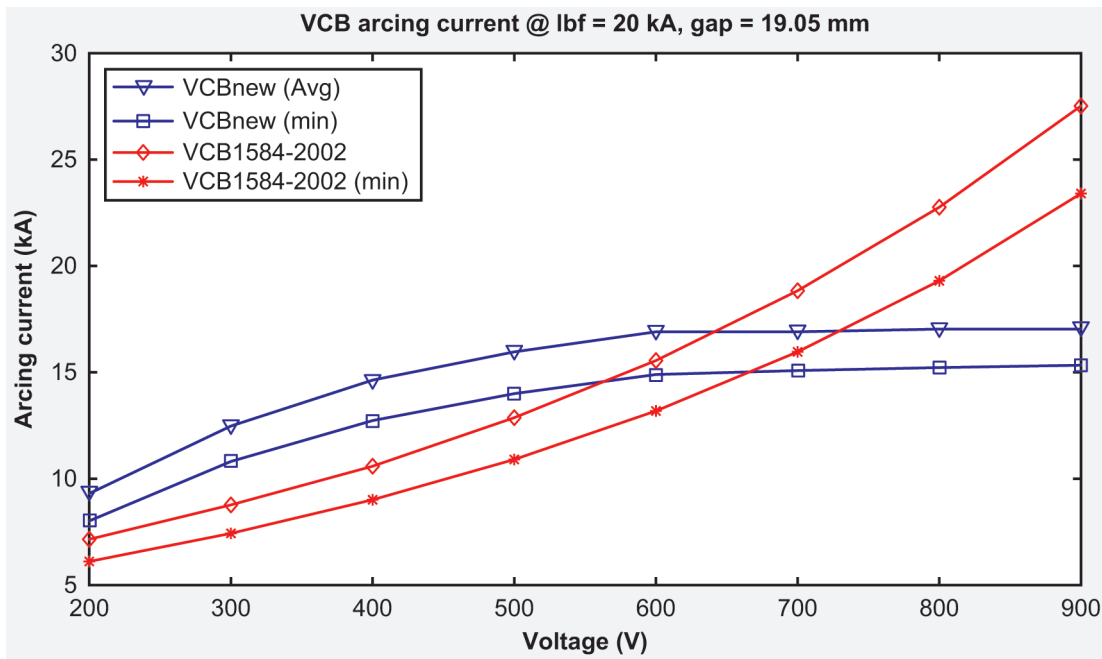


**Figure G.32— I_{arc} versus V_{oc} for 208 V to 1000 V
(comparison of IEEE 1584-2002 and IEEE 1584-2018)**

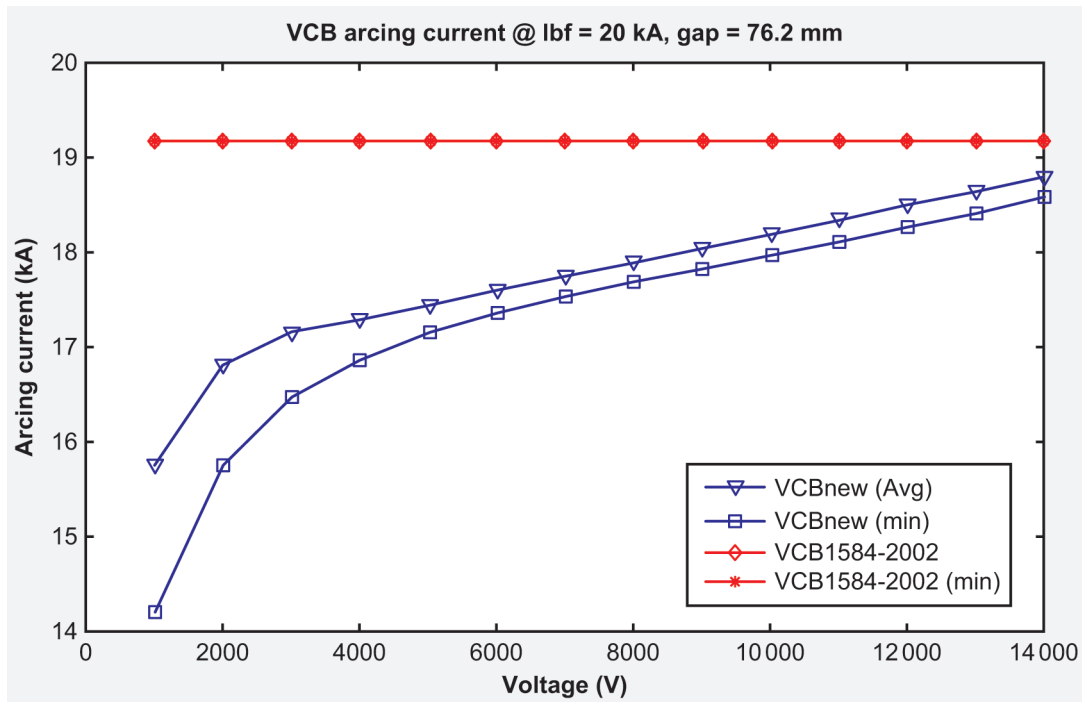


**Figure G.33— I_{arc} versus V_{oc} for 1 kV to 15 kV
(comparison of IEEE 1584-2002 and IEEE 1584-2018)**

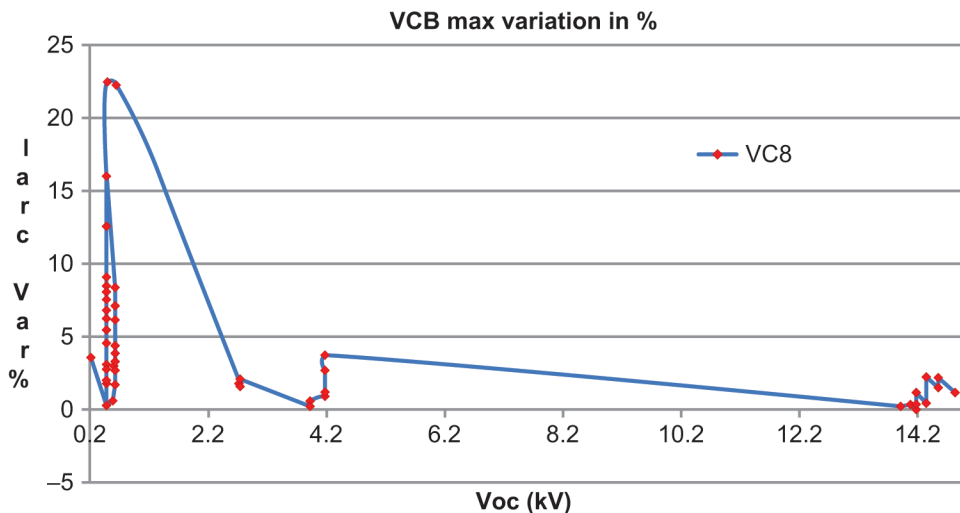


Figure G.34— I_{arc} variation versus V_{oc} for VCB test results

The arc current variation was applied to systems with voltage greater than 1000 V. Figure G.34 test results show a variation as high as 4% at the 2.3 kV to 5 kV range. In other words, for the same voltage, bolted fault current, gap between conductors, box size, and electrode configuration, the measured arc current ended up being approximately 4% different from max to low value. This variation should not be ignored when determining the operating time of overcurrent protective devices.

G.9.3 Enclosure sizes

IEEE Std 1584-2002 supported three enclosure sizes. The sizes and application to equipment types are listed in Table G.17. This number of enclosures is limited to represent available equipment in actual installations. The application of the model to a higher number of enclosure sizes was achieved by combining the results of the IEEE/NFPA Collaboration and IEEE 1584-2002 tests to validate the use of a larger number of enclosures in the new arc-flash model.

Table G.17—Enclosure sizes for IEEE 1584-2002 arc-flash model

Equipment class	Typical bus gaps (mm)	Enclosure size (H × W × D)
15 kV switchgear	152	1143 mm × 762 mm × 762 mm (45 in × 30 in × 30 in)
5 kV switchgear	104	1143 mm × 762 mm × 762 mm (45 in × 30 in × 30 in)
Low-voltage switchgear	32	508 mm × 508 mm × 508 mm (20 in × 20 in × 20 in)
Low-voltage MCCs and panelboards	25	355.6 mm × 304.8 mm × 203.2 mm (14 in × 12 in × 8 in)
Cable	13	355.6 mm × 304.8 mm × 203.2 mm (14 in × 12 in × 8 in)

Table G.18 shows the list of enclosures which have been validated for use with the new arc-flash model.

NOTE—Equipment enclosure sizes have doubled.

Table G.18—Enclosure sizes for IEEE 1584-2018 arc-flash model

Enclosure type	Equipment class	Default bus gaps (mm)	Enclosure size (H × W × D)
1	15 kV switchgear	152	1143 mm × 762 mm × 762 mm (45 in × 30 in × 30 in)
2	15 kV MCC	152	914.4 mm × 914.4 mm × 914.4 mm (36 in × 36 in × 36 in)
3	5 kV switchgear	104	914.4 mm × 914.4 mm × 914.4 mm (36 in × 36 in × 36 in)
4	5 kV switchgear	104	1143 mm × 762 mm × 762 mm (45 in × 30 in × 30 in)
5	5 kV MCC	104	660.4 mm × 660.4 mm × 660.4 mm (26 in × 26 in × 26 in)
6	Low-voltage switchgear	32	508 mm × 508 mm × 508 mm (20 in × 20 in × 20 in)
7	Shallow low-voltage MCCs and panelboards	25	355.6 mm × 304.8 mm × \leq 203.2 mm (14 in × 12 in × \leq 8 in)
8	Deep low-voltage MCCs and panelboards	25	355.6 mm × 304.8 mm × >203.2 mm (14 in × 12 in × >8 in)
7 or 8	Cable junction box	13	355.6 mm × 304.8 mm × \leq 203.2 mm (14 in × 12 in × \leq 8 in) or 355.6 mm × 304.8 mm × >203.2 mm (14 in × 12 in × >8 in)

Similar to how IEEE 1584-2002 is being applied, the new arc-flash model can be applied to similar size equipment plus some additional sizes. This was accomplished by adjusting the incident energy model to account for the additional sizes. The new model may yield accurate or slightly conservative results for the tested sizes in [Table G.18](#).

G.9.4 Enclosure sizes for voltage values between 208 V and 600 V

The effect of the enclosure depth is considered for some enclosures. A “shallow” enclosure is defined as one with a depth less than or equal to 203.2 mm (8 in). Enclosures with a depth greater than 203.2 mm (8 in) are considered as “typical.” The effect of depth is only considered if the system voltage is less than 600 V.

For example, the effect on the incident energy for an LV panelboard with two different depth values:

- Incident energy with depth > 203.2 mm (8 in) is 1.91 cal/cm² (typical)
- Incident energy with depth \leq 203.2 mm (8 in) is 1.27 cal/cm² (shallow)

The box opening size area (width × height) tends to be the dominant variable for the bigger box sizes and the depth did not seem to have as large an effect. The distance from electrodes to back wall and the distance from the tip of the electrodes to the bottom of the box may also be a factor but were not considered as parameter variables to be studied in the IEEE/NFPA collaboration tests. Future revisions of the model may incorporate their effect as more test data becomes available. In the low-voltage box enclosure sizes as previously observed by Wilkins [B97], [B99], the incident energy measurement may experience a reduction as the overall box size becomes smaller as shown in [Figure G.35](#). The triangle symbol curve represents the incident energy corrected with the factors derived by Wilkins (which were obtained by analyzing the IEEE Std 1584-2002 test results [B53]).

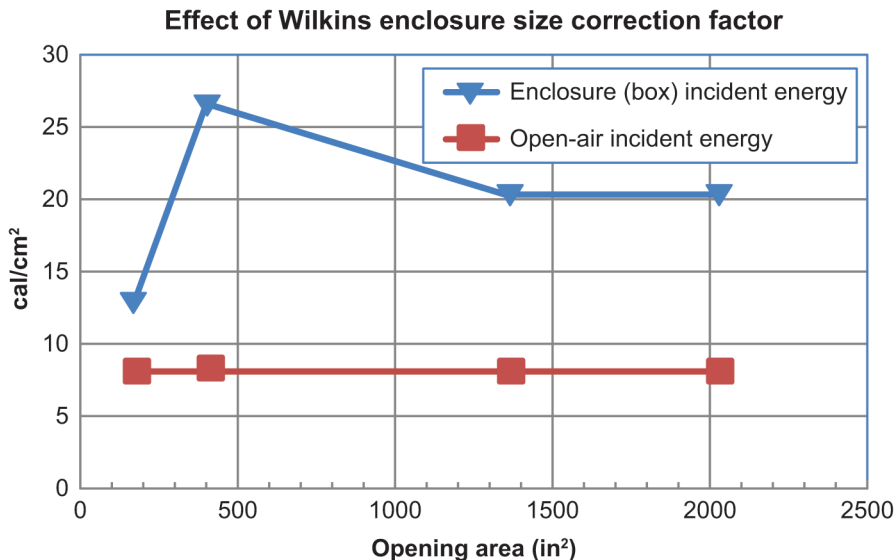


Figure G.35—Example of incident energy variation versus opening size (Wilkins)

The enclosure size and depth correction factor was implemented based on the effect shown in [Figure G.35](#), which shows the incident energy as a function of opening width. The incident energy test results of the enclosures with depth less than or equal to 203.2 mm (8 in) were slightly higher than those of depth > 228.6 mm (9 in).

G.9.5 Enclosure sizes for voltage values between 600 V and 15000 V

The IEEE/NFPA Collaboration tests included only (H × W × D) 660.4 mm × 660.4 mm × 660.4 mm (26 in × 26 in × 26 in) (at 3 kV) and 914.4 mm × 914.4 mm × 914.4 mm (36 in × 36 in × 36 in) (at 15 kV) enclosure sizes. There were two main items addressed during the validation of the MV box sizes.

- a) The first item was the use of an 1143 mm × 762 mm × 762 mm (45 in × 30 in × 30 in) box and how well the results would fit at 3 kV to 15 kV. The collaboration tests did not include this box size in their tests. To address this issue, the new model results were compared against the 2002 test results and the 2002 model predictions. The comparison results showed that the model could be extended for use to this box size for 3 kV to 15 kV.
- b) The second item was the use of 914.4 mm × 914.4 mm × 914.4 mm (36 in × 36 in × 36 in) enclosure sizes in the 3 kV voltage range. This item was addressed by comparing the model incident energy output against additional test results, which were available as part of the entire set of tests performed by the collaboration. The comparison results once again indicated that the new arc-flash model may conservatively handle larger box sizes in the 3 kV range.

[Figure G.36](#) shows a comparison of the new model incident energy results versus actual test results for VCB configuration using a 914.4 mm × 914.4 mm × 914.4 mm (36 in × 36 in × 36 in) box size. In the chart, the curve with the triangular symbols represents the model predictions and the square symbol curve represents the actual test results. The vertical axis is the incident energy and the horizontal axis is the test numbers (i.e., all the tests available at the specified box size, but with different short-circuit currents, gaps, etc.). [Figure G.37](#) and [Figure G.38](#) are similar charts but for VCBB and HCB, respectively (for the same box size).

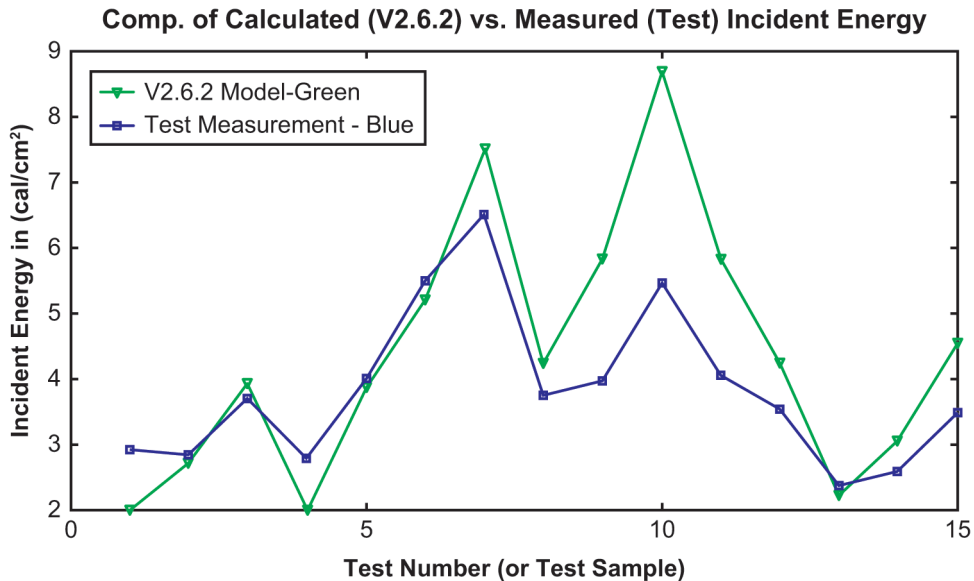


Figure G.36—VCB incident energy comparisons at different enclosure sizes

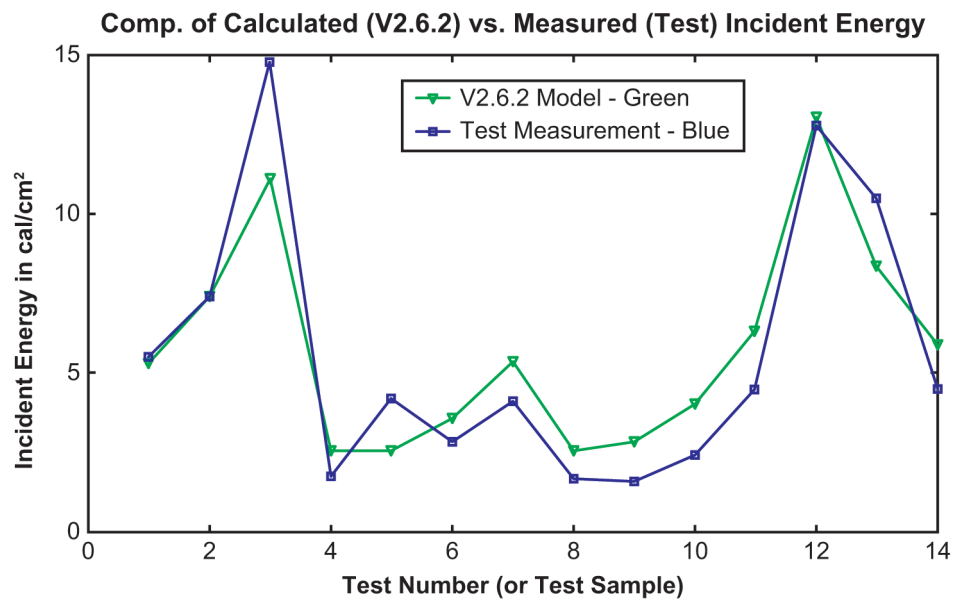


Figure G.37—VCBB incident energy comparisons at different enclosure sizes

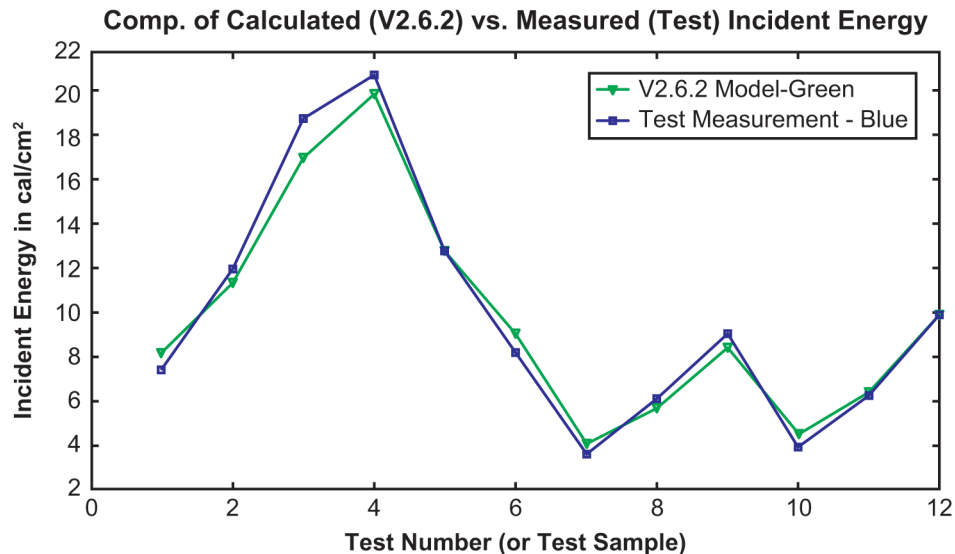


Figure G.38—HCB incident energy comparisons at different enclosure sizes

The incident energy results of the new arc-flash model were also compared against those of the IEEE 1584-2002 model to verify that the results were compatible for the VCB configuration. Based on the analysis of the charts of Figure G.36 through Figure G.38, the new AF model was extended for use in the equipment enclosure sizes described in Table G.18. Enclosure size correction factors were derived for each type of configuration. Subclause 4.8 provides individual correction factors for VCB, VCBB, and HCB.

G.9.6 Enclosure size application examples

G.9.6.1 General

Table G.18 can be used as an application guide when selecting the enclosure that is closest to the actual equipment. Depending on the application voltage the proper box size can be selected from the choices in Table G.18. The following are examples of how this can be accomplished.

G.9.6.2 Example 1

For voltage values between 0.208 kV and 0.6 kV, the box opening area range is between 355.6 mm × 304.8 mm (14 in × 12 in) all the way up to 508 mm × 508 mm (20 in × 20 in). Table G.18 has two standard opening sizes recommended which are 355.6 mm × 304.8 mm > 203.2 mm (14 in × 12 in > 8 in) or 355.6 mm × 304.8 mm × ≤ 203.2 mm (14 in × 12 in × ≤ 8 in) and 508 mm × 508 mm × 508 mm (20 in × 20 in × 20 in).

If a box opening size encountered in actual equipment is 406.4 mm × 406.4 mm (16 in × 16 in) with a depth of 8 in, then there are two methods to select a size to determine the incident energy:

- Select the 508 mm × 508 mm × 508 mm (20 in × 20 in × 20 in) as typical box size.
- Use the actual width, height as inputs in the model as 406.4 mm × 406.4 mm (16 in × 16 in) with shallow box selected [depth ≤ 203.2 mm (8 in)].

The incident energy results using option a will provide higher results. Using the second option for box size is expected to yield more accurate results.

G.9.6.3 Example 2

For voltage values between 0.6 kV and 2.7 kV the box opening area supported by the model is between 508 mm × 508 mm (20 in × 20 in) to 660.4 mm × 660.4 mm (26 in × 26 in). Depth is no longer a variable in this voltage range as previously described. [Table G.18](#) supports two sizes in this voltage range. 508 mm × 508 mm (20 in × 20 in) and 660.4 mm × 660.4 mm (26 in × 26 in).

If a box opening size encountered in actual equipment is 609.6 mm × 508 mm (24 in × 20 in), then there are two methods to select a size to determine the incident energy:

- a) Select the next smaller size available of 508 mm × 508 mm (20 in × 20 in).
- b) Enter the actual width and height as inputs into the model as 609.6 mm × 508 mm (24 in × 20 in). Depth can be specified but not used at this voltage level.

The incident energy results obtained using option a will be higher. Using option b is expected to yield more accurate results.

G.9.6.4 Example 3

For voltage values between 2.7 kV and 5.0 kV, the box opening area supported by the model is between 660.4 mm × 660.4 mm (26 in × 26 in) to 1143 mm × 762 mm (45 in × 30 in). [Table G.18](#) supports three sizes in this voltage range. 660.4 mm × 660.4 mm (26 in × 26 in), 914.4 mm × 914.4 mm (36 in × 36 in) and 1143 mm × 762 mm (45 in × 30 in).

If a box opening area encountered in actual equipment is 990.6 mm × 914.4 mm (39 in × 36 in), then there are two methods to select a size to determine the incident energy:

- a) Select the next smaller size available of 914.4 mm × 914.4 mm (36 in × 36 in)
- b) Enter the actual width, height as inputs into the model as 990.6 mm × 914.4 mm (39 in × 36 in)

The incident energy results obtained using option a will be higher. Using option b is expected to yield results that are more accurate.

If a box opening area encountered in actual equipment is 1016 mm × 762 mm (40 in × 30 in), then there are two methods to select a size to determine the incident energy:

- a) Select the next smaller size available of 914.4 mm × 914.4 mm (36 in × 36 in)
- b) Enter the actual width, height as inputs into the model as 1016 mm × 762 mm (40 in × 30 in)

The incident energy results obtained using option a will be higher. Using option b is expected to yield results that are more accurate. It is recommended to use the 1143 mm × 762 mm (45 in × 30 in) standard size for opening areas greater than 1143 mm × 762 mm (45 in × 30 in).

G.9.6.5 Example 4

For voltage values between 5 kV and 15 kV, the box opening area supported by the model is between 914.4 mm × 914.4 mm (36 in × 36 in) to 1244.6 mm × 1244.6 mm (49 in × 49 in) [Table G.18](#) supports two standard box-opening sizes in this voltage range, which are 914.4 mm × 914.4 mm (36 in × 36 in) and 1143 mm × 762 mm (45 in × 30 in)

If a box opening area encountered in actual equipment is 1320.8 mm × 1320.82 mm (52 in × 52 in), then the recommended methods to select the opening size are:

- a) Select the next smaller available opening area of 1143 mm × 762 mm (45 in × 30 in)
- b) Use an opening area of 1244.6 mm × 1244.6 mm (49 in × 49 in) (biggest opening size in model range) as inputs into the model.

The incident energy for method “a)” is expected to be higher. Method b takes the maximum box opening area that was analyzed. The test results were insufficient for validating the box opening size beyond 1244.6 mm × 1244.6 mm (49 in × 49 in)

If a box opening area encountered in actual equipment is 1016 mm × 1016 mm (40 in × 40 in), then the recommended methods to select the opening size are:

- a) Select the next smaller opening area of 914.4 mm × 914.4 mm (36 in × 36 in)
- b) Use 1016 mm × 1016 mm (40 in × 40 in) as opening area input into the model.

The incident energy for method “a)” is expected to be higher. Using option b) is expected to yield more accurate results.

G.9.7 Selection of model configuration

A representative configuration for arc-flash thermal hazard assessment has been provided in this subclause. It offers general guidance for selection proper configurations in estimating arcing current, incident energy, and arc-flash boundary

The results of the incident energy calculation can be utilized to define minimum arc thermal performance value (ATPV) or energy breakdown (E_{BT}) rating of the PPE for personnel working on energized equipment.

For the same equipment, the fault location may change the plasma direction and the arcing path. In general, electrode orientation determines the direction of the plasma during the incident. Some real equipment tests provide the examples for the way to determine configuration chosen for arc-flash event.

Figure G.39 to Figure G.43 provide typical equipment configuration and relevant electrode characteristics, which could be used to determine the configuration for incident energy calculations.

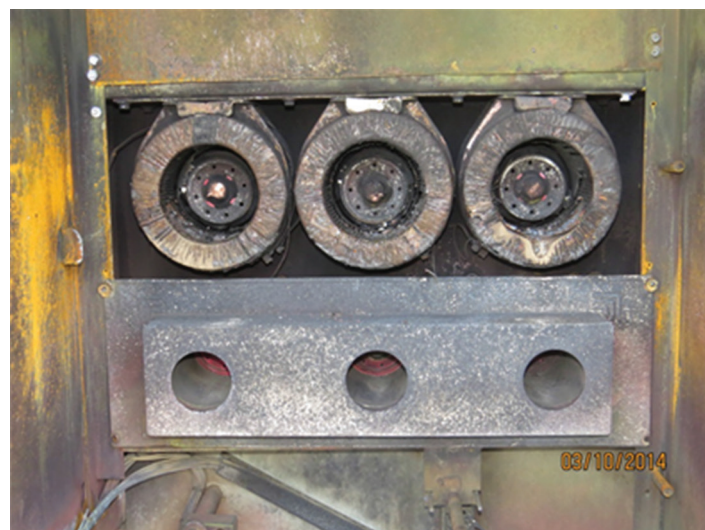


Figure G.39—HCB/HOA configuration in switchgear (depends on opening dimension)

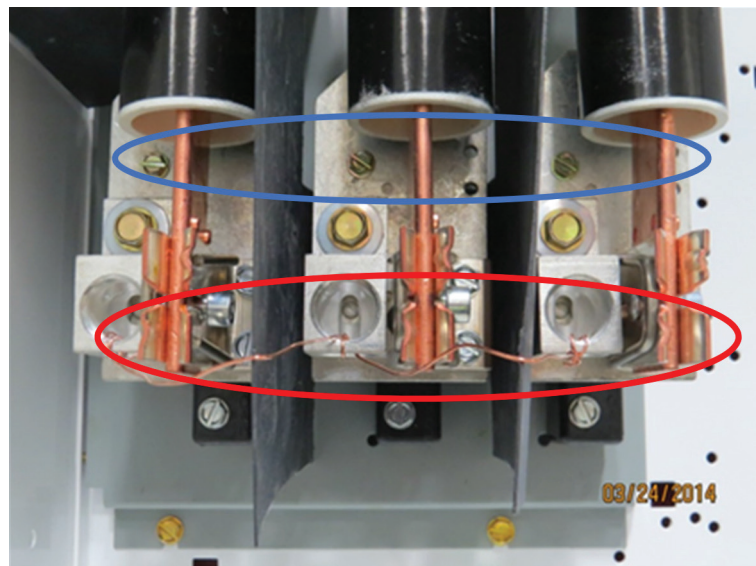


Figure G.40—VCB (upper circle) and HCB (lower circle) configuration on the fuse holder



Figure G.41—VCBB configuration on switchgear



Figure G.42—VCB configuration on switchgear

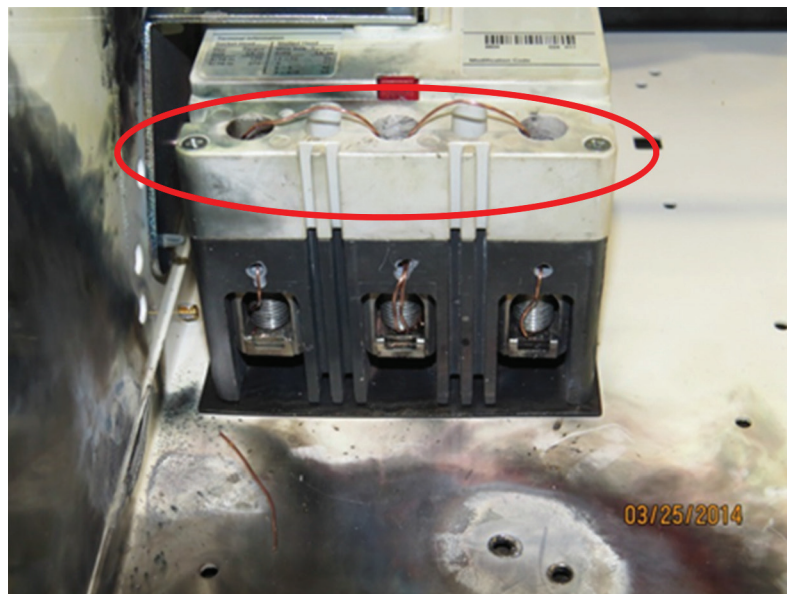


Figure G.43—HCB configuration on switchgear

Annex H

(informative)

Development of special model for current-limiting fuses

H.1 General

For the development of IEEE 1584-2002, it was found to be difficult to calculate incident energy in circuits protected by current-limiting fuses because of the reduced arc time and limited let-through current. Therefore, tests were conducted to determine the effect of current-limiting fuses on incident energy.

Three fuses were placed between the laboratory's source and a switchgear-sized enclosure 508 mm × 508 mm × 508 mm (20 in × 20 in × 20 in). Arcs were initiated in the enclosure, and incident energy, arc current, and arc time were recorded. The circuit was calibrated for open-circuit voltage and a range of bolted fault currents. The range of test currents was selected to enable development of a model of arc-flash characteristics, both within and below the fuses' current-limiting ranges. Three tests were performed for each fuse rating and each data point. The worst case was then selected. See [B25], [B33], and [B75] in the bibliography.

Fuses from one manufacturer were used, but results with other manufacturers' fuses of the same class should be similar. The manufacturer should be consulted.

Actual field results could be different for various reasons, as follows:

- a) Different system voltage
- b) Different closing angle on the voltage wave
- c) Different distance from the arc

The smallest fuse tested was a 100 A Class RK1 fuse. All data for lower amperage fuses is based upon the 100 A level. Incident energy values with actual 30 A and 60 A fuses would be considerably less than for 100 A fuses.

H.2 Development of curve-fitting equations

H.2.1 General

Equations for calculating arc-flash energies for use with current-limiting Class L and Class RK1 fuses have been developed. These equations were developed based upon testing at 600 V and a distance of 455 mm (17.913 in) using one manufacturer's fuses. They can be applied over the range of fuses below the tested fuse, e.g., the 200 A class RK1 fuse may be applied to fuses rated from 101 A to 200 A. The variables are as follows:

- I_{bf} is bolted fault current for three-phase faults
 E is incident energy (J/cm^2)

[Table H.1](#) to [Table H.8](#) show the test data used for one particular manufacturer, and [Figure H.1](#) to [Figure H.27](#) show the application of a curve-fitting program to develop the equations listed in [Table H.9](#).

These equations are applicable only to VCB configurations in 600 V systems only.

H.2.2 Class L 2000 A

Table H.1 shows the test data used for a 2000 A fuse for a particular manufacturer, and Figure H.1, Figure H.2, and Figure H.3 show the application of a curve-fitting program to develop the equations for this size.

Table H.1—Incident energy as a function of bolted fault current for one manufacturer's 2000 A class L current limiting fuses at 600 V, 460 mm (18.11 in)

Current limiting fuse	Bolted fault (kA)	Series average incident energy (J/cm ²)	Series mean max incident energy (J/cm ²)	Series maximum incident energy (J/cm ²)	Default for model ^a
Class L 2000 A	106.0	8.1	10.0	13.0	13
Class L 2000 A	65.9	27.0	34.0	100.0	100
Class L 2000 A	44.1	41.0	55.0	70.0	111
Class L 2000 A	22.6	97.0	121.0	123.0	123

NOTE—111.2944 was chosen as default value to linearize the values from 22 600 A to 65 900 A.

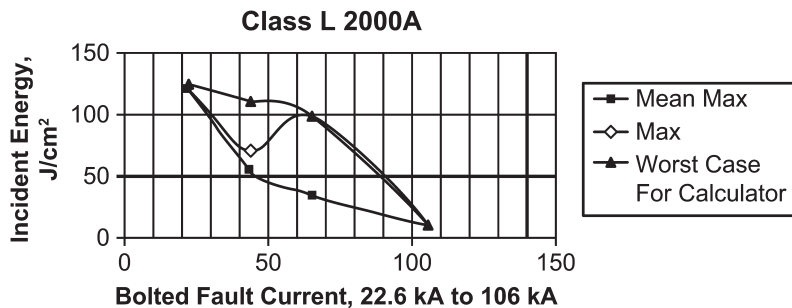


Figure H.1—Class L 2000 A fuse—incident energy versus bolted fault current

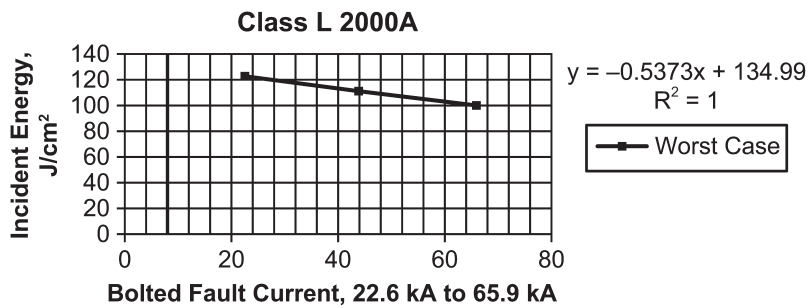


Figure H.2—Class L 2000 A fuse—low current segment of model

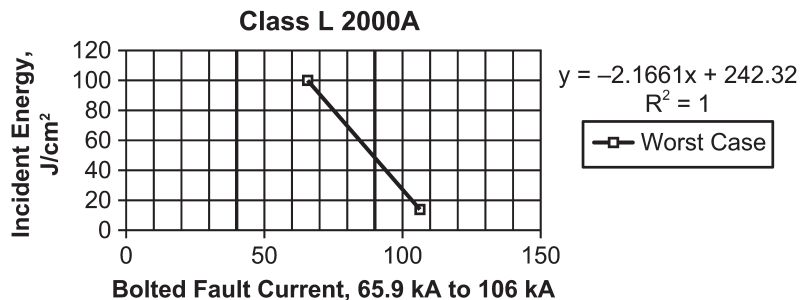


Figure H.3—Class L 2000 A fuse—high current segment of model

H.2.3 Class L 1600 A

Table H.2 shows the test data used for a 1600 A fuse for a particular manufacturer, and Figure H.4 through Figure H.8 show the application of a curve-fitting program to develop the equations for this size.

Table H.2—Incident energy as a function of bolted fault current for one manufacturer's 1600 A class L current limiting fuses at 600 V, 460 mm (18.11 in)

Current limiting fuse	Bolted fault (A)	Series average incident energy (J/cm ²)	Series mean maximum incident energy (J/cm ²)	Series maximum incident energy (J/cm ²)	Default for model
Class L 1600 A	106 000	1.2	1.5	1.5	1.7
Class L 1600 A	65 900	4.1	5.2	12.3	12.0
Class L 1600 A	44 100	3.1	3.8	4.9	12.0
Class L 1600 A	31 800	84.0	87.0	92.0	92.0
Class L 1600 A	22 600	29.0	40.0	49.0	99.0
Class L 1600 A	15 700	77.0	79.0	85.0	105.0

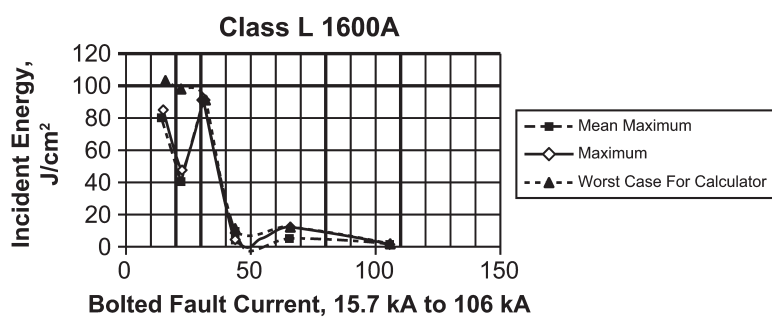


Figure H.4—Class L 1600 A fuse—incident energy versus bolted fault current

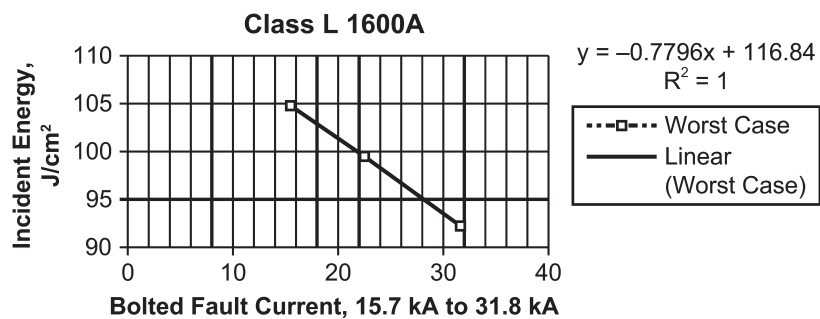


Figure H.5—Class L 1600 A fuse—low current segment of model

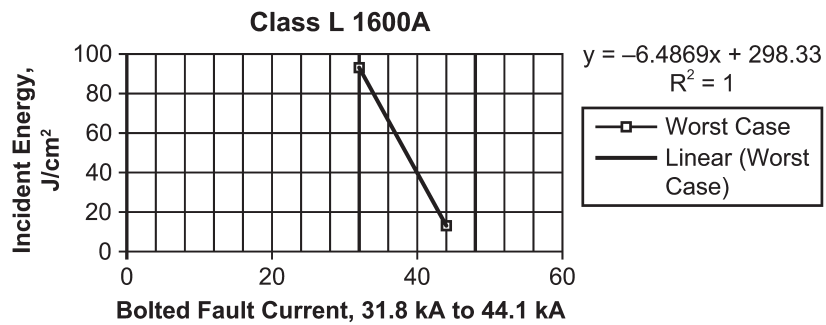


Figure H.6—Class L 1600 A fuse—upper-middle current segment of model

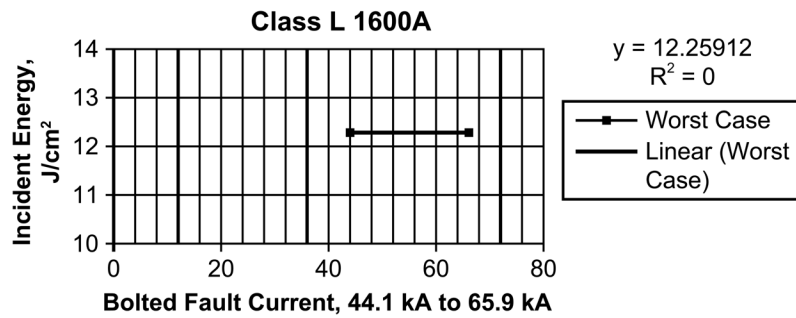


Figure H.7—Class L 1600 A fuse—upper-middle current segment of model

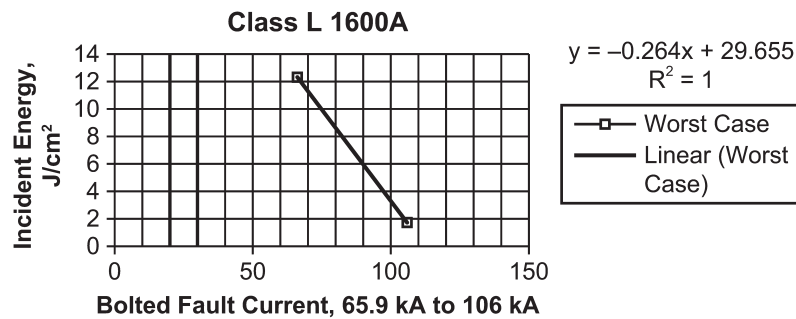


Figure H.8—Class L 1600 A fuse—upper current segment of model

H.2.4 L 1200 A

Table H.3 shows the test data used for a 1200 A fuse for a particular manufacturer, and Figure H.9 through Figure H.12 show the application of a curve-fitting program to develop the equations for this size.

Table H.3—Incident energy as a function of bolted fault current for one manufacturer's 1200 A class L current limiting fuses at 600 V, 460 mm (18.11 in)

Current limiting fuse	Bolted fault (A)	Series average incident energy (J/cm ²)	Series mean maximum incident energy (J/cm ²)	Series maximum incident energy (J/cm ²)	Default for spreadsheet calculation
Class L 1200 A	106 000	0.6	0.8	1.0	1.6
Class L 1200 A	65 900	0.8	1.0	1.0	1.6
Class L 1200 A	44 100	1.0	1.3	1.6	1.6
Class L 1200 A	31 800	7.1	1.7	18.0	18.0
Class L 1200 A	22 600	19.0	26.0	41.0	41.0
Class L 1200 A	15 700	37.0	43.0	47.0	47.0

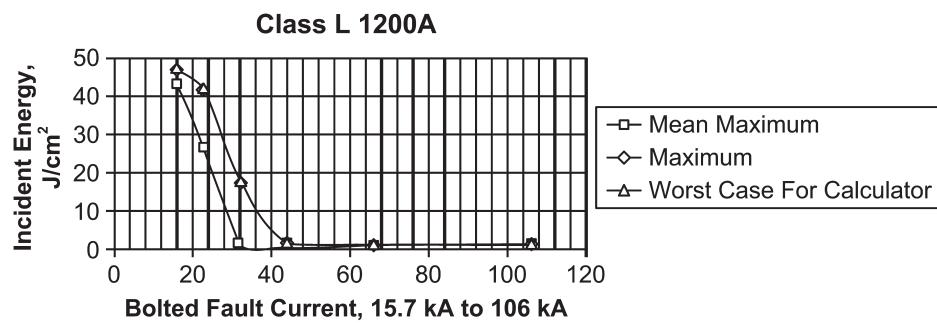


Figure H.9—Class L 2000 A fuse—incident energy versus bolted fault current

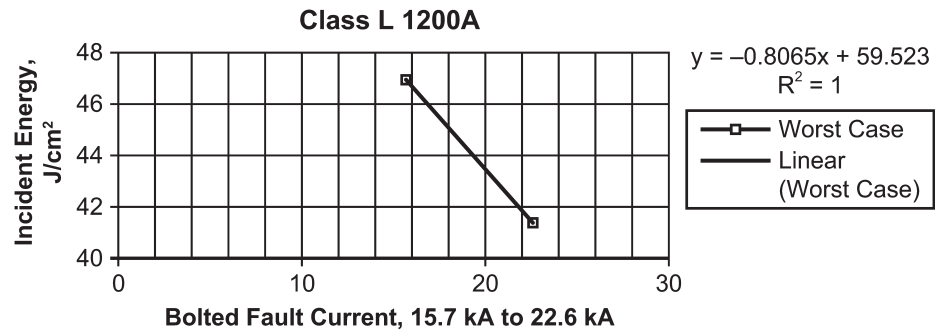


Figure H.10—Class L 1200 A fuse—lower current segment of model

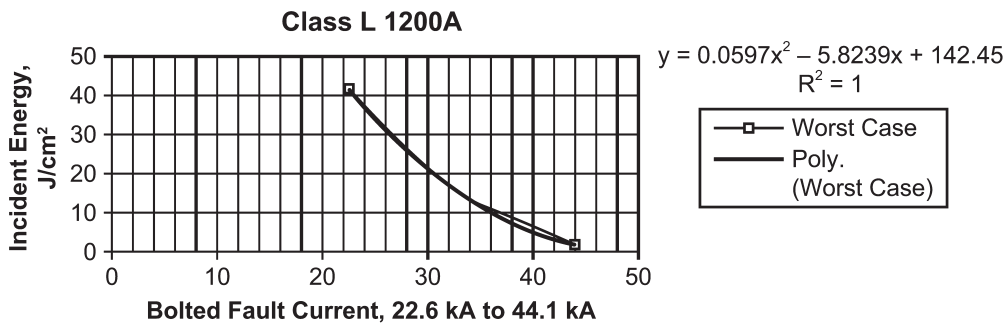


Figure H.11—Class L 1200 A fuse—middle current segment of model

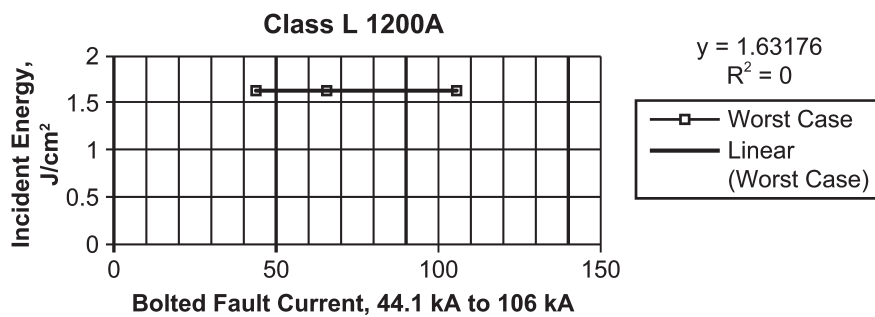


Figure H.12—Class L 1200 A fuse—upper current segment of model

H.2.5 Class L 800 A

Table H.4 shows the test data used for an 800 A fuse for a particular manufacturer, and Figure H.13, Figure H.14, and Figure H.15 show the application of a curve-fitting program to develop the equations for this size.

Table H.4—Incident energy as a function of bolted fault current for one manufacturer's 800 A class L current limiting fuses at 600 V, 460 mm (18.11 in)

Current limiting fuse	Bolted fault (A)	Series average incident energy (J/cm ²)	Series mean maximum Incident energy (J/cm ²)	Series maximum incident energy (J/cm ²)	Default for model
Class L 800 A	106 000	0.75	0.92	1.00	1.0
Class L 800 A	65 900	0.59	0.71	0.75	1.0
Class L 800 A	44 100	0.38	0.63	0.75	1.0
Class L 800 A	22 600	2.60	3.50	6.40	6.4
Class L 800 A	15 700	4.10	4.20	4.60	8.2

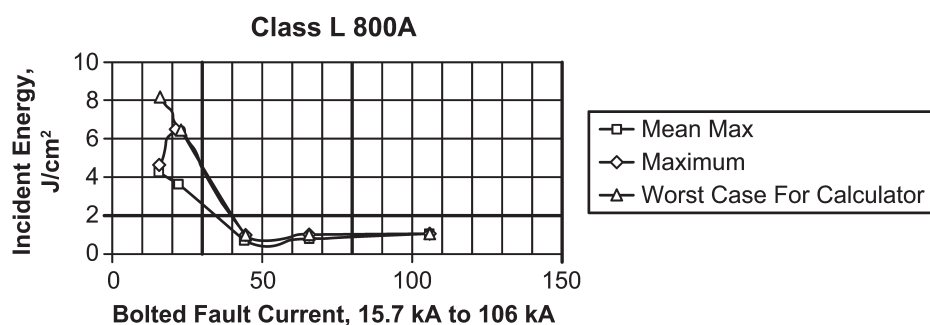


Figure H.13—Class RK1 800 A fuse—incident energy versus bolted fault current

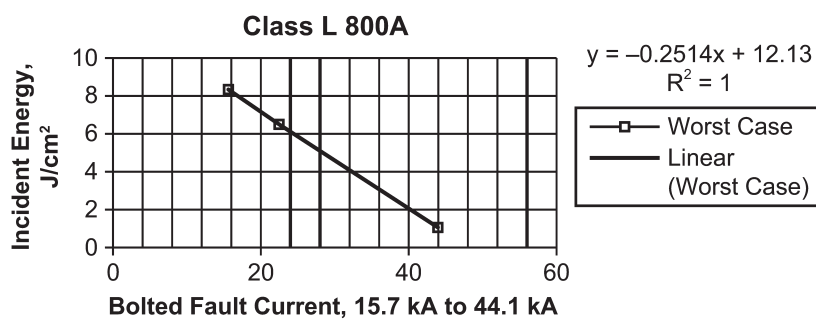


Figure H.14—Class RK1 800 A fuse—lower current segment of model

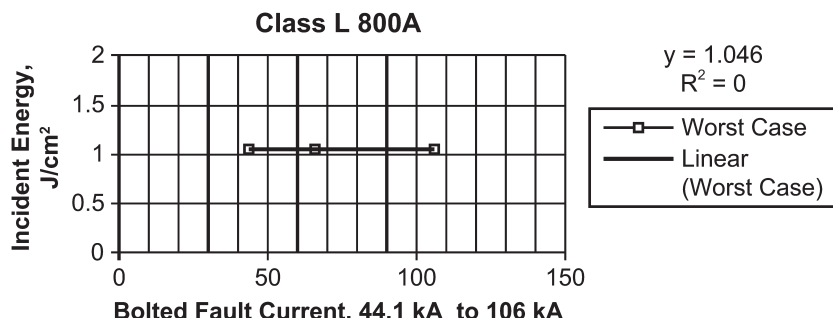


Figure H.15—Class RK1 800 A fuse—middle current segment of model

H.2.6 Class RK1 600 A

Table H.5 shows the test data used for a 600 A fuse for a particular manufacturer, and Figure H.16, Figure H.17, and Figure H.18 show the application of a curve-fitting program to develop the equations for this size.

Table H.5—Incident energy as a function of bolted fault current of one manufacturer's 600 A class RK1 current limiting fuses at 600 V, 460 mm (18.11 in)

Current limiting fuse	Bolted fault (A)	Series average incident energy (J/cm ²)	Series mean maximum incident energy (J/cm ²)	Series maximum incident energy (J/cm ²)	Default for model
Class RK1 600 A	106 000	0.13	0.17	0.17	1.0
Class RK1 600 A	65 900	0.21	0.38	0.46	1.0
Class RK1 600 A	44 100	0.21	0.29	0.33	1.0
Class RK1 600 A	22 600	0.42	0.63	0.63	1.0
Class RK1 600 A	15 700	1.50	1.30	2.10	2.5
Class RK1 600 A	14 000	1.50	1.30	2.50	2.5
Class RK1 600 A	8500	53.00	52.00	73.00	73.0

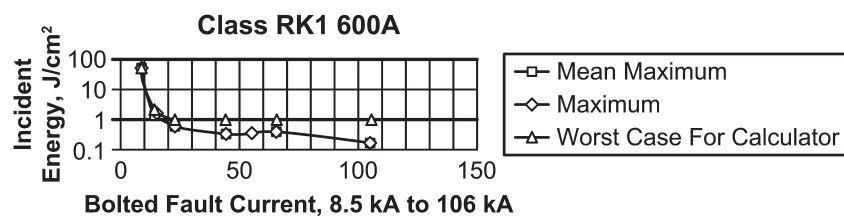


Figure H.16—Class RK1 600 A fuse—lower current segment of model

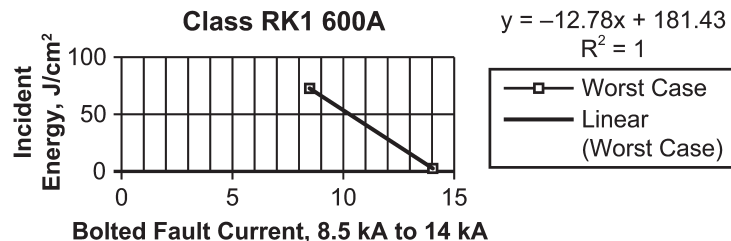


Figure H.17—Class RK1 600 A fuse—middle current segment of model

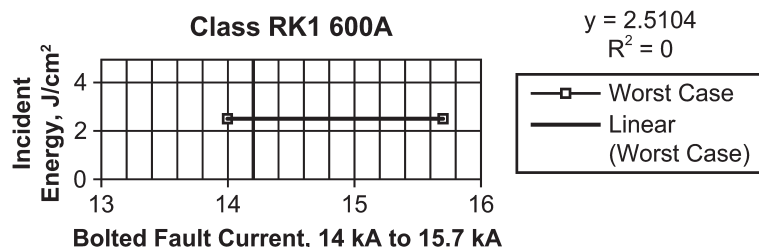


Figure H.18—Class RK1 200 A fuse—upper current segment of model

H.2.7 Class RK1 400 A

Table H.6 shows the test data used for a 400 A fuse for a particular manufacturer, and Figure H.19, Figure H.20, and Figure H.21 show the application of a curve-fitting program to develop the equations for this size.

Table H.6—Incident energy as a function of bolted fault current for one manufacturer's 400 A class RK1 current limiting fuses at 600 V, 460 mm (18.11 in)

Current limiting fuse	Bolted fault (A)	Series average incident energy (J/cm ²)	Series mean maximum incident energy (J/cm ²)	Series maximum incident energy (J/cm ²)	Default for model
Class RK1 400 A	22 600	0.08	0.13	0.13	1.0
Class RK1 400 A	5040	1.20	1.50	3.30	3.3
Class RK1 400 A	3160	92.00	92.00	153.00	153.0

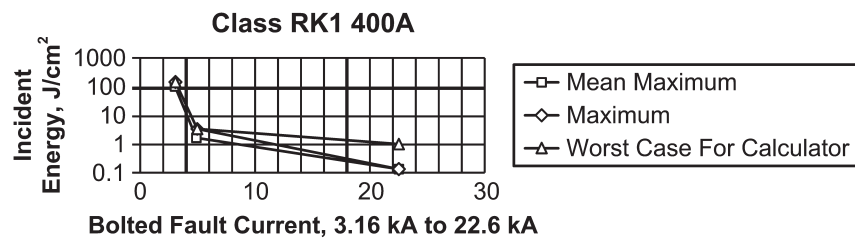


Figure H.19—Class RK1 400 A fuse—incident energy versus bolted fault current

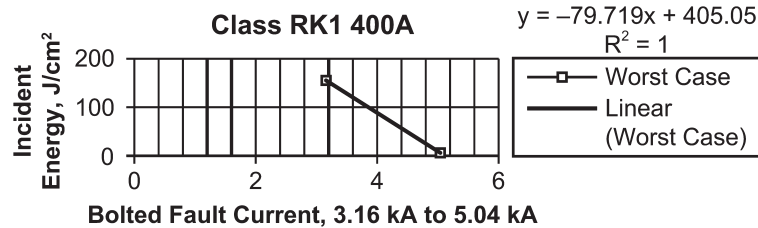


Figure H.20—Class RK1 400 A fuse—lower current segment of model

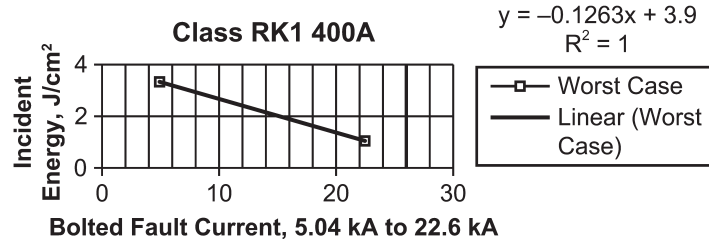


Figure H.21—Class RK1 400 A fuse—middle current segment of model

H.2.8 Class RK1 200 A

Table H.7 shows the test data used for a 200 A fuse for a particular manufacturer, and Figure H.22, Figure H.23, and Figure H.24 show the application of a curve-fitting program to develop the equations for this size.

Table H.7—Incident energy as a function of bolted fault current for one manufacturer's 200 A class RK1 current limiting fuses at 600 V, 460 mm (18.11 in)

Current limiting fuse	Bolted fault (A)	Series average incident energy (J/cm ²)	Series mean maximum incident energy (J/cm ²)	Series maximum incident energy (J/cm ²)	Default for model
Class RK1 200 A	3160	0.21	0.21	0.21	1.0
Class RK1 200 A	1600	5.40	0.63	29.00	29.0
Class RK1 200 A	1160	63.00	63.00	63.00	63.0

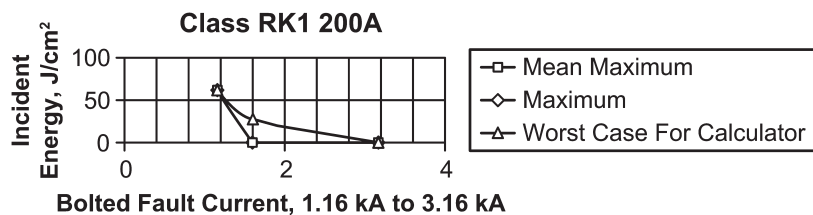


Figure H.22—Class RK1 200 A fuse—incident energy versus bolted fault current

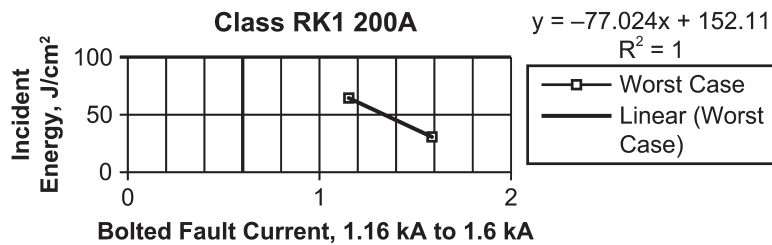


Figure H.23—Class RK1 200 A fuse—lower current segment of model

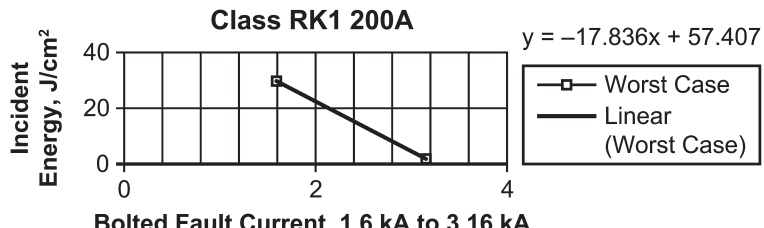


Figure H.24—Class RK1 200 A fuse—upper current segment of model

H.2.9 Class RK1 100 A

Table H.8 shows the test data used for a 100 A fuse for a particular manufacturer, and Figure H.25, Figure H.26, and Figure H.27 show the application of a curve-fitting program to develop the equations for this size.

Table H.8—Incident energy as a function of bolted fault current of one manufacturer's 100 A class RK1 current limiting fuses at 600 V, 460 mm (18.11 in)

Current limiting fuse	Bolted fault (A)	Series average incident energy (J/cm ²)	Series mean maximum incident energy (J/cm ²)	Series maximum incident energy (J/cm ²)	Default for model
Class RK1 100 A	1600	0.42	0.21	0.84	1.0
Class RK1 100 A	1400	0.92	0.84	1.05	1.0
Class RK1 100 A	1160	2.00	1.70	2.50	2.5
Class RK1 100 A	650	21.00	21.00	26.00	26.0

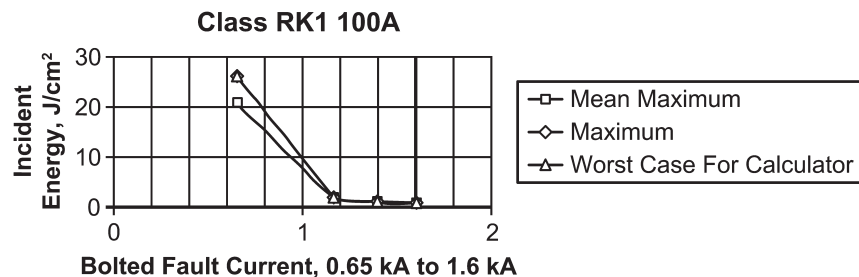


Figure H.25—Class RK1 100 A fuse—lower current segment of model

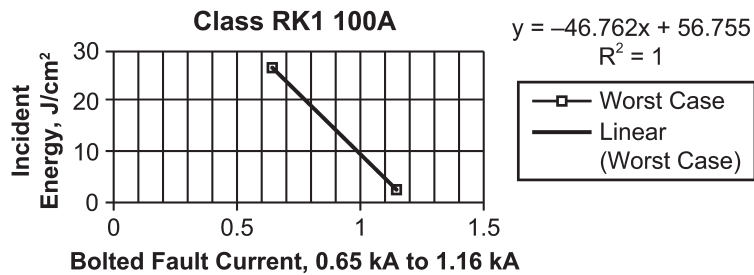


Figure H.26—Class RK1 100 A fuse—upper current segment of model

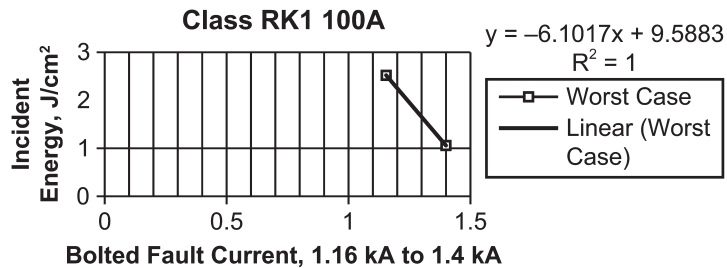


Figure H.27—Class L 100 A fuse—upper current segment of model

H.3 Special current-limiting fuse model equations

Equations for calculating arc-flash energies for use with current-limiting Class L and Class RK1 fuses have been developed. These equations were developed based upon testing at 600 V in the VCB configuration and at a distance of 457.2 mm (18 in) using one manufacturer's fuses. Where applicable, these formulae should be used as opposed to the equations in 4.3, 4.4, and 4.5. If any other working distance or electrode configuration is needed for the study, then 4.3, 4.4, and 4.5 should be used. Contact the individual manufacturers to determine the appropriateness of the following equations. The variables are as follows:

I_{bf} bolted fault current for three-phase faults (symmetrical rms) (kA)

E incident energy (J/cm^2)

$K1, K2, K3$ constants as found in Table H.9

$$E = 4.184 \cdot (K1 \cdot I_{bf}^2 + K2 \cdot I_{bf} + K3) \quad (\text{H.1})$$

For I_{bf} below the value in the “lower limit” column of Table H.9, use 4.3, 4.4, and 4.5 and time-current curves to calculate arcing current and determine estimated energy. For I_{bf} above 106 kA, contact the manufacturer for information.

Table H.9—Constants K1, K2, and K3 for special fuse model equation

Fuse type	Lower limit (kA)	From (kA)	To (kA)	K1	K2	K3
Class L fuses 1601–2000 A	22.6	22.6	65.9	0	-0.1284	32.262
		65.9	106	0	-0.5177	57.917
Class L fuses 1201–1600 A	15.7	15.7	31.8	0	-0.1863	27.926
		31.8	44.1	0	-1.5504	71.303
		44.1	65.9	0	0	2.941
		65.9	106	0	-0.0631	7.0878
Class L fuses 801–1200 A	15.7	15.7	22.6	0	-0.1928	14.226
		22.6	44.1	0.0143	-1.3919	34.045
		44.1	106	0	0	0.3898
Class L fuses 601–800 A	15.7	15.7	44.1	0	-0.0601	2.8992
		44.1	106	0	0	0.2501
Class RK1 fuses 401–600 A	8.5	8.5	14.0	0	-3.0545	43.364
		14.0	15.7	0	0	0.6002
		15.7	22.6	0	-0.0507	1.3964
		22.6	106	0	0	0.2501
Class RK1 fuses 201–400 A	3.16	3.16	5.04	0	-19.053	96.808
		5.04	22.6	0	-0.0302	0.9321
		22.6	106	0	0	0.2501
Class RK1 fuses 101–200 A	1.16	1.16	1.6	0	-18.409	36.355
		1.6	3.16	0	-4.2628	13.721
		3.16	106	0	0	0.2501
Class RK1 fuses up to 100 A	0.65	0.65	1.16	0	-11.176	13.565
		1.16	1.4	0	-1.4583	2.2917
		1.4	106	0	0	0.2501

Annex I

(informative)

Development of special model for circuit breakers

I.1 General

This annex is provided for information only. This model has not been validated using the IEEE/NFPA Collaboration test results

Where applicable, this model allows a calculation of incident energy if the potential arc current falls in the instantaneous trip range of the circuit breaker. See Gregory, Lytle, and Wellman [B47]. Equations have been developed for systems using low-voltage circuit breakers that will output values for incident energy and arc-flash boundary when the available bolted fault current is known or can be calculated. These equations do not require availability of the time-current curves for the circuit breaker, but they should be used within the appropriate range indicated in the circuit breaker model. These equations are only applicable for equipment in the VCB configuration.

Calculations were performed for a broad range of low-voltage circuit breakers in order to find those with the highest values for incident energy and arc-flash boundary. The output provided a range of information as indicated in [Figure I.1](#) for one grouping of circuit breakers. The calculations were performed using the model equations for arc current and incident energy with time-current characteristic curves for various ranges of circuit breakers for four manufacturers. Similar calculations were run for various groupings of circuit breaker types and ratings.

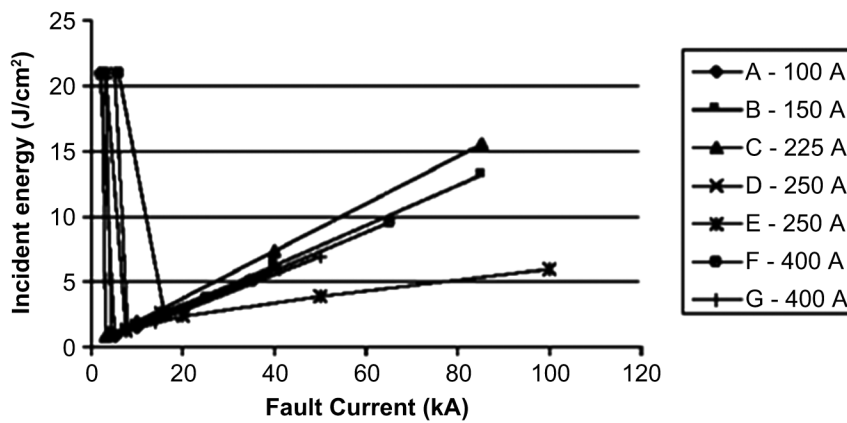


Figure I.1—Incident energy versus fault current for 100 A to 400 A circuit breakers

The format for both incident energy and arc-flash boundary appeared as indicated in [Figure I.1](#) for each grouping of circuit breakers. Even though the curves developed in this manner represent various designs from multiple manufacturers, the curves are somewhat bundled. This makes it practical to generate a single maximum energy or maximum distance curve representing each group of frames. The equations in the circuit breaker model were formed by taking the highest curve calculated using model equations for any circuit breaker found and by calculating the line $E = M I_{bf} + N$ for the portion between I_1 and I_2 . See [Figure I.2](#). These values represent the highest values for any equipment class, regardless of whether solidly grounded or resistance grounded.

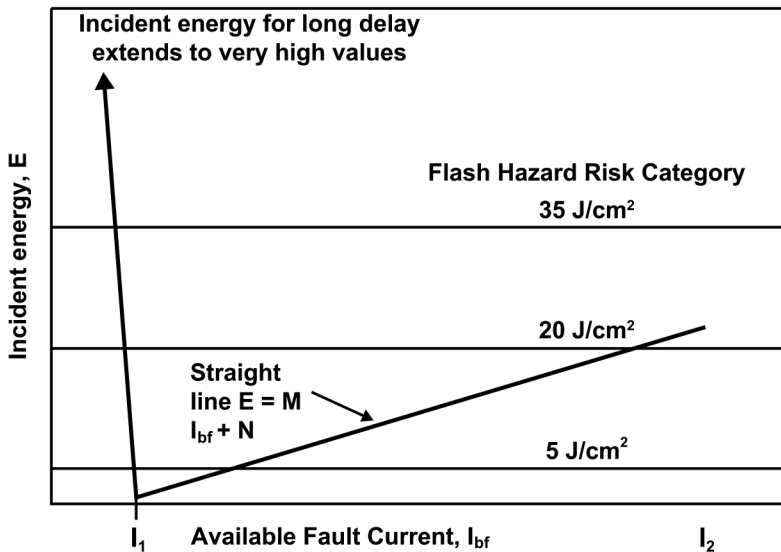


Figure I.2—Incident energy versus available fault current generalized for circuit breakers

Note that the curve reaches a low energy value at the bottom of the “V” at a fault current point labeled I_1 . Finding this current point is an essential part of calculating the incident energy. The user must confirm that the application is at a fault current above I_1 . The high current point on the line is the interrupting rating of the CB and is labeled I_2 . From I_1 on the chart to the highest current point, I_2 , the curve is roughly a straight line due to the fact that manufacturers represent instantaneous clearing times as a straight line. This line, $E = M I_{bf} + N$ represents the equation developed for that group. It is taken from a least squares regression of values calculated.

In the low current region (below I_1), in which the MCCBs are operating on their long-time characteristic, incident energy elevates quickly and may go above 100 cal/cm².

I.2 Special low-voltage circuit breaker model equations

Equations have been developed for systems using low-voltage circuit breakers that will output values for incident energy and arc-flash boundary when the available bolted fault current is known or can be calculated. These equations do not require availability of the time-current curves for the circuit breaker, but should be used within the appropriate range indicated below. For conditions of bolted fault current outside the range $I_1 < I_{bf} < I_2$ described below, or for different equipment configurations, the arc current and incident energy equations in Clause 4 are applicable. Similarly, when the time-current curves are available, the equations in Clause 4 are preferred.

The types of circuit breakers are as follows:

- MCCB: Molded-case circuit breaker
- ICCB: Insulated-case circuit breaker
- LVPCB: Low-voltage power circuit breaker

The types of trip units are briefly defined as follows:

- TM: Thermal-magnetic trip units.
- M: Magnetic (instantaneous only) trip units.

- E: Electronic trip units have three characteristics that may be used separately or in combination,
 - (L) long-time
 - (S) short-time and
 - (I) instantaneous.
- A trip unit may be designated LI when it has both long-time and instantaneous features. Other common designations are LS and LSI.

The range of these equations is 700 A to 106 000 A for the voltages shown in **Table I.1**. Each equation is applicable for the range $I_1 < I_{bf} < I_2$.

Table I.1—Equations for incident energy and arc-flash boundary by circuit-breaker type and rating^a

Rating (A)	Circuit breaker type	Trip unit type	480 V and lower		575–690 V	
			Incident energy (J/cm ²) ^b	Arc-flash boundary (mm)	Incident energy (J/cm ²)	Arc-flash boundary (mm)
100–400	MCCB	TM or M	0.189 I_{bf} + 0.548	9.16 I_{bf} + 194	0.271 I_{bf} + 0.180	11.8 I_{bf} + 196
600–1200	MCCB	TM or M	0.223 I_{bf} + 1.590	8.45 I_{bf} + 364	0.335 I_{bf} + 0.380	11.4 I_{bf} + 369
600–1200	MCCB	E, LI	0.377 I_{bf} + 1.360	12.50 I_{bf} + 428	0.468 I_{bf} + 4.600	14.3 I_{bf} + 568
1600–6000	MCCB or ICCB	TM or E, LI	0.448 I_{bf} + 3.000	11.10 I_{bf} + 696	0.686 I_{bf} + 0.165	16.7 I_{bf} + 606
800–6300	LVPCB	E, LI	0.636 I_{bf} + 3.670	14.50 I_{bf} + 786	0.958 I_{bf} + 0.292	19.1 I_{bf} + 864
800–6300	LVPCB	E, LS ^c	4.560 I_{bf} + 27.230	47.20 I_{bf} + 2660	6.860 I_{bf} + 2.170	62.4 I_{bf} + 2930

^aRefer to **Annex B** for conversion to cal/cm².

^b I_{bf} is in kA, working distance is 460 mm.

^cShort time delay is assumed to be set at maximum.

I_2 is the interrupting rating of the CB at the voltage of interest and is the endpoint of the time-current curve. The opening time of the circuit breaker is undetermined at current values above its interrupting rating.

I_1 is the minimum bolted fault current at which this method can be applied. I_1 is the lowest bolted fault current level that generates arcing current great enough for instantaneous tripping to occur or for circuit breakers with no instantaneous trip, the lowest current at which short time tripping occurs.

To find I_1 , use the manufacturer's time-current curve, if it is readily available, and take the instantaneous trip value, I_t , from the curve as shown in **Figure I.3**. If the curve is not available, but the instantaneous trip setting is shown on the circuit breaker, use that setting. When the tripping current, I_t , is not known, use a default value of 10 times the continuous current rating of the CB, except for CBs rated 100 A and below, use a default value of $I_t = 1300$ A. Where an LS trip unit is used, I_t is the short-time pick-up current.

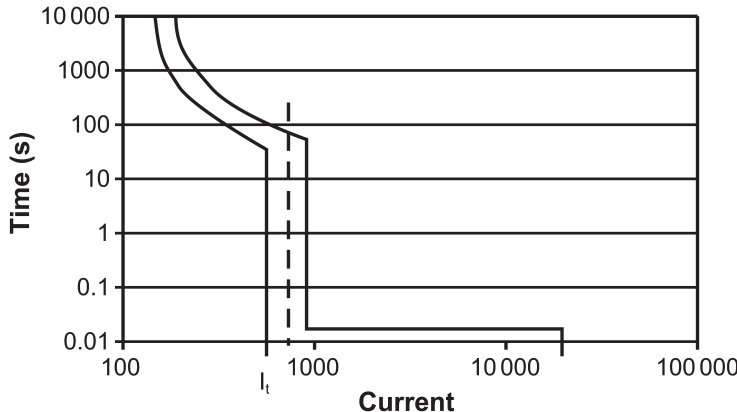


Figure I.3—Typical circuit breaker time-current characteristic

The corresponding bolted fault current, I_{bf} , is found by solving the model equation for arc current for box configurations by substituting I_t for arcing current. The 1.3 factor in [Equation \(I.1\)](#) adjusts current to the top of the tripping band.

$$\log(1.3 \cdot I_t) = -0.084 + 0.096V + 0.586(\log I_{bf}) + 0.559V(\log I_{bf}) \quad (I.1)$$

Solving for I_{bf} at the point I_t for 600 V:

$$\log I_{bf} = 0.0281 + 1.09 \log(1.3 \cdot I_t) \quad (I.2)$$

Solving for I_{bf} at the point I_t for 480 V and lower:

$$\log I_{bf} = 0.0407 + 1.17 \log(1.3 \cdot I_t) \quad (I.3)$$

$$I_{bf} = I_t = 10 \cdot \log^{11} \quad (I.4)$$

Consensus

WE BUILD IT.

Connect with us on:

-  **Facebook:** <https://www.facebook.com/ieeesa>
-  **Twitter:** @ieeesa
-  **LinkedIn:** <http://www.linkedin.com/groups/IEEESA-Official-IEEE-Standards-Association-1791118>
-  **IEEE-SA Standards Insight blog:** <http://standardsinsight.com>
-  **YouTube:** IEEE-SA Channel